



POLITECNICO DI MILANO
DIPARTIMENTO DI ELETTRONICA, INFORMAZIONE E BIOINGEGNERIA
DOCTORAL PROGRAMME IN INFORMATION TECHNOLOGY

HIERARCHICAL AND MULTILAYER CONTROL
STRUCTURES BASED ON MPC FOR
LARGE-SCALE SYSTEMS

Doctoral Dissertation of:
Xinglong Zhang

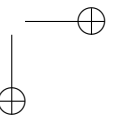
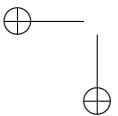
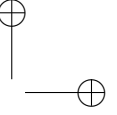
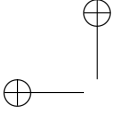
Supervisor:
Prof. Riccardo Scattolini

Co-supervisor:
Prof. Marcello Farina

Tutor:
Prof. Simone Garatti

The Chair of the Doctoral Program:
Prof. Andrea Bonarini

2014 – XXX Cycle

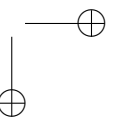
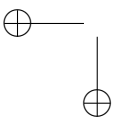
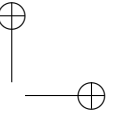
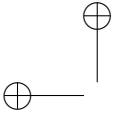


—

*Everything must be made as simple as possible.
But not simpler.*

by Albert Einstein

—



Abstract

OVER the last decades, the complexity of systems is continuously increasing due to economic reasons and technological advances. It is known that the centralized Model Predictive Control (MPC) solutions for such large-scale systems might result in unacceptable control performance due to various factors, such as high dimension of the system, computation efficiency and communication bandwidth. Moreover, centralized controllers are not scalable and difficult to maintain. For these reasons, in the last twenty years, decentralized and distributed MPC algorithms have been developed with a number of local problems solved in parallel to achieve global or local objectives. An alternative to decentralized and distributed control consists in the use of hierarchical control structures based on MPC. This approach is very powerful especially for control of systems with separable fast and slow dynamics, for the coordination of subsystems and when it is required to consider different objectives in the long term and regulation problems in the short term.

This Thesis addresses the theoretical development of hierarchical and multilayer control algorithms based on MPC for large-scale systems.

In Chapter 2, we develop a two-layer control structure for the coordination of independent linear dynamic systems with input and joint output constraints. At the higher layer, a reduced order dynamic model of the system’s components is used to state and solve an economic MPC algorithm in a long time scale. The outcomes of this layer are the components of the control variables to be held constant over the long sampling periods. At the lower layer, decentralized MPC controllers, one for each subsystem, are

implemented in a shorter time scale and according to a shrinking horizon strategy to compensate for the model inaccuracies at the high level. The overall convergence, recursive feasibility, as well as the fulfillment of the joint constraints, are obtained under mild assumptions.

A fully scalable hierarchical control scheme for coordination of similar independent systems with joint output and input constraints is presented in Chapter 3. Differently from Chapter 2, a scalable low-dimensional model mapping the common input to the collective output is used at the high layer, this model is easily determined from the impulse responses of the subsystems. The outcome of the high layer is the value of the common input to be held constant and to be distributed among the subsystems based on a specific weight associated with each subsystem. This approach allows to modify the system configuration with time varying weights, in terms of the contribution provided by any subsystem to the overall system performance, and to implement plug-and-play operations. The recursive feasibility is guaranteed also during plug-in and plug-out operations, and the overall convergence of the system output to the set-point is proven.

Finally, in Chapter 4, we extend the hierarchical control structure to large-scale interconnected systems. At the higher layer, a robust centralized MPC algorithm based on a reduced order dynamic model optimizes a long-term performance index, while at the lower layer local MPC regulators, are designed for the full order models of the subsystems to refine the control action computed at the higher layer. The recursive feasibility and robustness of the two layer algorithm are guaranteed and the overall convergence of the state to the steady state is fully discussed.

Several simulation examples are reported to show the effectiveness of all the proposed algorithms.

Riassunto

NEGLI ultimi decenni, la complessità dei sistemi ingegneristici è sempre più aumentata sia per motivi economici, sia per gli sviluppi tecnologici. Nel progetto dei sistemi di controllo, è noto che le soluzioni centralizzate basate sul Model Predictive Control (MPC) per tali sistemi su larga scala potrebbero risultare inefficienti a causa di vari fattori, come la dimensione del sistema, l'efficienza di computazione e la larghezza della banda di comunicazione. Inoltre, i controllori centralizzati non sono scalabili e sono difficili da mantenere. Per questi motivi, negli ultimi vent'anni sono stati progettati algoritmi MPC decentralizzati e distribuiti basati sulla soluzione in parallelo di una serie di problemi locali, con lo scopo di raggiungere obiettivi globali o locali. Un'alternativa al controllo decentralizzato e distribuito riguarda l'uso di strutture di controllo gerarchiche basate su MPC. Questo metodo è molto potente soprattutto per il controllo dei sistemi con dinamiche sia veloci che lente, per il coordinamento di sottosistemi e in generale quando è necessario prendere in considerazione diversi obiettivi a lungo termine e problemi di regolazione a breve termine.

Questa tesi affronta lo sviluppo teorico di algoritmi di controllo gerarchici e multilivello basati su MPC per sistemi a larga scala.

Nel 2° Capitolo, è progettata una struttura di controllo a due livelli per il coordinamento di sistemi dinamici lineari indipendenti con vincoli di input e di output congiunti. Al livello superiore, un modello dinamico in ordine ridotto dei componenti del sistema viene utilizzato per progettare un algoritmo MPC economico che consideri un lungo orizzonte temporale. I risultati prodotti da questo controllore sono le componenti delle varia-

bili di controllo che devono essere mantenute costanti durante periodi di campionamento lunghi. Al livello inferiore, i controllori MPC decentralizzati, uno per ciascun sottosistema, sono implementati considerando un orizzonte temporale più breve, secondo una strategia “shrinking horizon” per compensare le inaccuratezze del modello ad alto livello. La convergenza dell’intero sistema controllato, l’ammissibilità ricorsiva dei problemi di ottimizzazione e il soddisfacimento dei vincoli congiunti sono ottenuti sotto ipotesi non molto stringenti.

Uno schema di controllo gerarchico completamente scalabile per il coordinamento di sistemi indipendenti con vincoli congiunti di ingresso e uscita è presentato nel Capitolo 3. A differenza del Capitolo 2, al livello più alto viene utilizzato un modello scalabile di dimensioni ridotte che mappa l’ingresso comune all’uscita collettiva e questo modello è facilmente determinato dalla risposta all’impulso dei sottosistemi. Il risultato dello controllo al livello superiore è il valore dell’ingresso comune da mantenere costante e da distribuire tra i sottosistemi in base a un peso specifico associato a ciascun sottosistema. Questo approccio consente di modificare la configurazione del sistema con pesi variabili nel tempo, in termini di contributo fornito da qualsiasi sottosistema alle prestazioni generali del sistema, e di implementare operazioni plug-and-play. La fattibilità ricorsiva è garantita anche durante le operazioni di plug-in e plug-out, e viene provata la convergenza complessiva dell’uscita del sistema al riferimento.

Infine, nel 4° Capitolo, la struttura gerarchica di controllo è estesa a sistemi interconnessi a larga scala. Al livello superiore, un algoritmo MPC robusto e centralizzato, basato su un modello dinamico in ordine ridotto, ottimizza un indice di prestazione a lungo termine; mentre allo strato inferiore, i regolatori locali MPC sono progettati per i modelli in ordine completo dei sottosistemi per perfezionare l’azione di controllo calcolata al livello superiore. La fattibilità e la robustezza dell’algoritmo a due livelli sono garantite, e la convergenza complessiva dello stato allo stato stazionario è provata.

Diversi esempi di simulazione sono riportati per mostrare l’efficacia di tutti gli algoritmi proposti.

Contents

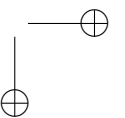
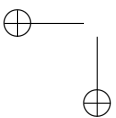
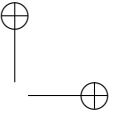
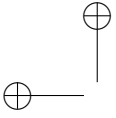
1	Introduction	1
1.1	Notation	2
1.2	Centralized MPC	3
1.2.1	Nominal MPC	4
1.2.2	Robust tube-based MPC	7
1.3	Decentralized and distributed MPC	9
1.3.1	Decentralized MPC	10
1.3.2	Distributed MPC	11
1.4	Hierarchical structures based on MPC	13
1.4.1	Hierarchical MPC for plantwide optimization	13
1.4.2	Coordination of independent systems	15
1.4.3	Hierarchical MPC for interconnected systems	15
1.4.4	Other hierarchical algorithms based on MPC	17
1.5	Structure of the Thesis and list of publications	19
2	Hierarchical MPC of independent systems with joint constraints	23
2.1	Introduction	23
2.2	The two-layer control structure	26
2.2.1	Reduced order models	29
2.2.2	The MPC problem at the high level	30
2.2.3	The MPC problem at the lower level	31
2.3	Design of the reduced order models	33
2.3.1	Construction of β and C_H	33
2.3.2	Model reduction	34

Contents

2.4	Properties of the two-layer control scheme	34
2.4.1	Feasibility	35
2.4.2	Convergence	36
2.5	Example	37
2.6	Conclusions	39
2.7	Appendix	40
2.7.1	Proof of Corollary 2.1	40
2.7.2	Proof of Proposition 2.1	40
2.7.3	Proof of Proposition 2.2	42
2.7.4	Proof of Proposition 2.3	44
3	A hierarchical MPC scheme for coordination of independent systems with shared resources and plug-and-play capabilities	47
3.1	Introduction	47
3.2	Statement of the problem and models	49
3.2.1	System model and control objectives	49
3.2.2	System decomposition and low-level models	51
3.2.3	High-level collective model	52
3.3	The high level regulator	53
3.3.1	Constraints in velocity form	53
3.3.2	The auxiliary control law and the maximal output admissible set	54
3.3.3	The high layer MPC problem	55
3.3.4	The high layer MPC problem with zero-terminal constraint	56
3.4	The low level regulators	57
3.5	Design issues and main results	58
3.6	Static and dynamic optimization of the weights α_i and plug and play operations	60
3.6.1	Time varying weights	61
3.6.2	Plug and play operations	62
3.7	Simulation example	64
3.7.1	Description of the models	64
3.7.2	Design of the sets	64
3.7.3	Simulation results without plug-and-play operations	65
3.7.4	Simulation results with plug-and-play operations	67
3.8	Conclusions	67
3.9	Appendix	69
3.9.1	Proof of Proposition 3.1	69
3.9.2	Proof of Proposition 3.2	70

Contents

3.9.3	Proof of Theorem 3.1	70
4	Hierarchical multi-rate MPC scheme for interconnected systems	73
4.1	Introduction and main idea	73
4.2	Models for the two-layer control scheme	75
4.2.1	Large-scale system model	75
4.2.2	Reduced order models	76
4.3	Design of the hierarchical control structure	77
4.3.1	Design of the high level regulator	77
4.3.2	Design of the low level regulators	79
4.4	Properties and algorithm implementation	83
4.4.1	Main assumptions and remarks	83
4.4.2	Main results and conservativeness of the scheme	86
4.4.3	Design	88
4.5	Simulation examples and implementation procedures	88
4.5.1	Temperature regulation of two apartments	88
4.5.2	Multi-rate control of a chemical plant	93
4.6	Extensions and conclusions	101
4.7	Appendix	102
4.7.1	Construction of β_i and of the reduced order model	102
4.7.2	Computation of the input constraint sets	103
4.7.3	Proof of Theorem 4.1	105
5	Conclusions	113
5.1	Conclusions	113
5.2	Hints for future research	114
	Bibliography	117



List of Figures

1.1	Traditional hierarchical structure for plantwide optimization	14
2.1	Hierarchical control scheme. E-MPC = Economic MPC, SH-MPC = Shrinking Horizon MPC	26
2.2	Open loop step responses of the continuous time models (continuous lines) of the generators and of the reduced order models in the long sampling time (dots).	39
2.3	Closed-loop control: outputs of the generators and their sum at the high layer (dots) and at the low layer (continuous lines).	40
2.4	Control variables at the high (continuous lines) and at the low (dots) layers.	41
3.1	Control variables of the controlled generators: overall control actions computed with the two-layer scheme (black solid lines) and control variables computed with the centralized scheme (red dashed lines).	66
3.2	Outputs of the controlled generators: outputs obtained with the two-layer scheme (black solid lines) and outputs obtained with the centralized scheme (red dashed lines).	67
3.3	Control variables of the controlled generators: overall control actions (u_1, \dots, u_6) , (magenta, blue, yellow, green, cyan, and red solid lines). Vertical dashed lines indicate the plug-in/unplug instants.	68

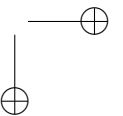
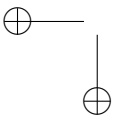
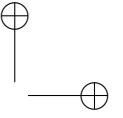
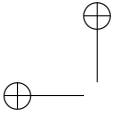
List of Figures

3.4	Outputs of the controlled generators: outputs $(y_1, \dots, y_6, \sum_{i=1}^6 y_i)$, (magenta, blue, yellow, green, cyan, red, and black solid lines) and reference power (black dash-dotted line). Vertical dashed lines indicate the plug-in/unplug instants.	68
4.1	Overall control scheme.	74
4.2	Adopted time scales: k (high layer design), $l_i = kN_i$ (low layer design of the i -th local regulator), $h = \zeta_i l_i = k\zeta_i N_i = kN_L$ (basic time scale).	81
4.3	Schematic representation of a building with two apartments .	89
4.4	Inputs of the controlled two apartments: blue * markers are the values of the inputs computed at the high level with the two-layer scheme, red dashed lines are the values of the overall control actions computed with the two-layer scheme, while black continuous lines are the values of the control variables computed with the centralized scheme.	91
4.5	States of the first apartment: red dashed lines are the values of the states with the two-layer scheme, while black continuous lines are the ones with the centralized scheme.	92
4.6	States of the second apartment: red dashed lines are the values of the states with the two-layer scheme, while black continuous lines are the ones with the centralized scheme.	93
4.7	Flow diagram of the chemical plant: for $i = 1, 2, 3$, R_i and C_i are the reactors and distillation columns, while D_i and B_i are the top and bottom products.	94
4.8	Control variables of the controlled linear system: black + markers (blue · markers) are the values of the inputs computed at the high level with the two-layer scheme with $N_L = 84$ and $N_H = 1$ (with $N_L = 28$ and $N_H = 3$), black continuous lines (blue dot-dashed lines) are the values of the overall control actions computed with the two-layer scheme with $N_L = 84$ and $N_H = 1$ (with $N_L = 28$ and $N_H = 3$), while red dashed lines are the values of the control variables computed with the centralized scheme.	99
4.9	Outputs of the controlled linear system: black continuous lines (blue dot-dashed lines) are the values of the outputs computed with the two-layer scheme with $N_L = 84$ and $N_H = 1$ (with $N_L = 28$ and $N_H = 3$), while red dashed lines are the values of the outputs computed with the centralized scheme.	100

List of Figures

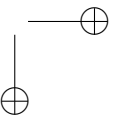
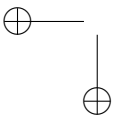
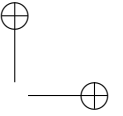
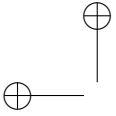
4.10 Control variables of the controlled nonlinear system: * markers are the values of the control variables computed at the high level in the long sampling time, i.e., (\bar{u}_1, \bar{u}_2) , (red, black, cyan, blue, green and magenta), while continuous lines are the values of the overall control actions in the multi rate, i.e., (u_1, u_2) , (red, black, cyan, blue, green and magenta). 100

4.11 Outputs of the controlled nonlinear system, i.e., (r_1, \dots, r_6) , (red, black, cyan, blue, green and magenta). 101



List of Tables

3.1 On-line computation time comparison	65
4.1 On-line computation time comparison: two apartments . . .	93
4.2 On-line computation time comparison: chemical plant . . .	98



CHAPTER *1*

Introduction

MPC is an effective process control method that has been widely employed in a large number of industrial plants, see [25, 62, 124, 140]. In MPC the control problem is reformulated as an optimization one with the capability to tackle multivariable systems and to handle constraints on input, state and output variables. Many MPC algorithms have been developed over the years with guaranteed fundamental properties, such as closed-loop stability and robustness with respect to external disturbances and/or model uncertainties, see [120].

Over the last decades, the complexity of systems such as smart grids [89], chemical plants [99], traffic systems [95], water supply networks [103] is continuously increasing due to economic concerns and technological advances. The control problem for such large-scale systems could be trivially solved by resorting to a single (centralized) stabilizing MPC. However, the centralized solution of the resulting control problem could be hampered by various factors, such as high dimension of the system, computation efficiency, and communication bandwidth. Moreover, centralized controllers are not scalable and difficult to maintain. For these reasons, in the last twenty years, decentralized and distributed MPC algorithms have been developed for large-scale systems, where the centralized optimization prob-

Chapter 1. Introduction

lem is replaced by a number of local ones solved in parallel to achieve global and/or local objectives. When using decentralized and distributed MPC, the values of input, state and output variables can be locally computed over the whole prediction horizon at each sampling time instant and can be broadcast to neighbour systems to obtain performance close to those of the centralized controllers.

An alternative to decentralized and distributed control consists in the use of hierarchical and multilayer control structures based on MPC. This approach is very powerful especially for control of systems with separable fast and slow dynamics, for the coordination of subsystems and when it is required to consider different objectives such as economic incomes and product throughput in the long term and regulation problems in the short term. In many hierarchical structures, centralized MPC is used at the high level at a slow time scale to achieve long-term goals, with the possibility to use a simplified model in the design phase, while decentralized or distributed MPC regulators are designed at the intermediate or low levels at a fast time scale to achieve short-term performance using full order models.

The aim of this Thesis is to design hierarchical and multilayer structures based on MPC for coordination. Specifically, independent systems with joint constraints are first considered, including the possibility to allow for plug-and-play operations. Then the analysis is extended to interconnected systems. Fundamental properties such as feasibility, convergence and robustness of the proposed structures are developed taking advantage of the recent developments of MPC, such as robust tube-based MPC.

This chapter describes the basic ideas on the main techniques used and the scientific motivations of this Thesis. Section 1.1 lists the adopted notation. Section 1.2 introduces the design of centralized stabilizing MPC algorithms for nominal deterministic systems without disturbances and robust tube-based MPC for systems affected by unknown, but bounded additive disturbances. Section 1.3, presents a short scientific review on decentralized and distributed MPC, while in Section 1.4 a literature review on hierarchical structures based on MPC is reported with emphasis on independent systems and interconnected systems. Section 1.5 presents the Thesis structure and its main contributions.

1.1 Notation

Our notation for symbols and technical terms used throughout the Thesis is listed below.

- For a given set of variables $z_i \in \mathbb{R}^{q_i}$, $i = 1, 2, \dots, M$, we define the

1.2. Centralized MPC

vector whose vector-components are z_i in the following compact form:
 $(z_1, z_2, \dots, z_M) = [z_1^T \ z_2^T \ \dots \ z_M^T]^T \in \mathbb{R}^q$, where $q = \sum_{i=1}^M q_i$.

- Given the signal x , the symbol $\vec{x}(k : k + N - 1)$ denotes the sequence $x(k) \dots x(k + N - 1)$, where k is the discrete time index and N is a positive integer.
- We denote by $\|\cdot\|$ the Euclidean norm. The expression $\|x\|_Q^2$ stands for $x^T Q x$.
- We use \mathcal{N} to denote the set of nonnegative integer numbers, \mathcal{N}_+ to denote the set of positive integer numbers, \mathbb{R} to denote the set of real numbers, \mathbb{R}_+ to denote the set of positive real numbers.
- We denote by I_n the identity matrix of order n , by 0 the matrix of proper dimensions with all entries equal to zero and by $\mathbb{1}_{m \times n}$ the $m \times n$ matrix whose entries are all equal to 1.
- Given two sets \mathcal{Z} and \mathcal{W} , their Minkowski sum (dilation) is $\mathcal{Z} \oplus \mathcal{W} = \{z + w | z \in \mathcal{Z}, w \in \mathcal{W}\}$, their Minkowski or Pontryagin difference is $\mathcal{Z} \ominus \mathcal{W} = \{v | v \oplus \mathcal{W} \in \mathcal{Z}\}$. We use $\bigoplus_{i=1}^N \mathcal{Y}_i$ to denote the Minkowski sum of the sets $\{\mathcal{Y}_1, \dots, \mathcal{Y}_N\}$.
- We denote $d(x, \mathcal{Y})$ the distance of a point $x \in \mathbb{R}^n$ from a set $\mathcal{Y} \subseteq \mathbb{R}^n$, which is defined by

$$d(x, \mathcal{Y}) := \inf\{\|x - y\| | y \in \mathcal{Y}\}.$$

- A ball with radius ρ_{ε_i} and centered at \bar{x} in the \mathbb{R}^{dim} space is defined as follow:

$$\mathcal{B}_{\rho_{\varepsilon_i}}(\bar{x}) := \{x \in \mathbb{R}^{dim} : \|x - \bar{x}\| \leq \rho_{\varepsilon_i}\}.$$
- Finally, \otimes denotes the Kronecker matrix product, i.e., $A \otimes B$ is the matrix whose ij -th block entry is $a_{ij}B$, where a_{ij} is the ij -th element of A .

1.2 Centralized MPC

The main features of MPC that make it popular for many industrial applications are:

- the control problem is transformed into an optimization one, with the possibility to handle many degrees of freedom in the performance index, which can represent different and even conflicting goals;

Chapter 1. Introduction

- static or dynamic constraints on input, state and output variables can be included naturally in the control problem formulation;
- it can be extended to multivariable systems and is generally more powerful than classic PID controllers;
- MPC algorithms guaranteeing fundamental properties such as feasibility, stability, and robustness are nowadays available.

For further indepth reading on the topics of MPC, the reader is referred to the textbooks [26, 112, 150] and to the survey papers [64, 120].

In this section we describe the fundamentals of several centralized linear MPC algorithms with the emphasis on MPC for nominal systems and on recent results on robust MPC for systems affected by unknown disturbances.

1.2.1 Nominal MPC

Consider the finite-dimensional, linear, time-invariant, discrete-time model described by

$$\Sigma: \begin{cases} x(k+1) = Ax(k) + Bu(k) \\ y(k) = Cx(k), \end{cases} \quad (1.1)$$

where k is the discrete time index; $x \in \mathcal{X} \subseteq \mathbb{R}^n$, $u \in \mathcal{U} \subseteq \mathbb{R}^m$ and $y \in \mathbb{R}^p$ are the state, input and output variables; \mathcal{U} and \mathcal{X} are convex sets containing the origin; the pair (A, B) is assumed to be stabilizable.

The control goal is usually to steer the control and state variables to zero (regulation problem) or to the pair (x_s, u_s) (tracking problem), where x_s and u_s are the steady-state state and control corresponding to a given constant reference signal y_r . It is assumed here that y_r is compatible with the state and control constraints, i.e., $x_s \in \mathcal{X}$, $u_s \in \mathcal{U}$. The latter tracking problem can be easily transformed into a regulation one by state and input transformation. For this reason, in the following only the regulation problem will be considered.

At each time instant k , given the current value of the state $x(k)$, the follow-

1.2. Centralized MPC

ing finite-horizon optimization problem is typically considered:

$$\begin{aligned} & \min_{\vec{u}(k:k+N-1)} J(x(k), \vec{u}(k:k+N-1)) \\ & \text{subject to:} \\ & \bullet \text{ the dynamics (1.1)} \\ & \bullet x(k+i) \in \mathcal{X}, i = 1, \dots, N-1 \\ & \bullet u(k+i) \in \mathcal{U}, i = 1, \dots, N-1 \\ & \bullet x(k+N) \in \mathcal{X}_f, \end{aligned} \tag{1.2}$$

where

$$J(x(k), \vec{u}(k:k+N-1)) = \sum_{i=0}^{N-1} (\|x(k+i)\|_Q^2 + \|u(k+i)\|_R^2) + \|x(k+N)\|_P^2, \tag{1.3}$$

N is the prediction horizon, $Q \in \mathbb{R}^{n \times n}$, $R \in \mathbb{R}^{m \times m}$ and $P \in \mathbb{R}^{n \times n}$ are positive definite matrices, and $\mathcal{X}_f \subseteq \mathcal{X}$ is a convex terminal set containing the origin. Note that the matrices Q and R are design parameters, while matrix P has to be chosen carefully, usually together with the terminal set \mathcal{X}_f to guarantee the properties of the control algorithm.

The optimization problem (1.2) can be recast as a quadratic programming one (or quadratically constrained quadratic programming one where also quadratic function is included in the constraint), see [166], whose solution is computed with efficient algorithms [148,178]. Denote by $u(k|k), \dots, u(k+N-1|k)$ the optimal control sequence at time instant k . Only the first element of this optimal control sequence $u(k|k)$ is applied at time k , then the values of states and outputs are updated, and the optimization problem (1.2) with cost (1.3) is solved again at the next time instant $k+1$, according to the receding horizon (or moving horizon) principle. Due to the state and input constraints, the control law computed at each time instant k might be implicit.

The properties usually required to MPC algorithms are:

- if the optimization problem is feasible at time instant k , then it is feasible at all the future time instants (*recursive feasibility*);
- the origin is an asymptotically stable equilibrium point of the closed-loop system (*stability*).

In many popular MPC methods, instead of stability the following weaker property is proven:

- the state of the closed-loop system asymptotically converges to the origin (*convergence*).

Chapter 1. Introduction

The above properties can be achieved see [120] by introducing an auxiliary state feedback law $u = Kx$, and by verifying that the optimal cost function J^o is a Lyapunov function of the closed-loop system. A typical choice is to select P as the solution of the Lyapunov equation

$$(A + BK)^T P(A + BK) - P = -(Q + K^T RK) \quad (1.4)$$

where K is the optimal infinite horizon LQ gain $K = (R + B^T P B)^{-1} B^T P A$. The terminal set must be chosen carefully such that $\mathcal{X}_f \subseteq \mathcal{X}$, $K \mathcal{X}_f \subseteq \mathcal{U}$ and $(A + BK) \mathcal{X}_f \subseteq \mathcal{X}_f$. One may take \mathcal{X}_f as the maximal invariant admissible set for system $x(k+1) = (A + BK)x(k)$ or define it as an ellipsoidal invariant set $\mathcal{X}_f = \{x | x^T P x < \alpha\}$, for some suitably chosen positive scalar α .

A sketch of the proof of recursive feasibility and convergence is now provided. Assume that at time instant k the optimal control sequence of the optimization problem (1.2) is found, i.e., $\vec{u}^o(k : k+N-1|k) = (u(k|k), \dots, u(k+N-1|k))$. Associated with this control sequence, the optimal cost function is $J^o(x(k))$ and the state evolution is such that $x(k+N|k) \in \mathcal{X}_f$. In view of the definition of \mathcal{X}_f and of the gain matrix K , the input sequence $\vec{u}^s(k+1 : k+N|k+1) = (u(k+1|k), \dots, u(k+N-1|k), Kx(k+N|k))$ is a feasible choice at the next time instant $k+1$. Associated with this input sequence the value of the suboptimal cost function is $J^s(x(k+1), \vec{u}^s(k : k+N|k+1))$, and the terminal constraint $x(k+N+1|k+1) \in \mathcal{X}_f$ is satisfied as well. Thus, the recursive feasibility follows. It is also possible to write

$$\begin{aligned} & J^s(x(k+1), \vec{u}^s(k+1 : k+N|k+1)) - J^o(x(k)) = \\ & = -(\|x(k)\|_Q^2 + \|u(k|k)\|_R^2) + \|x(k+N|k)\|_Q^2 + \|Kx(k+N|k)\|_R^2 + \\ & \quad \|(A + BK)x(k+N|k)\|_P^2 - \|x(k+N|k)\|_P^2 \\ & = -(\|x(k)\|_Q^2 + \|u(k|k)\|_R^2) + \|x(k+N|k)\|_{Q+K^T RK+(A+BK)^T P(A+BK)-P}^2 \end{aligned} \quad (1.5)$$

In view of (1.4) and from (1.5), one has

$$J^s(x(k+1), \vec{u}^s(k+1 : k+N|k+1)) - J^o(x(k)) = -(\|x(k)\|_Q^2 + \|u(k|k)\|_R^2)$$

Recalling that $J^o(x(k+1|k)) \leq J^s(x(k+1), \vec{u}^s(k+1 : k+N|k+1))$, then

$$J^o(x(k+1|k)) - J^o(x(k)) \leq -(\|x(k)\|_Q^2 + \|u(k|k)\|_R^2) \quad (1.6)$$

(1.6) implies that $J^o(x(k+1|k)) - J^o(x(k))$ converges to zero. Furthermore, from (1.6), $J^o(x(k)) - J^o(x(k+1|k)) \geq \|x(k)\|_Q^2 + \|u(k|k)\|_R^2$, then

1.2. Centralized MPC

$\|x(k)\|_Q^2 + \|u(k|k)\|_R^2 \rightarrow 0$ as well. Recalling the definition of Q and R , the convergence of the state and input variables follows.

1.2.2 Robust tube-based MPC

The MPC formulation reported in Section 1.2.1 assumes that the nominal model (1.1) used for prediction is exactly the same as the real plant. However, due to the presence of additive unknown disturbances acting on the system being controlled, the standard MPC setup may lead to issues of stability and constraint satisfaction even when the disturbance is arbitrarily small, see [68]. This has motivated the development of a robust MPC theory, within which three main approaches have been proposed: the first one is based on min-max formulations of MPC optimization problems where a worst-case cost is minimized, see [15, 16, 94, 102, 142, 165] and the reference therein. The second approach is based on input-to-state stability for robust MPC with tightened state constraints, see [115, 116]; while the last one is the so-called “tube-based” approach, relying on the concept of tubes with tightened constraints used for predicted input and state variables over the prediction horizon, see [32, 60, 98, 119, 121]. In tube-based MPC, an online standard MPC problem is solved at any time instant with tightened constraints on the nominal model to generate the trajectory of the nominal state, i.e., the center of a tube, while an auxiliary feedback policy is introduced to steer the trajectory of the uncertain system to the nominal one. The online-computational load of the resultant controller is comparable to that of nominal MPC. The implementation of tube-based MPC relies on set theory, see [21, 22] and on recently developed computation approaches for robust positive invariant (RPI) sets, see [144–147].

Since the tube-based approach will be extensively used in the following chapters, its main ideas for linear discrete-time LTI systems are now introduced based on the theory described in [121, 150].

Consider the finite-dimensional, linear, time-invariant, discrete-time perturbed model described by

$$x(k+1) = Ax(k) + Bu(k) + w(k) \quad (1.7)$$

where $x \in \mathcal{X} \subseteq \mathbb{R}^n$, $u \in \mathcal{U} \subseteq \mathbb{R}^m$ and $w \in \mathcal{W} \subseteq \mathbb{R}^n$; \mathcal{U} and \mathcal{X} are polytopic sets containing the origin in its interior, and \mathcal{W} is a compact set.

The nominal system for (1.7) is referred as

$$\hat{x}(k+1) = A\hat{x}(k) + B\hat{u}(k) \quad (1.8)$$

Select a control gain K such that $F = A + BK$ is Schur stable and define the

Chapter 1. Introduction

control law for the real system (1.7) as

$$u(k) = \hat{u}(k) + K(x(k) - \hat{x}(k)) \quad (1.9)$$

where $\hat{u}(k)$ is the solution of a standard MPC optimization problem for the nominal model (1.8).

Define by $e = x - \hat{x}$ the deviation of the real state from the nominal one, then the difference autonomous system derived from the subtraction of (1.7) and (1.8) with (1.9) is

$$e(k+1) = Fe(k) + w(k) \quad (1.10)$$

Denote by \mathcal{L} a minimal (if possible) RPI set satisfying $F\mathcal{L} \oplus \mathcal{W} \subseteq \mathcal{L}$ for the autonomous system (1.10). If the current state $x(k) - \hat{x}(k) \in \mathcal{L}$, then it holds that $x(k+i) - \hat{x}(k+i) \in \mathcal{L}$ for all $i > 0$.

Therefore, the main idea of tube-based MPC can be summarized as follows: the first term $\hat{u}(k)$ in (1.9) is computed by solving a nominal MPC optimization problem with the goal to generate the center trajectory of the tube, where tightened constraints are enforced on the state and input of the nominal model (1.8) by using a priori knowledge of the RPI set \mathcal{L} for the satisfaction of real constraints; while the auxiliary feedback term $K(x(k) - \hat{x}(k))$ is introduced to steer the trajectories of the uncertain system (1.7) to the nominal ones.

Accordingly, the optimization problem to be solved at each time instant k is given by

$$\begin{aligned} & \min_{\hat{x}(k), \vec{\hat{u}}(k:k+N-1)} J(\hat{x}(k), \vec{\hat{u}}(k:k+N-1)) \\ & \text{subject to:} \\ & \bullet \text{ the dynamics (1.8)} \\ & \bullet x(k) - \hat{x}(k) \in \mathcal{L} \\ & \bullet \hat{x}(k+i) \in \hat{\mathcal{X}}, i = 1, \dots, N-1 \\ & \bullet \hat{u}(k+i) \in \hat{\mathcal{U}}, i = 1, \dots, N-1 \\ & \bullet \hat{x}(k+N) \in \hat{\mathcal{X}}_f, \end{aligned} \quad (1.11)$$

where

$$J(x(k), \vec{\hat{u}}(k:k+N-1)) = \sum_{i=0}^{N-1} (\|\hat{x}(k+i)\|_Q^2 + \|\hat{u}(k+i)\|_R^2) + \|\hat{x}(k+N)\|_P^2, \quad (1.12)$$

N is the prediction horizon, $\hat{\mathcal{X}} = \mathcal{X} \ominus \mathcal{L}$, $\hat{\mathcal{U}} = \mathcal{U} \ominus K\mathcal{L}$ and $\hat{\mathcal{X}}_f$ is a positively invariant set for the nominal system (1.8) with the auxiliary control law $\hat{u}(k) = K\hat{x}(k)$ such that $\hat{\mathcal{X}}_f \subseteq \hat{\mathcal{X}}$, $K\hat{\mathcal{X}}_f \subseteq \hat{\mathcal{U}}$ and $F\hat{\mathcal{X}}_f \subseteq \hat{\mathcal{X}}_f$.

1.3. Decentralized and distributed MPC

Q , R , and P are positive definite matrices. The control gain K can be selected arbitrarily as long as F is stable, also in this case a simple choice is to consider the optimal gain computed according to the infinite horizon LQ criterion. The matrix P can be computed as the solution of the following Lyapunov function

$$F^T P F - P = -(Q + K^T R K)$$

Let $\vec{u}(k : k + N - 1 | k) = (\hat{u}(k | k), \dots, \hat{u}(k + N - 1 | k))$ be the optimal solution of the optimization problem (1.11), then the control action of the real system (1.7) at time k is given by

$$u(k) = \hat{u}(k | k) + K(x(k) - \hat{x}(k | k))$$

If the initial condition satisfies $x(k) - \hat{x}(k) \in \mathcal{Z}$ and all the parameters are properly selected, a feasible solution of the optimization problem (1.11) can be found. The proof of recursive feasibility is similar to that of standard MPC, to this regard note that the initial condition of the nominal system is an optimization parameter at any time instant. The recursive feasibility also implies that the real input and state constraints are fulfilled at any time instant, i.e., $x \in \mathcal{X}$ and $u \in \mathcal{U}$.

As for the convergence proof, let $\hat{x}(k + 1) = \hat{x}(k + 1 | k)$, then $\vec{u}^s(k + 1 : k + N | k + 1) = (\hat{u}(k + 1 | k), \dots, \hat{u}(k + N - 1 | k), K\hat{x}(k + N | k))$ is a feasible choice at time instant $k + 1$ associated with the suboptimal cost $J^s(\hat{x}(k + 1 | k), \hat{u}^s(k + 1 : k + N | k + 1))$. It holds that

$$J^o(x(k + 1)) \leq J^s(\hat{x}(k + 1 | k), \hat{u}^s(k + 1 : k + N | k + 1)) \quad (1.13)$$

where $J^o(\cdot)$ is the optimal cost. Then, according to arguments similar to the ones introduced for nominal MPC, it is easy to show that

$$J^o(x(k + 1)) - J^o(x(k)) \leq -(\|\hat{x}(k | k)\|_Q^2 + \|\hat{u}(k | k)\|_R^2)$$

The monotonic property of the optimal cost function implies that the nominal inputs and states exponentially converge to zero. Recall that the real state always remains inside the tube whose center are the nominal state trajectories, i.e., $x \in \hat{x} \oplus \mathcal{Z}$, then the robustness and convergence properties of the uncertain system (1.7) can be guaranteed, that is

$$\lim_{k \rightarrow \infty} d(x(k), \mathcal{Z}) \rightarrow 0.$$

1.3 Decentralized and distributed MPC

Many efforts have been devoted in recent years to develop decentralized and distributed MPC algorithms for large-scale interconnected systems. The

Chapter 1. Introduction

literature is very wide, see e.g. [113], so that in this section reference will be only made to the main contributions and ideas in this field.

1.3.1 Decentralized MPC

In decentralized MPC structures, the large-scale system is usually decomposed into non-overlapping subsystems, interacting due to direct input couplings or indirect effects of internal states. Each subsystem is controlled by an independent MPC regulator, see [14, 169], with no information exchange between the local controllers. In the design phase, the input and/or state couplings are neglected, which makes the design of the local MPC regulators trivial; however fundamental properties, like stability and convergence, can usually be guaranteed when the interactions are weak, while strong interactions can lead to issues of stability and poor performances. In addition, some systems cannot be stabilized by a decentralized control structure due to the presence of unstable fixed modes, see [41, 185].

Since many large-scale systems can be decomposed into subsystems with very small interconnections, see [31, 67, 71, 74, 159, 170, 187], decentralized MPC can be very useful. However, in spite of the importance of decentralized MPC, very few algorithms with guaranteed properties can be found in the literature. This is due to the fact that the stability analysis relying on the idea to use the optimal cost used as a Lyapunov function, typical of centralized MPC, is difficult to extend to decentralized MPC problems. A stabilizing decentralized state-feedback MPC controller for nonlinear discrete-time systems with bounded decaying disturbances has been reported in [114], where a contractive terminal state constraint is included in the formulation of the decentralized MPC problems. The closed-loop stability is obtained despite the influences of couplings between the subsystems and the presence of external disturbances. In [143], decentralized regulators with both open-loop and closed-loop formulations have been developed by resorting to robust min-max MPC: the interconnections are considered as perturbations to be rejected and the concept of Input-to-State Stability is used to guarantee the stability properties. A decentralized MPC of dynamically coupled linear systems with input constraint has been described in [5], where the large-scale system is decomposed into overlapping sub-models for local predictions. The asymptotic stability with respect to input constrained open-loop stable systems and to unconstrained open-loop unstable systems are obtained and extended to the cases of tracking reachable output set-points and constant disturbances. Plug-and-play decentralized MPC problems have been studied in [153, 154], where the sta-

1.3. Decentralized and distributed MPC

bility is guaranteed by resorting to robust tube-based MPC algorithms and maintained when the addition and removal of new units are considered.

1.3.2 Distributed MPC

Unlike decentralized MPC structures, in the context of distributed MPC information is transmitted among local controllers. The information exchange usually consists in predicted input and state variables computed over the prediction horizon. Hence, each local MPC regulator can estimate the interconnection effects and/or the models of other agents.

As presented in the survey paper [161], several classifications can be considered. A first classification can be based on the adopted protocols for information exchanges: in non-iterative algorithms, information is transmitted (and received) by the local controllers once at each sampling interval; on the contrary, in iterative algorithms, information can be transmitted (and received) by the local controllers many times at each sampling time interval. Iterative distributed MPC algorithms need a larger amount of information within each sampling time interval which may be helpful for large-scale networked systems to reach a global consensus. However, consensus does not imply optimality, which leads to another possible classification: in non-cooperative algorithms, each local controller has its own local objective function, while in cooperative algorithms, all the regulators share a global performance index. As discussed in [184], and according to classical results of game theory, iterative non-cooperative algorithms admit a Nash equilibrium, while iterative cooperative algorithms can reach the Pareto optimal solution. Another classification can be made relying on the topology of the information transmission network: in fully connected algorithms information is transmitted (and received) from any regulator to the other agents, while in partially connected algorithms only information exchanges among neighboring subsets are allowed. A partially connected algorithm may be used for large-scale systems that are made by loosely connected subsystems, where information exchanges are limited for the reduction of communication burden without deteriorating performance.

Several distributed algorithms based on MPC have been developed in the literature. A non-cooperative and noniterative solution has been proposed for discrete-time linear systems in [27], where a contractive constraint is included and stability can be proved a-posteriori with an analysis of the resulting closed-loop dynamics. A non-cooperative, iterative and fully connected algorithm has been developed in [44, 104] for discrete-time unconstrained input-output models with Nash equilibrium achieved, while a cooperative

Chapter 1. Introduction

and iterative approach has been studied in [184] for discrete-time linear systems, where the Pareto optimal solution is obtained when the iterative procedure converges, and feasibility, as well as stability can be guaranteed even when the information exchange is stopped at any intermediate iteration. This approach has been extended to output feedback systems with verified properties, see [173] and to nonlinear systems resulting in a non-convex problem without guaranteed convergence of the closed-loop system, see [174]. A non-cooperative, noniterative and partially connected algorithm has been proposed in [46] and extended in [45] for nonlinear continuous-time systems with stability verified under the assumption that a consistency constraint is included to guarantee the real trajectory does not differ too much from the predicted ones. Another non-cooperative, noniterative and partially connected MPC has been addressed in [58, 59] for linear systems, where each agent only knows the reference trajectories of the state variables of the neighbours, and the convergence property is verified by resorting to robust tube-based MPC. Other approaches designed according to closed-loop robust MPC can be found in [35, 43, 84, 155]. In [193], two cooperative, iterative and partially connected solutions are presented for cascade processes, where communication delays are considered and stability is obtained in the unconstrained case. Lyapunov-based cooperative and iterative algorithms for nonlinear systems have been developed recently, see [106, 107].

A specific class of distributed MPC algorithms has been developed for the coordinated control of independent systems with coupling state and input constraints or with the possibility to consider a global performance index such as the overall output throughput. In [63] a cooperative cost function is used and the stability analysis relies on Input-to-State Stability arguments. Distributed control of decoupled nonlinear discrete-time nonlinear systems with coupling constraints and cost has been considered in [90] and extended in [91]. Each local regulator computes its control actions based on its states and neighbors and the stability is achieved with a zero terminal constraint. In [151], a robust algorithm has been developed for linear independent systems with coupled constraints, in which the reference signals related to the coupled constraints are communicated. The constraint fulfillment is guaranteed by including a constraint tightening approach and the robustness is verified also in presence of bounded disturbances. An extension of this approach resorting to tube-based MPC is described in [182]. A stochastic distributed algorithm has been developed for linear discrete-time independent systems with coupled state and input constraints in [135], where the coupling constraints are reformulated and decoupled as deterministic ones

1.4. Hierarchical structures based on MPC

by means of the Cantelli inequality.

1.4 Hierarchical structures based on MPC

An alternative to decentralized and distributed control schemes consists of considering hierarchical and multilayer structures based on MPC. Hierarchical control structures are useful at least in the following cases:

- Coordination control: local controllers possibly designed with MPC to achieve local goals work at the low level, while a coordinator is placed at the high level with the goal to minimize a global performance index and satisfy coherence constraints, see [127–130]. A negotiation procedure must be activated between the two layers when the coherence constraints are not fulfilled.
- Control systems of hierarchical structures: multilayer schemes are used naturally, where the higher level controller usually works at a slow time scale computing the reference signals to be used at the low level, while the low level controllers solve tracking problems at a fast time scale, see [136, 137, 162, 163].

In the following subsections, a review of some typical applications of hierarchical MPC is reported according to the survey paper [161]. Specifically, the following topics will be considered: plantwide optimization, coordination of independent systems, control of interconnected systems.

1.4.1 Hierarchical MPC for plantwide optimization

A traditional hierarchical structure for the process industry is shown in Fig.1.1. At the upper-layer, Real Time Optimization (RTO) is used to compute the steady-state operating points for the low level controllers according to an economic optimization problem and based on a static model, while a dynamic model is used at the intermediate layer for the supervisory control, possibly designed with MPC. The basic control layer usually includes PID controllers for computation of the control actions of the actuators. In this context, steady-state optimization based on a detailed nonlinear model has to be solved at the upper level, while a linear dynamic model, possibly obtained with identification techniques, is used for the design of the MPC regulator at the intermediate layer. Another approach is taken in [133], where an abstract model is used at the high level for the optimization of the long term performance, while detailed models are used for the design

Chapter 1. Introduction

of local controllers at the low level for computing the control actions of the actuators. Due to the set-point it generates, RTO at the upper layer plays a fundamental role in the hierarchical structure. In the design phase of the upper and intermediate layers, the issues to be considered are: (i) the models used for computing the set-points at the upper layer must be updated periodically to account for possible model mismatches and slow disturbances, (ii) the consistency of the upper layer and the intermediate layer should be guaranteed and the set-points computed by the upper-layer should be reachable by the MPC regulator. Time scale separation can be employed naturally when long term goals such as economic indices have to be achieved with a sampling rate of days or hours, while the short-term behavior of the actuators should be considered at a much faster sampling interval of minutes or seconds.

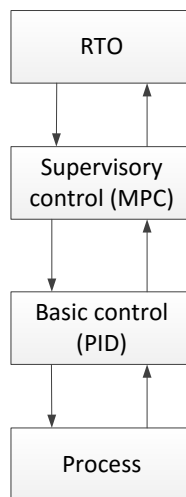


Figure 1.1: *Traditional hierarchical structure for plantwide optimization*

The literature on the hierarchical structure described in Fig.1.1 is rich. The hierarchical algorithms resorting to RTO based on a static nonlinear system can be found in [37, 118, 168, 176, 177]. An integration of nonlinear RTO layer and linear MPC layer has been developed in [100]. Despite this paradigm has been successful in the process industry, the need of dynamic economic process optimization caused by various factors, such as market-driven price variations, requires new solutions for the upper-layer RTO, see [50]. In [52, 77, 87, 189, 191], the extensions of RTO to transient optimization, i.e., dynamic RTO, a form of economic MPC, has been studied with dynamic models introduced at the upper layer. Similar

1.4. Hierarchical structures based on MPC

to classic RTO, the upper-layer economic MPC computes the references for the lower-layer MPC at a slower rate for the reduction of computational requirements. Although many results on hierarchical structures regarding plantwide optimization have been presented, only limited work, see [52, 189], has been devoted to the analysis of closed-loop properties, such as stability and robustness. Future work in this area must be made to develop new algorithms with verified closed-loop properties, in particular by resorting to recent theoretical results in economic MPC, see [8, 42, 69, 75, 82, 149] and the survey papers [50, 180].

1.4.2 Coordination of independent systems

Hierarchical MPC algorithms have been developed for the solution of control problems with multiple and conflicting goals. A hierarchical structure for multi-robot navigation has been discussed in [81], where a centralized MPC works at the high level while a decentralized controller is designed for each robot at the low level. Reachable sets are employed to decouple the formation problem, and properties of feasibility and stability are guaranteed. In [57], a hierarchical algorithm based on distributed MPC has been studied for the coordination of unicycle autonomous robots. The high-level optimizer computes the reference signals for the low-level controllers with the possibility to consider various objectives such as formation control or obstacle collision avoidance. At the low level, a robust MPC is designed for each robot to track the trajectories and neighbor-to-neighbor communications are allowed among the controllers.

Indeed, the lack of hierarchical algorithms for this class of problems and with closed-loop properties motivates the work of Chapter 2 of this Thesis.

1.4.3 Hierarchical MPC for interconnected systems

The connections of complex networked systems may lead to strong couplings between the control loops, which can be addressed within a plantwide control setting similar to the one described in Section 1.4.1. A hierarchical distributed control structure for interconnected systems with limited communication has been presented in [85] where the high-level regulator works at a slower time scale for distinct clusters of subsystems, while the low-level decentralized controllers operate at a higher rate. In [172], a hierarchical cooperative distributed MPC algorithm has been proposed for interconnected systems grouped by a hierarchy. Communication between neighbors is allowed at every iteration, but information between different groups is exchanged at a reduced frequency. A further development

Chapter 1. Introduction

of [172] has been discussed in [54] with application to automated irrigation channels. Detailed proof of feasibility, convergence and optimality is provided. A hierarchical distributed MPC algorithm is proposed in [109] for heating, ventilation, and air-conditioning (HVAC) systems with the objective to minimize the energy consumption at the high level and to generate the reference signals to be tracked by distributed low-level controllers. Recursive feasibility is guaranteed based on a contraction property of the building’s dynamics.

Many process systems are characterized by multiple time-scale dynamics, in which the main time constant of each subsystem may differ from the others, then the faster subsystems reach their final state quickly while the slower subsystems may have begun their main motion, see examples such as energy integrated networks in [86] and chemical plants in [10]. For interconnected systems with clearly separable fast and slow dynamics, a “fast-slow” composite controller based on singular perturbation theory can be employed, where a regulator acting at a slower rate is designed for the reduced slow dynamics with the aim to compute the “slow” control actions and to generate the fast reference signals, while a “fast” regulator is implemented to compute the “fast” control variables by solving a tracking problem with the approximated fast dynamical model. Many works based on singularly perturbed systems have been studied in the past forty years, see the examples in [92, 96, 158] and the algorithms with stability properties described in [1, 2, 92, 194]. Recently, several efforts have been made to develop MPC algorithms for multi-timescale systems. Among them, a MPC solution for multi-timescale Wind Energy Conversion Systems has been studied in [194]. In [188], a two-layer MPC algorithm has been developed for continuous linear singularly perturbed systems, where the quasi-infinite horizon is used in the design of each MPC controller to guarantee the stability of the closed-loop system. A two time-scale MPC controller has been presented in [132] for input and output models. The stability properties are guaranteed and a case study on models with delays is studied. In [30], a composite “fast-slow” controller based on Lyapunov-based MPC has been proposed for continuous nonlinear singularly perturbed systems. The stability and near optimality are verified under the assumption that the slow and fast dynamics are clearly separable. This approach has been then extended in [51], where the “slow” controller is reformulated with Lyapunov-based economic MPC accounting for process economic optimization on the slow subsystem.

It is worth mentioning that the stability analysis in singular perturbation theory relies on the assumption of clear separation of fast and slow dynam-

1.4. Hierarchical structures based on MPC

ics of the system. Possibly, for large-scale systems, the complexity of fast subsystems resulting from time-scale separation based on singular perturbation theory remains still high and the interconnections between inseparable fast modes might not be negligible, see [138]. For these reasons, the “fast” control layer may be designed according to decentralized and/or distributed structures. Very few works have been addressed on this point and only decentralized standard feedback solutions are described, see [9, 175], for the control of fast dynamics. Further research could rely on decentralized or distributed MPC described in Section 1.3 within the framework of multi-rate hierarchical structures.

1.4.4 Other hierarchical algorithms based on MPC

A three-level hierarchical algorithm has been presented in [17] for balance control of a smart grid electric power system with intelligent consumers where the high-level regulator minimizes energy consumption at a slow time scale with energy balance constraints satisfied; the intermediate-level regulators, each one designed for an aggregator (MPC controller) that is gathered by a certain number of units, track the reference signals computed by the high level at a faster time scale; while at the low level autonomous units are used. The detailed exact constraint aggregation of this approach has been addressed in [181]. An MPC approach has been proposed in [72] with the scope to balance power production and consumption with thermal loads. The aggregator is used at the high level to minimize power consumption of the aggregated thermal loads via an estimated ARMAX model mapping price and temperature set points, where the temperature set points are used as references for each unit at the low level. In [73], a distributed algorithm has been developed based on Douglas-Rachford splitting algorithm for power balancing control of large-scale smart grids with flexible consumers. A global cost function is defined in an aggregator while a decomposition method is introduced to decompose the problem into smaller subproblems. The total power consumption is controlled through a negotiation procedure between all units and the aggregator that coordinates the overall objective. In [190], a coordination based distributed approach has been proposed for residential energy systems (RES) where each RES consists of a generation, a battery and residential loads. Each distributed MPC penalizes the energy profile for the local RES respectively, meanwhile, each RES can communicate with a centralized entity, where an iterative negotiation is proposed to update prices. A cascade hierarchical MPC approach has been discussed in [89] for energy management of smart grids. The

Chapter 1. Introduction

outer-loop MPC follows reference trajectories of conventional power stations and vehicle fleets at the slow time scale with the prediction of one day ahead, while the inner-loop MPC tracks the reference trajectories generated by the outer-loop regulator at the fast time scale. An aggregator is utilized to provide profiles based on the current mobility and statistical mobility behavior to the hierarchical MPC controller. In [139], a multi-layer decentralized MPC approach has been presented for drinking water networks where high-level centralized MPC optimizes a global economic cost function at daily time scale, while intermediate-level decentralized MPC controllers solve local economic costs using partition-based network models at hourly time scale, finally the low-level PID controllers, each one designed for a reservoir, track the reference signals computed by the upper layer. In [186], a scalable hierarchical power consumption control of an entire modern data center made by independent servers has been considered. The high-level and the intermediate-level regulators manage the total power consumption of the entire data center and of each power distribution unit at the slow time scale, while the low-level regulator manages the power consumption of each rack by manipulating the CPU frequency of the processors of each server at the fast time scale. A hierarchical scheduling and control strategy for thermal energy storage systems (TESS) is addressed in [179], where centralized economic MPC is utilized at the high level for energy consumption management of TESS in a slow time scale while a faster MPC regulator is applied at the low level with a shorter horizon for managing passive TESS. In [47], a hierarchical control architecture has been presented for dynamic real-time optimization and control of a wastewater treatment process with external disturbance, where a mixed-integer dynamic optimization problem is solved at the high level to compute reference signal for the low-level linear MPC while a PID controller is applied at the base level. A two-layer hierarchical MPC for dynamic real-time optimization has been developed in [191] where an economic objective is optimized at a slow time scale dealing with slow uncertainties while a faster neighboring-external controller is applied for reference tracking with fast disturbances. An extension to a class of hybrid systems with the same hybrid nonlinear models, the same constraints and the same economic indices of the two levels has been presented in [189] to overcome inconsistencies. In [34], a two-layer stochastic MPC algorithm has been discussed for the energy management of a microgrid where the high-level mixed-integer optimizer works at the low frequency to compute operating condition as well as economic indices while the low-level stochastic regulator acts at the fast time scale to compensate disturbances and to guarantee probabilistic constraints sat-

1.5. Structure of the Thesis and list of publications

isfaction. Another multi-layer MPC scheme has been addressed in [33] for energy management of microgrids. Dispatchable units with similar characteristics are gathered as cluster models to be used at the high level for optimizing energy exchanges with the main network. At the intermediate level, each regulator allocates the energy requested to the units of the corresponding cluster and computes the reference signal for the lowest-level PID controller of each unit. A hierarchical multi-rate control approach has been addressed in [12] for linear systems with input and output constraints, where a linear regulator is designed at a fast rate at the low level without considering the constraints, while the high-level regulator works at a lower frequency and defines the reference signal for the low-level controller by means of a maximum admissible output set. Quantitative results for choosing the ratio of the sampling period between the high and the low levels are provided to guarantee closed-loop stability and constraints satisfaction.

1.5 Structure of the Thesis and list of publications

The Thesis is organized as follows:

Chapter 2 In this chapter we develop a hierarchical control structure for the coordination of independent linear dynamic systems with input and joint output constraints. At the higher layer, a “long” sampling time compatible with the prediction horizon required for economic optimization is adopted and reduced order dynamic models of the system’s components are used to state and solve an economic MPC algorithm guaranteeing feasibility and convergence. The outcomes of this layer are the components of the control variables to be held constant over the long sampling periods. At the lower layer, decentralized MPC controllers, one for each subsystem, are implemented in the “short” time scale and according to a shrinking horizon strategy to compensate for the model inaccuracies at the high level and to guarantee that the state computed at the high level is recovered with endpoint state constraints. In doing so, the overall convergence, recursive feasibility, as well as the fulfillment of the joint constraints are obtained. In order to derive the main results, a novel model reduction procedure is proposed. Simulation results in terms of power coordination of two generators are illustrated.

Chapter 2 is based on the following paper.

- B. Picasso, X. Zhang, and R. Scattolini. Hierarchical Model Predictive Control of independent systems with joint constraints. *Automatica*, 74: 99-106, 2016.

Chapter 1. Introduction

Chapter 3 In this chapter we extend the control scheme described in Chapter 2 to the case where plug-and-play operations are allowed, so fully scalable MPC algorithm (with the number of the subsystems) at the high level is expected. In particular, a fully scalable hierarchical control scheme for coordination of similar independent systems with joint output and input constraints is presented. At the higher layer, a low-dimensional model mapping the common input to the collective output is used to define and solve a centralized offset-free MPC algorithm in the long term so as to fulfill the global output request. Different from the algorithm described in Chapter 2, the outcome of this layer is the value of the common input to be held constant and to be distributed among the subsystems based on a specific weight of each subsystem. At the lower layer, for any subsystem a fast MPC controller is designed to remove the effects of the model mismatch introduced at the higher layer, to satisfy local constraints and to optimize the individual performance. The proposed design method allows to modify the system configuration with time varying weights, in terms of the contribution provided by any subsystem to the overall system performance, and to implement plug-and-play operations. The recursive feasibility of the MPC problems to be solved at the high and low levels is guaranteed also during plug-in and plug-out operations, and the overall convergence of the system output to the set-point is proven. Simulation results regarding coordination of a number of Diesel generators with plug-and-play operations are reported.

Chapter 3 is based on the following paper.

- M. Farina, X. Zhang, and R. Scattolini. A hierarchical MPC scheme for coordination of independent systems with shared resources and plug-and-play capabilities. *IEEE Transactions on Control System Technology*, Submitted.

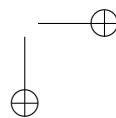
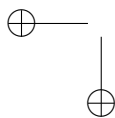
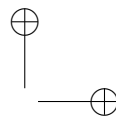
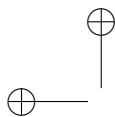
Chapter 4 This chapter presents a hierarchical control scheme for interconnected linear systems with input constraints. At the higher layer of the control structure a robust tube-based centralized MPC algorithm based on a reduced order dynamic model of the overall system optimizes a long term performance index penalizing the deviation of the state and the control input from their nominal values to compensate for additive disturbances caused by neglected dynamics and by low-level control actions, and to compute the control signals which must be held constant over the long time scale. At the lower layer local MPC regulators, possibly working at different rates, solve finite-horizon optimization problems for the full order models of the subsystems and refine the control action computed at the higher

1.5. Structure of the Thesis and list of publications

layer to guarantee feasibility and robustness of the overall control structure. Simulation results in terms of temperature regulation of two apartments and tracking control of a multi-rate chemical plant are presented to describe the implementation aspects and the potentialities of the proposed approach. Chapter 4 is based on the following publications.

- M. Farina, X. Zhang, and R. Scattolini. A hierarchical multi-rate MPC scheme for interconnected systems. *Automatica*, 90: 38-46, 2018.
- M. Farina, X. Zhang, and R. Scattolini. A hierarchical MPC scheme for interconnected systems. In 20th IFAC World Congress, 2017.
- M. Farina, X. Zhang, and R. Scattolini. A hierarchical multirate MPC scheme for interconnected systems-*extended version* [Online]. arXiv preprint arXiv:1705.08818, 2017.

Chapter 5 This chapter summarizes the main contributions of the Thesis and proposes some hints for future research on hierarchical MPC. \square



CHAPTER 2

Hierarchical MPC of independent systems with joint constraints

2.1 Introduction

Hierarchical control structures made by regulators working at different time scales are widely used in the process industry to cope with many significant problems, see the survey paper [161] and the review in Chapter 1. For instance, in the case of singularly perturbed systems, i.e. systems characterized by separable slow and fast dynamics, low level “fast” feedback controllers are designed to stabilize the fast dynamics, while at the higher level of the control structure a regulator working at lower frequency is in charge of stabilizing the slow dynamics and satisfy performance requirement, see e.g. [24, 78] for a couple of industrial examples. An in-depth theoretical analysis of multilayer structures for singularly perturbed systems made by MPC has been recently reported in [28, 29].

In a different setting, two-layer architectures are used for economic optimization. Typically RTO is placed at the higher layer of the control structure with the goal of periodically computing the optimal working conditions by maximizing profits and/or minimizing costs with respect to a static

Chapter 2. Hierarchical MPC of independent systems with joint constraints

model under the implicit assumption that, in the periods between successive optimizations, the system reaches its steady-state conditions, see e.g. [167]; while at the lower layer, MPC is applied to track the reference signals computed with RTO, with its stabilizing properties guaranteed and with the possibility to deal with state, input, and output constraints see [150]. Many methods in terms of stabilizing economic MPC have been developed recently to merge the two layers by minimizing an economic cost, see e.g. [47, 77, 191]. However, as it has been well recognized in [183], in economic MPC a sufficiently large prediction horizon must often be used to consider the long-term performance of the system, so that the resulting optimization problem can be difficult to solve in real-time.

Furthermore, as it has been pointed out in [189], a single-layer economic MPC that merges the RTO layer and the supervisory MPC layer is undesirable for industry application, and in general, an additional safety layer is needed. An alternative choice is to maintain the hierarchical control structure, but to replace the RTO layer with an economic MPC that works possibly at a slow time scale to reduce computational load and computes the optimal economic conditions for the lower layer. However, only limited work in terms of hierarchical control algorithms with closed-loop stability of the two layers have been developed in this direction, see [48, 49, 189] and the review in Section 1.4.2. Among them, a two-layer integrated framework has been presented in [48, 49] for nonlinear process systems, where the high layer includes an economic MPC regulator computing economically optimal time-varying operating conditions for the lower layer by optimizing an economic cost while at the lower layer, a Lyapunov-based MPC controller is designed to track the economic operating trajectories computed at the high layer. The practical closed-loop stability has been proved under a contractive constraint. In [189], a consistent hierarchical control algorithm has been developed for a class of hybrid systems. At the high layer of the control structure, a hybrid economic MPC problem is formulated at a low sampling rate while a faster hybrid neighboring-extremal controller is adopted at the lower layer based on the same objective function, the same constraint and the same model used at the high-level to avoid performance degradation and infeasibilities.

Indeed, with this setting, a significant problem concerns the design of hierarchical control systems for the coordination and control of independent subsystems which must cooperate to achieve prescribed performance. As a first example, consider the problem of controlling micro-grids made by independent components, such as batteries, gas-turbines, photovoltaic panels, wind generators, and loads. For these systems a high level MPC, work-

2.1. Introduction

ing at a slow timescale, typically fifteen minutes, and relying on simplified models of the system components computes the nominal operating conditions guaranteeing that the overall energy balance of the grid is satisfied and optimized according to an economic performance index. At low level MPC controllers act at higher frequency, typically one minute, and adjust the micro-grid operation to reduce the effect of disturbances or unmodeled dynamics, [134], [34]. Conceptually similar problems arise in many different engineering fields, such as in the control of the temperature in a building when the available thermal power generators must be coordinated according to an economic criterion, see for instance the problem considered in [125], or in industrial applications with many generation units, see for example the problem considered in [117] where two oxygen generators must feed three consumer units.

Motivated by these examples, in this chapter we develop a hierarchical control structure for the coordination of independent linear dynamic systems with input and joint output constraints. At the high layer, a “long” sampling time compatible with the prediction horizon required for economic optimization is adopted and reduced order dynamic models of the system’s components are used to state and solve an economic MPC algorithm guaranteeing feasibility and convergence. The outcomes of this layer are the components of the control variables to be held constant over the long sampling periods. At the lower layer, decentralized MPC controllers, one for each subsystem, are implemented in the “short” time scale and according to a shrinking horizon strategy to compensate for the model inaccuracies at the high level and to guarantee the overall stability, convergence, and the fulfillment of the joint constraints. In order to derive the main results, a novel model reduction procedure is proposed.

The chapter is organized as follows: in Section 2.2 the original models of the subsystems are introduced together with their reduced order representation, and the MPC problems at the high and low levels are formulated. Section 2.3 describes the model reduction procedure, while in Section 2.4 the feasibility and convergence properties of the scheme are proven. An example is described in Section 2.5, while some conclusions are discussed in Section 2.6. For readability, the proofs of the main results are reported in an appendix.

Chapter 2. Hierarchical MPC of independent systems with joint constraints

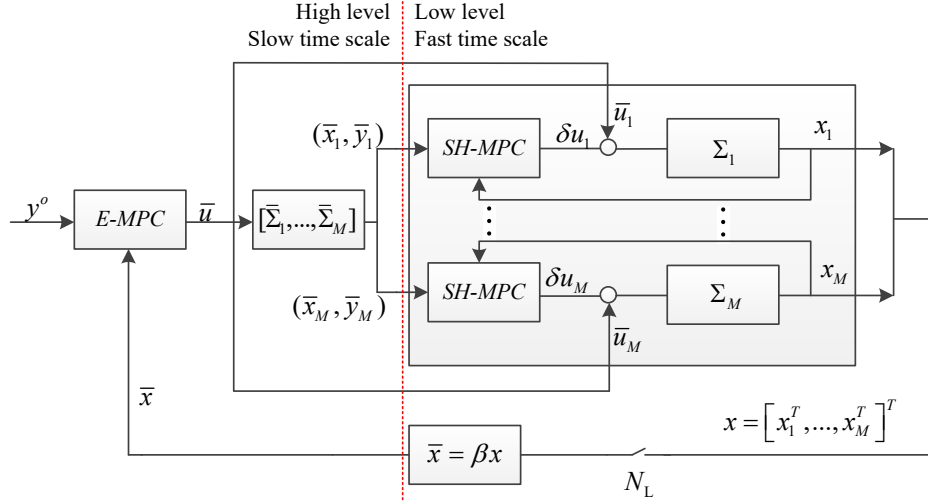


Figure 2.1: Hierarchical control scheme. *E-MPC* = Economic MPC, *SH-MPC* = Shrinking Horizon MPC

2.2 The two-layer control structure

The overall system under control is composed by M independent, discrete-time, linear dynamical systems described by

$$\Sigma_i : \begin{cases} x_i(h+1) = A_L^i x_i(h) + B_L^i u_i(h) \\ y_i(h) = C_L^i x_i(h), \end{cases} \quad i = 1, 2, \dots, M, \quad (2.1)$$

where h is the time index of the base (fast) time scale, $p_i \leq n_i$, $m_i \leq n_i$, $x_i \in \mathbb{R}^{n_i}$, $u_i \in \mathcal{U}_i \subseteq \mathbb{R}^{m_i}$ and $y_i \in \mathbb{R}^{p_i}$. The following assumption holds.

Assumption 2.1.

For any $i = 1, 2, \dots, M$:

- (1) the state x_i is measurable;
- (2) A_L^i is Schur stable;
- (3) the pair (A_L^i, B_L^i) is reachable;

2.2. The two-layer control structure

(4) B_L^i is full column rank and C_L^i is full row rank.

Assumption 2.1.(1) is introduced for simplicity, otherwise an observer would be required, while Assumption 2.1.(2-3) are quite standard requirements for the development of basic properties of both layers of the control structure. As for Assumption 2.1.(4), it simply states that the ranks of B_L^i and C_L^i are equal to the number of the column m_i and of the row p_i respectively, which are in general smaller than the order n_i . In turn, this means that there is no linear dependence among the subsystems’ inputs and outputs. Note that this assumption is not restrictive in practice, since starting from B_L^i and/or C_L^i not fulfilling it, we can always compute new matrices B_L^i and/or C_L^i with this property, and such that the corresponding inputs and/or outputs are linear combinations of the original ones.

For the overall system $\Sigma = (\Sigma_1, \dots, \Sigma_M)$ the goal is to design a controller such that, letting $y = (y_1 \cdots y_M) \in \mathbb{R}^p$ be the collective output, for a given $N_L \in \mathcal{N}$, $N_L > 1$, and for a given reference signal $y^o(k) \in \mathbb{R}^{\bar{p}}$ (where $\bar{p} \leq p$, $k \in \mathcal{N}$ being the time index of the slow time scale), the following joint output constraint is satisfied

$$\forall k \geq 1, \quad \mu(y(kN_L), y^o(k)) \geq 0, \quad (2.2)$$

for some specified function μ . For instance, with $\mu(z_1, z_2) = \varepsilon - \|z_1 - z_2\|$, condition (2.2) amounts to requiring that $\forall k \geq 1, \|y(kN_L) - y^o(k)\| \leq \varepsilon$.

The stated control problem can be trivially solved by considering the overall system Σ as a whole and by resorting to well known (stabilizing) MPC for systems subject to constraints. However, in this way, the centralized solution of the resulting problem could be hampered by various factors, such as the high dimension of Σ and/or the need to consider its long-term behavior, with the consequent need to use long prediction horizons, see [49]. For this reason, the two-layer control scheme described in the following and depicted in Figure 2.1 is proposed. The hierarchical structure is such that:

- at the high layer an MPC controller, running at a slow time scale, i.e. every N_L time steps of the fast time scale, is designed for an overall low-order centralized model made by the ensemble of reduced order models of the Σ_i 's. This controller must guarantee some fundamental properties, such as convergence in the long time scale and the fulfillment of the joint constraint (2.2), and can be designed according to economic criteria, see for example [7], [42], [69].
- at the lower layer a set of M decentralized MPC controllers, each one designed for the full model (2.1) of the corresponding subsystem Σ_i ,

Chapter 2. Hierarchical MPC of independent systems with joint constraints

are implemented in the fast time scale according to a shrinking horizon strategy. The low-level controllers are in charge of adjusting the nominal input computed by the high-level controller so as to compensate for unmodelled dynamics and to guarantee stability and performance.

Remark 2.1.

A similar solution for integrating economic optimization and MPC by means of a hierarchical control scheme has been proposed in [49]. However, in our approach the higher layer directly computes the nominal control action to be held constant over the long sampling time, and the lower layer can correct it at a higher frequency to compensate for model inaccuracy. On the contrary, in [49] the higher layer computes the reference signals for the systems (2.1) locally controlled at the lower layer. As an additional difference, in our scheme the higher layer relies on simplified models of the systems, so reducing the size of the control problem to be solved, while in [49] the full models (2.1) are used.

Remark 2.2.

When the reference signal y^o is constant and the problem is feasible at the initial time instant $h = 0$, the recursive feasibility at the high layer is guaranteed by the properties of the selected economic MPC algorithm, while at the lower layer it is proven in the following Section 2.4.1. In other cases, if at $h = 0$ the problem at the high layer is infeasible due to the control constraints and to the joint output constraint (2.2), or the reference signal is time varying, a typical solution is to transform (2.2) into soft constraints by introducing slack variables, see for instance [112]; this solution is the one adopted in the following Section 2.5. Another possible solution consists in considering also $y^o(k)$ as an optimization variable and computing it as the feasible signal nearest to the ideal one, according to an approach already used in [105] and [19].

Remark 2.3.

The constraints (2.2) have been formulated in the slow time scale; this is coherent with many practical problems. For instance, in the motivating example discussed in the Introduction 2.1 concerning the control of microgrids, what really matters is to constrain the energy and power management of each generation and storage unit over the long sampling interval of fifteen minutes. The main contribution of the low level regulator is to reduce, in the short sampling time, the production and storage discrepancies with respect to the strategy planned at the high level due to high frequency disturbances. Similar considerations can be done for the other motivating examples previously described.

2.2. The two-layer control structure

The resulting hierarchical control scheme requires coherence of the states of the full and reduced models at the sampling times of the slow time scale, so that the centralized MPC algorithm running at the slow time scale can be feeded by a proper linear combination of the sampled states of the subsystems Σ_i , see again Figure 2.1. Therefore, in order to avoid inconsistencies between both layers of the control structure, proper low-dimensional descriptions of the full-order models with rather smaller sets of variables must be selected establishing a linear connection between the states of the reduced models and the states of the original models (2.1) with the main properties such as convergence preserved.

2.2.1 Reduced order models

For each subsystem Σ_i , $i = 1, \dots, M$, consider the following reduced order model:

$$\bar{\Sigma}_i : \begin{cases} \bar{x}_i(h+1) = A_H^i \bar{x}_i(h) + B_H^i \bar{u}_i(h) \\ \bar{y}_i(h) = C_H^i \bar{x}_i(h), \end{cases} \quad (2.3)$$

where $\bar{x}_i \in \mathbb{R}^{\bar{n}_i}$, $p_i \leq \bar{n}_i < n_i$, $m_i \leq \bar{n}_i$, $\bar{u}_i \in \mathcal{U}_i \subseteq \mathbb{R}^{m_i}$ and $\bar{y}_i \in \mathbb{R}^{p_i}$. Each reduced model is endowed with a projection (matrix) $\beta_i : \mathbb{R}^{n_i} \rightarrow \mathbb{R}^{\bar{n}_i}$ that establishes a relation between the state variable of system (2.1) and that of system (2.3). More specifically, letting

$$G_{L_i}^x = (I - A_L^i)^{-1} B_L^i \quad (2.4)$$

$$G_{H_i}^x = (I - A_H^i)^{-1} B_H^i \quad (2.5)$$

the following consistency assumption is considered:

Assumption 2.2.

For any $i = 1, 2, \dots, M$,

(1) A_H^i is Schur stable;

(2) the projection β_i is full rank and such that

$$C_H^i \beta_i = C_L^i. \quad (2.6)$$

(3) the static gain $G_{H_i}^x$ of the reduced order model is full rank and such that

$$\beta_i G_{L_i}^x = G_{H_i}^x \quad (2.7)$$

Chapter 2. Hierarchical MPC of independent systems with joint constraints

Assumption 2.2.(1) trivially requires that the stability properties of the subsystems Σ_i are maintained also in the reduced models $\bar{\Sigma}_i$, while Assumption 2.2.(2) implies that, if at a given time instant h , $\bar{x}_i(h) = \beta_i x_i(h)$, then $\bar{y}_i(h) = y_i(h)$. Finally, Assumption 2.2.(3) requires the equivalence of the static gains from the input to the state, also considering the state transformation due to projection β_i .

Many methods related to model reduction technique has been developed, see, such as, Balanced Truncation in [122], Hankel Norm Approximation in [66], Singular Perturbation Approximation in [93], Krylov subspace projection algorithm in [70, 83], consistent aggregation approach in [133].

However, the selection of reduced order models (2.3) satisfying Assumption 2.2 is not trivial and cannot be accomplished with standard model reduction techniques, see [170]. For this reason, the following Section 2.3 will be devoted to present a novel model reduction method specifically developed for the case at hand.

2.2.2 The MPC problem at the high level

In order to develop the MPC algorithm at the high level running at a slow time scale, consider the systems $\bar{\Sigma}_i^{[N_L]}$ consisting of the sampling of systems $\bar{\Sigma}_i$ with period N under the assumption that, $\forall k \in \mathcal{N}$, \bar{u}_i is held constant over the interval $h \in [kN_L, kN_L + N_L - 1]$. Denoting by $\bar{u}_i^{[N_L]}(k)$ this constant value and by $\bar{x}_i^{[N_L]}, \bar{y}_i^{[N_L]}$ the state and output variables of $\bar{\Sigma}_i^{[N_L]}$, $i = 1, \dots, M$, one has

$$\bar{\Sigma}_i^{[N_L]} : \begin{cases} \bar{x}_i^{[N_L]}(k+1) = A_H^{i[N_L]} \bar{x}_i^{[N_L]}(k) + B_H^{i[N_L]} \bar{u}_i^{[N_L]}(k) \\ \bar{y}_i^{[N_L]}(k) = C_H^i \bar{x}_i^{[N_L]}(k), \end{cases} \quad (2.8)$$

where $A_H^{i[N_L]} = (A_H^i)^{N_L}$, $B_H^{i[N_L]} = \sum_{j=0}^{N_L-1} (A_H^i)^j B_H^i$. Thus, as long as $\bar{u}_i(h) = \bar{u}_i^{[N_L]}(\lfloor h/N_L \rfloor)$, it holds that $\bar{x}_i^{[N_L]}(k) = \bar{x}_i(kN_L)$ and $\bar{y}_i^{[N_L]}(k) = \bar{y}_i(kN_L)$.

Assume now that at time k the reference signal y^o is known for the future $\ell - 1$ long sampling instants, that is $y^o(l)$ is known $\forall l = k, k+1, \dots, k+\ell-1$. Then, for the overall system $\bar{\Sigma}^{[N_L]} = (\bar{\Sigma}_1^{[N_L]}, \dots, \bar{\Sigma}_M^{[N_L]})$ made by the ensemble of the M subsystems (2.8) with $\bar{x}^{[N_L]} = (\bar{x}_1^{[N_L]}, \dots, \bar{x}_M^{[N_L]})$, $\bar{u}^{[N_L]} = (\bar{u}_1^{[N_L]}, \dots, \bar{u}_M^{[N_L]})$, $\bar{y}^{[N_L]} = (\bar{y}_1^{[N_L]}, \dots, \bar{y}_M^{[N_L]})$, an MPC algorithm is used to compute the *nominal* control law $\bar{u}^{[N_L]}(k)$ satisfying the constraint

$$\forall l = 1, \dots, \ell - 1, \quad \mu(\bar{y}^{[N_L]}(k+l), y^o(k+l)) \geq 0 \quad (2.9)$$

2.2. The two-layer control structure

possibly reformulated as discussed in Remark 2.2 to guarantee feasibility. In principle, at this stage, any MPC method can be chosen to satisfy also additional requirements, such as the closed-loop stability and/or the optimization of some economic performance index.

Specifically, we can consider an economic MPC problem based on the contents described in [6]. First a static steady-state optimization problem for the full order models is stated as follows:

$$\begin{aligned}
 & \min_{x,u} l_e(x,u) \\
 & \text{subject to:} \\
 & \bullet \mu(y,y^o) \geq 0 \\
 & \bullet x_i = A_L^i x_i + B_L^i u_i \text{ and } y_i = C_L^i x_i, \forall i = 1 \cdots, M \\
 & \bullet u_i \in \mathcal{U}_i, \forall i = 1 \cdots, M
 \end{aligned} \tag{2.10}$$

where $l_e(\cdot)$ is the economic stage cost, $x = (x_1, \cdots, x_M)$, and $u = (u_1, \cdots, u_M)$. Let the pairs $(x_{i,s}, u_{i,s})$, $i = 1, \cdots, M$, be the solution of optimization problem (2.10) and we assume this solution to be unique throughout this chapter. Correspondingly, we define $\bar{u}_{i,s} = u_{i,s}$ as the steady-state input reference for the reduced-order system $\bar{\Sigma}_i$, then under Assumption 2.2.(3), the corresponding reference steady-state value can be represented as $\bar{x}_{i,s} = \beta_i G_{L_i}^x u_{i,s} = \beta_i x_{i,s}$.

The high layer optimization problem consists of N_H ($N_H < \ell$) slow time steps. Accordingly, at each slow time-step k the following optimization problem can be stated:

$$\begin{aligned}
 & \min_{\overrightarrow{\bar{u}^{[N_L]}(k:k+N_H-1)}} J_e(\overrightarrow{\bar{x}^{[N_L]}(k)}, \overrightarrow{\bar{u}^{[N_L]}(k:k+N_H-1)}) \\
 & \text{subject to:} \\
 & \bullet \text{the dynamics (2.8), } \forall i = 1, \cdots, M \text{ and the constraint (2.9)} \\
 & \bullet \bar{u}_i^{[N_L]}(k+j) \in \mathcal{U}_i, j = 1, \dots, N_L - 1, \forall i = 1, \cdots, M \\
 & \bullet \bar{x}_i^{[N_L]}(k+N_H) = \bar{x}_{i,s}, \forall i = 1, \cdots, M
 \end{aligned} \tag{2.11}$$

where

$$J_e = \sum_{j=0}^{N_H-1} l_e(\bar{x}^{[N_L]}(k+j), \bar{u}^{[N_L]}(k+j)) \tag{2.12}$$

2.2.3 The MPC problem at the lower level

Due to the use of the reduced order models (2.3), (2.8) in the design of the high level MPC algorithm (2.11) with cost (2.12), it is not guaranteed

Chapter 2. Hierarchical MPC of independent systems with joint constraints

that the outputs of the full order systems Σ_i satisfy the constraint (2.2) for $h = kN_L$ when the nominal control law $u_i(h) = \bar{u}_i^{[N_L]}(\lfloor h/N_L \rfloor)$ is applied. The nominal control law is hence amended by a set of decentralized low-level controllers designed for the dynamics of the full order systems Σ_i , $i = 1, \dots, M$, written in the form

$$\Sigma_i : \begin{cases} x_i(h+1) = A_L^i x_i(h) + B_L^i (\bar{u}_i^{[N_L]}(\lfloor h/N_L \rfloor) + \delta u_i(h)) \\ y_i(h) = C_L^i x_i(h), \end{cases} \quad (2.13)$$

where $\delta u_i(h)$ is the new decision variable. To this end, first consider the high-level systems $\bar{\Sigma}_i$, described by (2.3), in the time scale h and let $\bar{y}_i^*(h)$ be their output resulting from the nominal control law $\bar{u}_i(h) = \bar{u}_i^{[N_L]}(\lfloor h/N_L \rfloor)$. This signal is such that

$$\bar{y}_i^*(kN_L + N_L) = \bar{y}_i^{[N_L]}(k+1)$$

and, in view of the high-level control design, it satisfies the desired control goal. Therefore, it is reasonable to take $\bar{y}_i^*(h)$ as the reference for the i -th low-level controller. Accordingly, at time $h = kN_L + t$, shrinking-horizon MPC algorithms based on the following $i = 1, \dots, M$ optimization problems are considered:

$$J_L^i = \min_{\overrightarrow{\delta u_i(t:N_L-1)}} J_L^i(x_i(h)) + \sum_{j=0}^{N_L-t-1} \|y_i(h+j|h) - \bar{y}_i^*(h+j)\|_{Q_i}^2 + \|\delta u_i(h+j|h)\|_{R_i}^2 \quad (2.14)$$

where

$$\overrightarrow{\delta u_i(t:N_L-1)} = [\delta u_i(h|h) \cdots \delta u_i(h+N_L-t-1|h)] \in (\mathbb{R}^{m_i})^{N_L-t} \quad (2.15)$$

and subject to the dynamics (2.13) and

$$\beta_i x_i(kN_L + N_L) = \bar{x}_i^{[N_L]}(k+1) \quad (2.16)$$

$$\bar{u}_i^{[N_L]}(\lfloor h/N_L \rfloor) + \delta u_i(h|j) \in \mathcal{U}_i, \quad \forall j = 0, \dots, N_L - t - 1.$$

Notice that, in view of Assumption 2.2, the terminal constraint $\beta_i x_i(kN_L + N_L) = \bar{x}_i^{[N_L]}(k+1)$ ensures that $y_i(kN_L + N_L) = \bar{y}_i^{[N_L]}(k+1)$ so that the control goal is achieved.

Remark 2.4. *The signal $\bar{y}_i^*(h)$, as previously defined, is generated by an open-loop reduced order model and hence may have an undesired transient behavior. In this case, the use of a suitable interpolation of $\bar{y}_i^{[N_L]}(k)$ and $\bar{y}_i^{[N_L]}(k+1)$ to build an ad hoc reference signal $\bar{y}_i^*(h)$ is an advisable choice.*

2.3. Design of the reduced order models

2.3 Design of the reduced order models

In this section a constructive procedure is given for the selection of the reduced order models $\bar{\Sigma}_i$ defined by (2.3) and satisfying the conditions of Assumption 2.2.

Since all the results reported below are independent from the specific subsystem, for the sake of clarity, in the following developments the index $i = 1, \dots, M$ specifying the i -th subsystem will be omitted unless otherwise specified.

The following problem can be stated:

Problem 2.1. *Find β , C_H and G_H^x such that Assumption 2.2 is satisfied.*

Letting

$$\mathcal{L} = \text{Im } G_L^x \cap \text{Ker } C_L$$

the following result holds:

Proposition 2.1. *A solution to Problem 2.1 exists if and only if*

$$\bar{n} \geq p + \dim(\mathcal{L}). \quad (2.17)$$

Corollary 2.1. *A sufficient condition for the existence of a solution to Problem 2.1 is that $m \leq p$ and the low-level system (A_L, B_L, C_L) does not have transmission zeroes in 1.*

2.3.1 Construction of β and C_H

The proof of Proposition 2.1 (see the Appendix at the end of Chapter 2) provides a constructive procedure for the computation of the matrix β . Specifically, the following steps are required:

- a** find a subspace \mathcal{K}_β of dimension $n - \bar{n}$ so that $\mathcal{K}_\beta \subseteq \text{Ker } C_L$ and $\mathcal{L} \cap \mathcal{K}_\beta = \{0\}$;
- b** let $\{\kappa_1, \dots, \kappa_{n-\bar{n}}\}$ be a set of independent vectors in \mathcal{K}_β and complete this set to a basis $\mathcal{B} = \{v_1, \dots, v_{\bar{n}}, \kappa_1, \dots, \kappa_{n-\bar{n}}\}$ of the whole space \mathbb{R}^n ;
- c** let $\{r_1, \dots, r_{\bar{n}}\}$ be a basis of $\mathbb{R}^{\bar{n}}$, define

$$\hat{\beta} = [r_1 | \dots | r_{\bar{n}} | 0 | \dots | 0]$$

and T_L as the matrix whose columns are the vectors in \mathcal{B} , set $\beta = \hat{\beta} T_L^{-1}$;

- d** define $C_H = C_L \beta^\dagger$, where the symbol \dagger denotes the pseudoinverse.

Chapter 2. Hierarchical MPC of independent systems with joint constraints

2.3.2 Model reduction

Once solved Problem 2.1, C_H and G_H^x are available. In order to complete the construction of the reduced order model (A_H, B_H, C_H) , one has to find A_H and B_H so that $G_H^x = (I - A_H)^{-1} B_H$. To this regard, one can proceed as follows: fix a matrix A_H and let

$$B_H = (I - A_H) G_H^x.$$

The only restriction is that the matrix A_H has to be Schur stable. Suitable choices for A_H are those modeling the most relevant dynamics (*e.g.*, the dominant ones) of the low-level system.

Note that the proposed model reduction procedure is to be used independently for each subsystem, so that scalability in terms of the number of subsystems is guaranteed. In addition, since it is based on standard linear algebra, even subsystems with large dimensions can be considered.

2.4 Properties of the two-layer control scheme

In this Section the feasibility and convergence properties of the hierarchical control scheme previously described are analyzed. In order to derive the main results, and besides Assumption 2.2, the following additional hypothesis is required:

Assumption 2.3.

- (1) The sampling period N_L is so that, letting $\mathcal{R}(N_L) = [B_L A_L B_L \cdots A_L^{N_L-1} B_L]$ be the reachability matrix in N_L steps associated to (A_L, B_L) , the matrix

$$\mathcal{H}(N_L) = \beta \mathcal{R}(N_L) \in \mathbb{R}^{\bar{n} \times m N_L}$$

is full-rank.

- (2) $\mathcal{U} = \{u \in \mathbb{R}^m \mid \|u\| \leq \rho_u\}$, for some specified $\rho_u > 0$.

Notice that, in view of Assumption 2.3.(1), β has full rank and the pair (A_L, B_L) is reachable, so that $\text{rank}(\beta) = \bar{n}$, $\text{rank}(\mathcal{R}(N_L)) = n$ for all N_L satisfying $m N_L \geq n$. According to Sylvester’s rank inequality, *i.e.*, $\text{rank}(\beta) + \text{rank}(\mathcal{R}(N_L)) \leq \text{rank}(\beta \mathcal{R}(N_L)) + n$, condition (1) in Assumption 2.3 is attained by taking N_L such that $m N_L \geq n$. Moreover, denoting by $\sigma_{\bar{n}}(N_L)$ the minimal singular value of $\mathcal{H}(N_L)$, this condition is equivalent to

$$\sigma_{\bar{n}}(N_L) > 0.$$

2.4. Properties of the two-layer control scheme

2.4.1 Feasibility

Let us consider the feasibility issue for the $i = 1, \dots, M$ optimization problems (2.14).

First notice that, in view of the adopted shrinking horizon MPC approach, if the problem is feasible at time $t = 0$ (*i.e.*, at the beginning of the sampling interval $[kN_L, kN_L + N_L)$), then feasibility is ensured $\forall t = 1, \dots, N_L - 1$. Thus, without loss of generality, let us consider $h = 0$. Also recall that $\bar{x}^{[N_L]}(k) = \bar{x}(kN_L)$, $\forall k \in \mathcal{N}$.

Suppose that, for $h = 0$, the projection of the low-level state coincides with the high-level state, that is

$$\beta x(0) = \bar{x}(0). \quad (2.18)$$

We are interested in finding conditions on $\bar{u}^{[N_L]}(0)$ (*i.e.*, on the high-level control variable) guaranteeing the existence of a feasible choice for the low-level input signal $\overrightarrow{\delta u}_{(0:N_L-1)} \in \mathbb{R}^{mN_L}$ (see equation (2.15)) so that the terminal constraint in problem (2.14), that is

$$\beta x(N_L) = \bar{x}(N_L), \quad (2.19)$$

is recursively satisfied.

To this end, it is useful to introduce the following notation: let $\hat{y} \in \mathbb{R}^{\bar{n}}$ be an auxiliary output variable for system Σ defined by

$$\hat{y}(h) = \beta x(h) \quad (2.20)$$

and denote by $\hat{G}_L(z) = \beta(zI_n - A_L)^{-1}B_L$ the low-level model transfer function from u to \hat{y} . Let $G_H(z) = (zI_{\bar{n}} - A_H)^{-1}B_H$ be the high-level model transfer function from \bar{u} to \bar{x} and define a constant $\kappa > 0$ such that

$$\|\hat{G}_L - G_H\|_{\infty} \leq \kappa. \quad (2.21)$$

Then we can prove the following result:

Proposition 2.2. *Under Assumption 2.3, let $\mathcal{A}(N_L) = A_H^{N_L}\beta - \beta A_L^{N_L} \in \mathbb{R}^{\bar{n} \times n}$ and assume that $\beta x(0) = \bar{x}(0)$.*

1. *If*

$$\|x(0)\| \leq \frac{\sigma_{\bar{n}}(N_L) \cdot \rho_u}{\|\mathcal{A}(N_L)\|} := \lambda(N_L), \quad (2.22)$$

then there exist $\bar{u}^{[N_L]} \in \mathcal{U}$ and $\overrightarrow{\delta u}_{(0:N_L-1)} \in \mathcal{U}^{N_L}$ so that $u(j) = \bar{u}^{[N_L]} + \delta u(j|0) \in \mathcal{U}$, $\forall j = 0, 1, \dots, N_L - 1$ and the terminal constraint (2.19)

Chapter 2. Hierarchical MPC of independent systems with joint constraints

is attained. Moreover, any $\bar{u}^{[N_L]}$ such that

$$\|\bar{u}^{[N_L]}\| \leq \frac{\|\mathcal{A}(N_L)\|(\lambda(N_L) - \|x(0)\|)}{\sigma_{\bar{n}}(N_L) + \kappa\sqrt{N_L}} \quad (2.23)$$

is a feasible choice.

2. If $\|x(0)\|$ satisfies condition (2.22), $u(j) = \bar{u}^{[N_L]} + \delta u(j|0) \in \mathcal{U}$, $\forall j = 0, 1, \dots, N_L - 1$, N_L is such that $\|A_L^{N_L}\| < 1$ and

$$\chi(N_L) := \frac{\|\mathcal{R}(N_L)\| \cdot \sqrt{N_L} \cdot \|\mathcal{A}(N_L)\|}{\sigma_{\bar{n}}(N_L) \cdot (1 - \|A_L^{N_L}\|)} \leq 1, \quad (2.24)$$

then $\|x(N_L)\| \leq \lambda(N_L)$ and recursive feasibility of the terminal constraint is guaranteed.

3. It holds that

$$\lim_{N_L \rightarrow +\infty} \lambda(N_L) = +\infty, \quad \lim_{N_L \rightarrow +\infty} \|A_L^{N_L}\| = 0, \quad \lim_{N_L \rightarrow +\infty} \chi(N_L) = 0$$

so that, for sufficiently large N_L , both feasibility and recursive feasibility are ensured.

2.4.2 Convergence

Assume that the state, input and output of system (2.8) have reached steady-state conditions, thus

$$\bar{u}^{[N_L]}(k) \equiv \bar{u}_s, \quad \bar{x}^{[N_L]}(k) \equiv \bar{x}_s, \quad \bar{y}^{[N_L]}(k) \equiv \bar{C}_H \bar{x}_s.$$

In view of the terminal constraint $\beta x(kN_L + N_L) = \bar{x}^{[N_L]}(k+1)$ in the low-level optimization problem (2.14), and recalling the definition of \hat{y} given in equation (2.20), the state of the low-level system evolves so that

$$\forall k \in \mathcal{N}, \quad \hat{y}(kN_L) = \bar{x}_s.$$

Moreover, in view of the solution to Problem 2.1, the output \hat{y} corresponding to the equilibrium pair $(\bar{u}_s, x_s = G_{L1}^x \bar{u}_s)$ for the low-level system is $\hat{y} = \beta x_s = \bar{x}_s$. Thus, letting

$$\delta x(k) = x(kN_L) - x_s \quad \text{and} \quad \delta \hat{y}(k) = \hat{y}(kN_L) - \bar{x}_s,$$

as well as $\mathcal{A}_L = A_L^{N_L}$ and $w(k) = \sum_{j=0}^{N_L-1} A_L^{N_L-1-j} B_L \delta u(kN_L + j)$, the dynamics of the low-level system in the time scale k is given by

$$\begin{cases} \delta x(k+1) = \mathcal{A}_L \delta x(k) + w(k) \\ \delta \hat{y}(k) = \beta \delta x(k) \end{cases}$$

2.5. Example

and it holds that

$$\delta\hat{y}(k) \equiv 0.$$

Therefore, letting $\delta\hat{y}_L$ be the free motion of this system, the forced motion component $\delta\hat{y}_F$ of $\delta\hat{y}$ is such that

$$\delta\hat{y}_F(k) = -\delta\hat{y}_L(k) \quad (2.25)$$

and, since \mathcal{A}_L is Schur stable, $\lim_{k \rightarrow +\infty} \delta\hat{y}_F(k) = 0$.

Proposition 2.3. *If $\tilde{G}(z) = \beta(zI_n - \mathcal{A}_L)^{-1}$ has no zeros on the unitary circle $\mathcal{S}^1 = \{z \in \mathbb{C} \mid |z| = 1\}$, then*

$$\lim_{k \rightarrow +\infty} w(k) = 0.$$

Consequently, $\lim_{k \rightarrow +\infty} \delta x(k) = 0$, $\lim_{h \rightarrow +\infty} \delta u(h) = 0$, and $\lim_{h \rightarrow +\infty} x(h) = x_s$.

In conclusion, both the recursive feasibility property and the convergence to the equilibrium computed by the high level controller are established.

2.5 Example

Consider two generators ($M = 2$) that must provide a total electrical power. The first one is the 3.125-MW, 2400-V/60Hz Diesel generator described in [192], its input u_1 is the fuel flow rate, while its output y_1 is the produced power. The poles of its ninth order transfer function are $\{-2191.2 \pm j172.1, -111.1, -83.3, -26, -18.5, -13.1, -1.16, -0.017\}$, the zeros are $\{-2581, -33.1, -12.1, -4, -0.051, 83.3\}$, and the steady-state gain is $K_1 = 1.5$. The second subsystem is the 3.125-MW, 2400-V/60Hz Gas-turbine Generator described in [157]. Also in this case, the input and output variables, u_2 and y_2 , are the fuel flow rate and the produced power. The tenth order transfer function has poles $\{-2191.2 \pm j103, -200, -20, -26, -18.8, -12.5, -5, -1.67, -0.038\}$, zeros $\{-4362, -2151, -21, -11.9, -0.045, 200\}$, and steady-state gain $K_2 = 0.8$. The control variables are limited, i.e. $0 \leq u_1, u_2 \leq 0.9$, and the joint output constraint (2.2) is

$$y_1 + y_2 = y^o \quad (2.26)$$

where y^o is the total required power.

The two systems' continuous-time models have been sampled with $\Delta t = 1s$ to obtain their discrete-time counterpart in the fast time scale. Then, the

Chapter 2. Hierarchical MPC of independent systems with joint constraints

procedure described in Section 2.3 has been used to compute the following discrete-time reduced first order models

$$\bar{\Sigma}_1 : \begin{cases} \bar{x}_1(h+1) = 0.98\bar{x}_1(h) + 0.03\bar{u}_1(h) \\ \bar{y}_1(h) = \bar{x}_1(h), \end{cases} \quad (2.27)$$

$$\bar{\Sigma}_2 : \begin{cases} \bar{x}_2(h+1) = 0.95\bar{x}_2(h) + 0.04\bar{u}_2(h) \\ \bar{y}_2(h) = \bar{x}_2(h), \end{cases} \quad (2.28)$$

as well as the transformation matrices

$$\beta_1 = [0 \ 0 \ 0 \ 0 \ 4.14 \ 0 \ 0 \ 0 \ 0],$$

$$\beta_2 = [0 \ 0 \ 0 \ 0 \ 0 \ 6.31 \ 0 \ 0 \ 0 \ 0].$$

The reduced order models in the slow time scale $\bar{\Sigma}_1^{[N_L]}$ and $\bar{\Sigma}_2^{[N_L]}$ have been obtained with $N_L = 25$. The unitary step responses of the original full order continuous-time models of the generators and of $\bar{\Sigma}_1^{[N_L]}$ and $\bar{\Sigma}_2^{[N_L]}$ are compared in Figure 2.2.

The ninth and tenth order discrete-time models of the generators have been used to compute the optimal steady-state values of the inputs $u_s = [u_{1,s} \ u_{2,s}]^T$ and states $x_s = [x_{1,s} \ x_{2,s}]^T$ by means of the optimization algorithm (2.10) minimizing the stage cost $l(x, u) = u_1 + u_2$ under the constraint (2.26); then the corresponding values of the states of the reduced order models have been obtained as $\bar{x}_{i,s} = \beta_i x_{i,s}$, $i = 1, 2$. The dissipative property of subsystems (2.27) and (2.28) required by the adopted economic MPC algorithm, see [6], has been verified by constructing a quadratic storage function, i.e.,

$$\lambda(\bar{x}) = \frac{1}{2} [\bar{x}_1 \ \bar{x}_2] \begin{bmatrix} -\Pi_1 & 0 \\ 0 & -\Pi_2 \end{bmatrix} [\bar{x}_1 \ \bar{x}_2]^T$$

where Π_1, Π_2 are the solutions of discrete Riccati equations for (2.27) and (2.28) respectively, with penalties $\bar{Q}_1 = \bar{Q}_2 = 1, \bar{R}_1 = \bar{R}_2 = 0.01$. The computed values are i.e. $\Pi_1 = 1.43, \Pi_2 = 1.13$. Economic MPC according to the algorithm (2.11) has been designed at the high level with prediction horizon $N_H = 15$, control horizon equal to two, stage cost $l_e(\bar{x}, \bar{u}) = \bar{u}_1 + \bar{u}_2$, and terminal constraints $\bar{x}_1(N_H) = \bar{x}_{1,s}, \bar{x}_2(N_H) = \bar{x}_{2,s}$. Since at time $h = 0$ the problem is infeasible due to the control constraints, the joint output constraint (2.26) has been transformed into a soft constraint by introducing a slack variable and by including it into the cost function with a weigh equal to 1000.

2.6. Conclusions

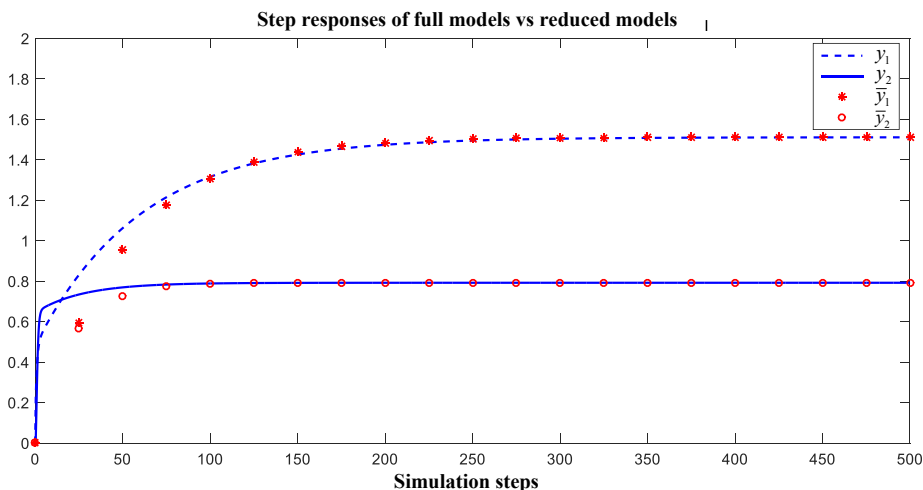


Figure 2.2: Open loop step responses of the continuous time models (continuous lines) of the generators and of the reduced order models in the long sampling time (dots).

At the low level, the shrinking horizon MPC algorithms described in Section (2.2.3) have been implemented with $Q_1 = 10^5$, $Q_2 = 10^4$, $R_1 = R_2 = 1$.

The hierarchical control scheme has been simulated starting from null initial conditions and by initially considering $y^o = 1$ in (2.26); then, at the time instant $t = 375s$, the reference power has been set equal to $y^o = 0.7$. The transients of the main output and control variables are reported in Figures 2.3 and 2.4. These results show the stabilizing action and the effectiveness of the algorithm implemented. Note also that in transient conditions the upper saturation limit on u_1 is active.

2.6 Conclusions

A two-layer control scheme has been proposed for the control of independent systems subject to joint output constraints. Its theoretical properties have been established and simulation results have been reported to show the potentialities of the method. A novel model reduction procedure has also been developed.

An extension of the solutions here considered can concern the design of algorithms with robustness properties. This can allow to cope with model uncertainties, possibly due to the model reduction phase, and to consider subsystems with dynamic couplings. Results in this direction will be presented in the following Chapter 4.

Chapter 2. Hierarchical MPC of independent systems with joint constraints

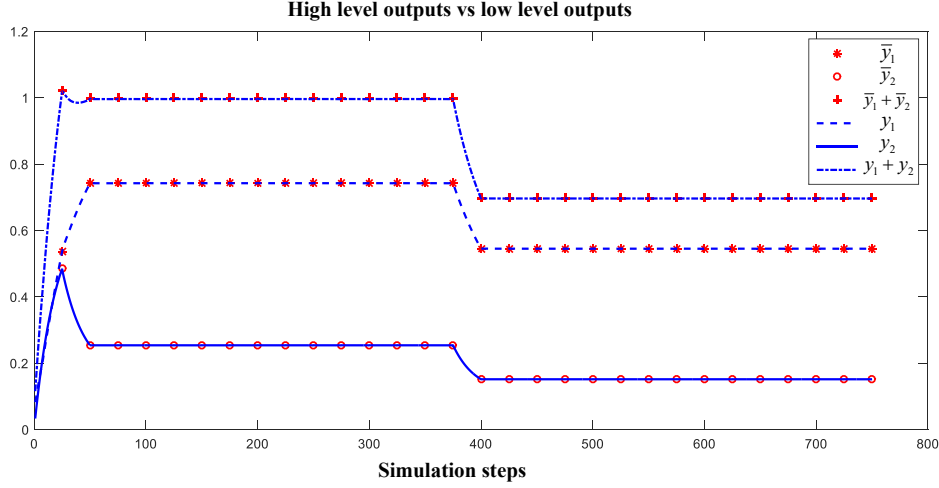


Figure 2.3: Closed-loop control: outputs of the generators and their sum at the high layer (dots) and at the low layer (continuous lines).

2.7 Appendix

2.7.1 Proof of Corollary 2.1

The low-level system (A_L, B_L, C_L) does not have transmission zeroes in 1 if and only if the input/output static gain $C_L G_L^x$ is full-rank and, for $m \leq p$, this condition is equivalent to $\mathcal{L} = \{0\}$. Therefore, condition (2.17) reduces to $\bar{n} \geq p$, which is satisfied by assumption. \square

2.7.2 Proof of Proposition 2.1

Assume that a solution to Problem 2.1 exists and let us focus on the properties holding for the mapping β . Since β has full rank, then

$$\dim(\text{Ker } \beta) = n - \bar{n}.$$

Moreover,

$$\text{Ker } \beta \subseteq \text{Ker } C_L \quad (2.29)$$

Indeed, if $v \in \text{Ker } \beta$ and $v \notin \text{Ker } C_L$, then $0 \neq C_L v = C_H \beta v = 0$. Finally, since $m \leq \bar{n}$ and G_H^x is full-rank, then G_H^x is injective, *i.e.*, $\text{Ker } G_H^x = \{0\}$. Thus, as long as $\beta G_L^x = G_H^x$, the restriction of β to $\text{Im } G_L^x$ is injective: this is equivalent to $\text{Im } G_L^x \cap \text{Ker } \beta = \{0\}$ and, under condition (2.29), to

$$\mathcal{L} \cap \text{Ker } \beta = \{0\}.$$

2.7. Appendix

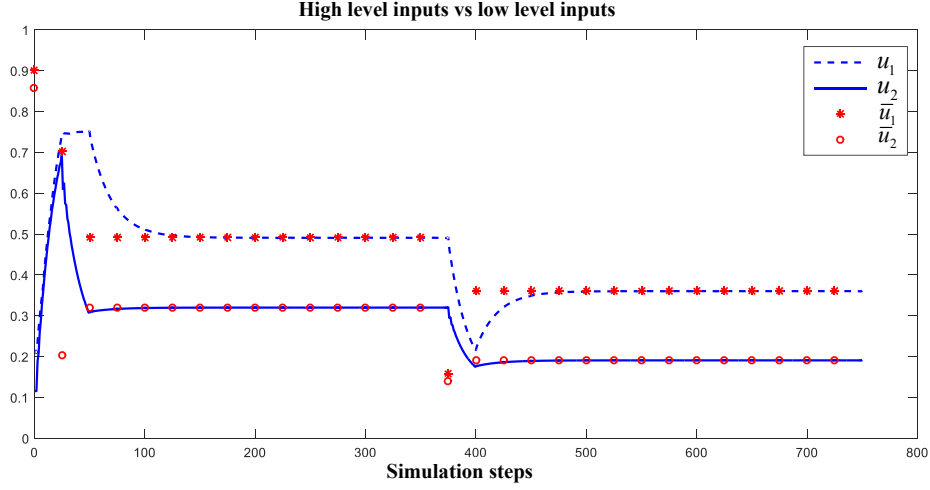


Figure 2.4: Control variables at the high (continuous lines) and at the low (dots) layers.

In view of this, it holds that $\dim(\text{Ker } \beta) + \dim(\mathcal{L}) = \dim(\mathcal{L} \cup \text{Ker } \beta) + \dim(\mathcal{L} \cap \text{Ker } \beta) = \dim(\mathcal{L} \cup \text{Ker } \beta)$. Since $\mathcal{L} \subseteq \text{Ker } C_L$, and $\text{Ker } \beta \subseteq \text{Ker } C_L$, then $\dim(\mathcal{L} \cup \text{Ker } \beta) \leq \dim(\text{Ker } C_L)$. To sum up, one has

$$\dim(\text{Ker } \beta) + \dim(\mathcal{L}) \leq \dim(\text{Ker } C_L). \quad (2.30)$$

Since C_L is surjective, then $\dim(\text{Ker } C_L) = n - p$ and, being $\dim(\text{Ker } \beta) = n - \bar{n}$, condition (2.30) rewrites as $n - \bar{n} + \dim(\mathcal{L}) \leq n - p$ that is condition (2.17).

Let us now show that under condition (2.17) it is indeed possible to solve Problem 2.1. In view of the above discussion, if $\bar{n} \geq p + \dim(\mathcal{L})$ it is possible to find a subspace \mathcal{K}_β of dimension $n - \bar{n}$ so that $\mathcal{K}_\beta \subseteq \text{Ker } C_L$ and $\mathcal{L} \cap \mathcal{K}_\beta = \{0\}$. Fix any of these \mathcal{K}_β 's, let $\{\kappa_1, \dots, \kappa_{n-\bar{n}}\}$ be a set of independent vectors in \mathcal{K}_β and complete this set to a basis $\mathcal{B} = \{v_1, \dots, v_{\bar{n}}, \kappa_1, \dots, \kappa_{n-\bar{n}}\}$ of the whole space \mathbb{R}^n . Hence define β as follows:

$$\begin{cases} \beta v_i = r_i \in \mathbb{R}^{\bar{n}}, & i = 1, \dots, \bar{n} \\ \beta \kappa_i = 0, & i = 1, \dots, n - \bar{n} \end{cases}$$

with the sole restriction that $\{r_1, \dots, r_{\bar{n}}\}$ form a basis of $\mathbb{R}^{\bar{n}}$. In doing so, $\text{Ker } \beta = \mathcal{K}_\beta$ and β is full-rank. Now, define C_H by

$$C_H r_i = C_L v_i \in \mathbb{R}^p, \quad i = 1, \dots, \bar{n}.$$

Chapter 2. Hierarchical MPC of independent systems with joint constraints

Hence, the coincidence of C_L and $C_H\beta$ holds by construction, just notice that since $\text{Ker } \beta \subseteq \text{Ker } C_L$, then $C_L \kappa_i = 0 = C_H\beta \kappa_i$. Finally, let

$$G_{H1}^x = \beta G_{L1}^x$$

that has full rank because, by construction, $\text{Im } G_{L1}^x \cap \text{Ker } \beta = \mathcal{Z} \cap \text{Ker } \beta = \{0\}$. \square

2.7.3 Proof of Proposition 2.2

1. In view of equation (2.13), it holds that

$$\beta x(N_L) = \hat{y}(N_L) = \beta A_L^{N_L} x(0) + \hat{y}_F^{[\bar{u}]}(N_L) + \hat{y}_F^{[\vec{\delta u}]}(N_L) \quad (2.31)$$

where $\hat{y}_F^{[\bar{u}]}$ is the forced output motion originated by the constant signal $u(h) \equiv \bar{u}^{[N_L]}$ and

$$\hat{y}_F^{[\vec{\delta u}]}(N_L) = \mathcal{H}(N_L) \vec{\delta u}_{(0:N_L-1)} \quad (2.32)$$

Since $\bar{x}(0) = \beta x(0)$, then

$$\begin{aligned} \bar{x}(N_L) &= A_H^{N_L} \bar{x}(0) + \bar{x}_F^{[\bar{u}]}(N_L) = \\ &= A_H^{N_L} \beta x(0) + \bar{x}_F^{[\bar{u}]}(N_L) \end{aligned} \quad (2.33)$$

Therefore, letting

$$\Delta \hat{y}_F^{[\bar{u}]}(N_L) = \bar{x}_F^{[\bar{u}]}(N_L) - \hat{y}_F^{[\bar{u}]}(N_L)$$

and combining equations (2.31), (2.32) and (2.33), the terminal constraint (2.19) is attained provided that

$$\mathcal{H}(N_L) \vec{\delta u}_{(0:N_L-1)} = \mathcal{A}(N_L) x(0) + \Delta \hat{y}_F^{[\bar{u}]}(N_L) \quad (2.34)$$

In view of (2.21), one has $\|\Delta \hat{y}_F^{[\bar{u}]}(N_L)\| \leq \kappa \sqrt{N_L} \|\bar{u}^{[N_L]}\|$ and

$$\begin{aligned} \|\mathcal{A}(N_L) x(0) + \Delta \hat{y}_F^{[\bar{u}]}(N_L)\| &\leq \\ &\leq \|\mathcal{A}(N_L)\| \cdot \|x(0)\| + \|\Delta \hat{y}_F^{[\bar{u}]}(N_L)\| \\ &\leq \|\mathcal{A}(N_L)\| \cdot \|x(0)\| + \kappa \sqrt{N_L} \|\bar{u}^{[N_L]}\| \end{aligned} \quad (2.35)$$

The constraint $u(j) \in \mathcal{U}$ is satisfied as long as

$$\|\delta u(j|0)\| \leq \rho_u - \|\bar{u}^{[N_L]}\| \quad (2.36)$$

2.7. Appendix

The norm constraint $\|\vec{\delta u}_{(0:N_L-1)}\| \leq \rho_u - \|\bar{u}^{[N_L]}\|$ on the overall signal $\vec{\delta u}_{(0:N_L-1)} \in \mathbb{R}^{mN_L}$ ensures that condition (2.36) is satisfied $\forall j = 0, 1, \dots, N_L - 1$. The image through $\mathcal{H}(N_L)$ of the ball

$$\{\vec{\delta u}_{(0:N_L-1)} \in \mathbb{R}^{mN_L} \mid \|\vec{\delta u}_{(0:N_L-1)}\| \leq \rho_u - \|\bar{u}^{[N_L]}\|\}$$

contains the ball

$$\{z \in \mathbb{R}^{\bar{n}} \mid \|z\| \leq \sigma_{\bar{n}}(N_L) \cdot (\rho_u - \|\bar{u}^{[N_L]}\|)\}$$

where $\sigma_{\bar{n}}(N_L) > 0$ in view of Assumption 2.3.(2). Therefore, according to inequality (2.35), a solution to system (2.34) satisfying condition (2.36) exists if

$$\sigma_{\bar{n}}(N_L) \cdot (\rho_u - \|\bar{u}^{[N_L]}\|) \geq \|\mathcal{A}(N_L)\| \cdot \|x(0)\| + \kappa\sqrt{N_L}\|\bar{u}^{[N_L]}\|$$

that is

$$\|\mathcal{A}(N_L)\| \cdot \|x(0)\| + (\sigma_{\bar{n}}(N_L) + \kappa\sqrt{N_L})\|\bar{u}^{[N_L]}\| \leq \sigma_{\bar{n}}(N_L) \cdot \rho_u \quad (2.37)$$

In other words, if $\|x(0)\|$ satisfies condition (2.22), then any $\bar{u}^{[N_L]} \in \mathcal{U}$ satisfying condition (2.23) ensures that condition (2.37) is satisfied and the latter guarantees the desired result.

2. Let $\vec{u}^{[N_L]}_{(0:N_L-1)} = [\bar{u}^{[N_L]} \dots \bar{u}^{[N_L]}] \in \mathbb{R}^{mN_L}$. Since

$$x(N_L) = A_L^{N_L}x(0) + \mathcal{R}(N_L)(\vec{u}^{[N_L]}_{(0:N_L-1)} + \vec{\delta u}_{(0:N_L-1)})$$

and, $\forall j = 0, \dots, N_L - 1$, $\|\bar{u}^{[N_L]} + \delta u(j|0)\| \leq \rho_u$, then

$$\begin{aligned} \|x(N_L)\| &\leq \\ &\leq \|A_L^{N_L}\| \cdot \|x(0)\| + \|\mathcal{R}(N_L)\| \cdot \|\vec{u}^{[N_L]}_{(0:N_L-1)} + \vec{\delta u}_{(0:N_L-1)}\| \\ &\leq \|A_L^{N_L}\| \cdot \frac{\sigma_{\bar{n}}(N_L) \cdot \rho_u}{\|\mathcal{A}(N_L)\|} + \|\mathcal{R}(N_L)\| \cdot \rho_u\sqrt{N_L} \end{aligned}$$

Thus, condition (2.22) is satisfied by $x(N_L)$ if

$$\|A_L^{N_L}\| \cdot \frac{\sigma_{\bar{n}}(N_L) \cdot \rho_u}{\|\mathcal{A}(N_L)\|} + \|\mathcal{R}(N_L)\| \cdot \rho_u\sqrt{N_L} \leq \frac{\sigma_{\bar{n}}(N_L) \cdot \rho_u}{\|\mathcal{A}(N_L)\|} \quad (2.38)$$

and, if $\|A_L^{N_L}\| < 1$, inequality (2.38) is equivalent to condition (2.24).

Chapter 2. Hierarchical MPC of independent systems with joint constraints

3. Let us first show that $\sigma_{\bar{n}}(N_L)$ is a non decreasing function of N_L : it holds that

$$\mathcal{H}(N_L + 1) = [\mathcal{H}(N_L) \quad g(N_L + 1)]$$

with

$$g(N_L + 1) = \beta A_L^{N_L} B_L$$

so that

$$\begin{aligned} \sigma_{\bar{n}}(N_L + 1) &= \sqrt{\lambda_{\min}(\mathcal{H}(N_L + 1)\mathcal{H}(N_L + 1)^\top)} \\ &= \sqrt{\lambda_{\min}(\mathcal{H}(N_L)\mathcal{H}(N_L)^\top + g(N_L + 1)g(N_L + 1)^\top)} \\ &\geq \sqrt{\lambda_{\min}(\mathcal{H}(N_L)\mathcal{H}(N_L)^\top)} = \sigma_{\bar{n}}(N_L) \end{aligned}$$

As for the norm of $\mathcal{A}(N_L)$, one has $\|\mathcal{A}(N_L)\| \leq (\|A_H^{N_L}\| + \|A_L^{N_L}\|) \cdot \|\beta\|$ and the latter is exponentially decreasing to 0 in N_L since both A_L and A_H are Schur stable. Hence, the divergence of $\lambda(N_L)$ and the convergence to 0 of $\|A_L^{N_L}\|$ easily follows.

As for $\chi(N_L)$, notice that: $\|\mathcal{B}(N_L)\|$ is a bounded function of N_L as a consequence of the Schur stability of A_L ; the exponential decrease of $\|\mathcal{A}(N_L)\|$ entails that

$$\lim_{N_L \rightarrow +\infty} \sqrt{N_L} \cdot \|\mathcal{A}(N_L)\| = 0$$

and, finally, $\sigma_{\bar{n}}(N_L)$ is a lower bounded function of N_L .

□

2.7.4 Proof of Proposition 2.3

Since the control space \mathcal{U} is bounded, then the signal $w(k)$ is bounded as well and, consequently, its Z-transform $W(z)$ has its poles in the unitary disk $\mathcal{D}_1 = \{z \in \mathbb{C} \mid |z| \leq 1\}$. In view of equation (2.25), the Z-transform of the forced motion $\delta\hat{y}_F(k)$ is given by

$$\Delta\hat{Y}_F(z) = -z\beta(zI_n - \mathcal{A}_L)^{-1}\delta x(0)$$

it is hence a rational function having its poles in the unitary ball $\mathcal{B}_1 = \{z \in \mathbb{C} \mid |z| < 1\}$. Since

$$\Delta\hat{Y}_F(z) = \tilde{G}(z)W(z)$$

2.7. Appendix

then, denoted by $\mathcal{P}(K(z))$ and $\mathcal{Z}(K(z))$ the set of the poles and of the zeros, respectively, of $K(z)$, one has

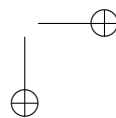
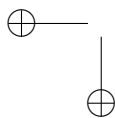
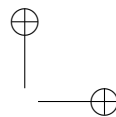
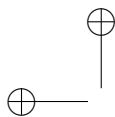
$$\left\{ \begin{array}{l} \mathcal{P}(\Delta\hat{Y}_F(z)) \subset \mathcal{B}_1 \\ \mathcal{P}(\tilde{G}(z)) \subset \mathcal{B}_1 \\ \mathcal{P}(W(z)) \subset \mathcal{D}_1 \\ \mathcal{P}(\Delta\hat{Y}_F(z)) \subset \mathcal{P}(\tilde{G}(z)) \cup \mathcal{P}(W(z)) \\ \left(\mathcal{P}(\tilde{G}(z)) \cup \mathcal{P}(W(z)) \right) \setminus \mathcal{P}(\Delta\hat{Y}_F(z)) \subseteq \mathcal{Z}(\tilde{G}(z)) \cup \mathcal{P}(\tilde{G}(z)) \end{array} \right.$$

From these relations, and from the assumption that $\tilde{G}(z)$ has no zeros on the unitary circle \mathcal{S}^1 , it promptly follows that

$$\mathcal{P}(W(z)) \subset \mathcal{B}_1$$

so that $\lim_{k \rightarrow +\infty} w(k) = 0$.

Finally, $\lim_{k \rightarrow +\infty} \delta x(k) = 0$ is an immediate consequence of the asymptotic stability of the low-level system; $\lim_{h \rightarrow +\infty} \delta u(h) = 0$ follows from the fact that, when $x(0) = x_s$, the null input sequence $\delta u \equiv 0$ solves the low-level optimization problem (2.14); once more $\lim_{h \rightarrow +\infty} x(h) = x_s$ follows from the asymptotic stability of the low-level system. \square



CHAPTER 3

A hierarchical MPC scheme for coordination of independent systems with shared resources and plug-and-play capabilities

3.1 Introduction

In many industrial and civil contexts, there is the need to coordinate a number of independent subsystems with limited resources to guarantee a given behavior of the overall system. Examples can be found in buildings, where different thermal power generators must be controlled to provide the required cooling or heating and to minimize an economic cost, see [125]. In [117], the considered problem consists in coordinating different oxygen generators available in a distribution network to satisfy a given request under shared resources. In isolated microgrids, possibly including renewable energy sources, the available dispatchable Diesel generators must be managed to satisfy the load request and eventually provide frequency and voltage regulation, see for example [36, 123]. Other examples, concerning irrigation systems and chemical processes, are discussed in [17]. In all

Chapter 3. A hierarchical MPC scheme for coordination of independent systems with shared resources and plug-and-play capabilities

these problems it can also be useful to allow for plug and play operations to improve the economic performance and guarantee better flexibility, adaptation to changing conditions, and fault tolerance, see for instance [152, 171]. A simple approach for the solution to these coordination problems consists of considering a unique model of the entire system and to design a centralized MPC described in Section 1.2.1. However, this could be computationally expensive when the overall system is large-scale, as recognized for instance in [17], since the computational complexity would scale with the number of subsystems. For this reason, different hierarchical control schemes have been proposed. The general idea is to design a centralized high level regulator for a simplified model with the scope to consider the long-term behavior of the system, while local regulators are used at the lower levels for stability and disturbance rejection, see for example [17] and Chapter 2. In this scenario, this chapter presents a novel hierarchical control algorithm for the coordination of independent asymptotically stable (or pre-stabilized), square systems with joint input and output constraints. At the higher layer of the control structure, a centralized MPC problem is solved at a slow rate and considering a reduced order model of the overall system to compute the input to the independent subsystems so as to fulfill the global output request. At the lower layer, for any subsystem a fast MPC controller is designed to remove the effects of the model mismatch introduced at the higher layer, to satisfy local constraints and to optimize the individual performance. The proposed design method allows to modify the system configuration, in terms of the contribution provided by any subsystem to the overall system performance, and to implement plug and play operations. The recursive feasibility of the MPC problems to be solved at the high and low levels is guaranteed also during plug-in and plug-out operations, and overall convergence of the system output to the set-point is proven. The adopted control structure is similar to the one considered in Chapter 2, but the solution proposed here represents a significant improvement for the following reasons: (i) the problem at the high level is fully scalable with the number of subsystems, so allowing for plug and play operations, (ii) the high level model is easily determined from the impulse responses of the subsystems and its state is measurable, being composed by past inputs, (iii) constraints on the shared resources (inputs) are included, (iv) the possibility to perform static high level optimization is explicitly considered to optimize the subsystems’ usage and provide flexibility to the control configuration.

The chapter is organized as follows. In Section 3.2 the problem is stated and the models used at the high and low levels of the control structure are

3.2. Statement of the problem and models

defined. The design of the high and low level MPC regulators is presented in Sections 3.3 and 3.4, respectively, while the main theoretical results of recursive feasibility and convergence are described in Section 3.5. The static optimization problem to be solved for the definition of the optimal usage of the subsystems is presented in Section 3.6, where it is also defined the plug and play procedure to be followed to guarantee the properties of the system. A simulation study is discussed in Section 3.7 to illustrate the performance of the method, while some conclusions are drawn in Section 3.8. The proofs of the main results are collected in an Appendix.

3.2 Statement of the problem and models

In this section we present the model of the overall system under study and the main idea allowing to simplify the control problem both at high and at low hierarchical levels.

3.2.1 System model and control objectives

We assume that the overall system Σ is composed by M discrete-time, linear, independent subsystems described by

$$\Sigma_i : \begin{cases} x_i(h+1) &= A_i x_i(h) + B_i u_i(h) \\ y_i(h) &= C_i x_i(h) \end{cases} \quad (3.1)$$

$i = 1, 2, \dots, M$, where $x_i \in \mathbb{R}^{n_i}$, $u_i \in \mathbb{R}^m$, and $y_i \in \mathbb{R}^p$ are the state, input, and output vectors, while h is the discrete-time index in the basic time scale. Subsystems Σ_i , $i = 1, \dots, M$ are similar, in the sense that the inputs $u_i(h)$ [respectively the outputs $y_i(h)$] are homogeneous vectors. The following properties are assumed to hold.

Assumption 3.1.

- (1) A_i is Schur stable, $i = 1, \dots, M$;
- (2) $m = p$;
- (3) $\det(C_i(I_{n_i} - A_i)^{-1}B_i) \neq 0$, $i = 1, \dots, M$;
- (4) (A_i, C_i) is observable, $i = 1, \dots, M$.

We will use also, for all $i = 1, \dots, M$, the equivalent infinite impulse response (IIR) form

$$y_i(h) = \sum_{j=1}^{+\infty} G_j^i u_i(h-j) \quad (3.2)$$

Chapter 3. A hierarchical MPC scheme for coordination of independent systems with shared resources and plug-and-play capabilities

where $G_j^i = C_i A_i^{(j-1)} B_i \in \mathbb{R}^{p \times m}$ are the impulse response matrices. The control scheme to be designed must allow to coordinate the M subsystems in such a way that the following objectives are attained.

- (i) **Collective output tracking and constraint satisfaction:** solve a constrained control problem for the collective output

$$y(h) = \sum_{i=1}^M y_i(h) \quad (3.3)$$

Specifically, we aim to drive $y(h)$ to a desired reference value y_{ref} while verifying collective output constraints

$$y(h) \in \mathcal{Y} \quad (3.4)$$

where \mathcal{Y} is a specified bounded and convex output constraint set.

- (ii) **Local constraints satisfaction:** verify local input constraints, for each subsystem Σ_i , $i = 1, \dots, M$, of the type

$$u_i(h) \in \mathcal{U}_i \quad (3.5)$$

- (iii) **Resource sharing:** assuming that a subset of agents $\mathcal{S} \subseteq \{1, \dots, M\}$ shares the same (limited) input resource, we may require that

$$u_{\text{shared}}(h) = \sum_{i \in \mathcal{S}} u_i(h) \in \mathcal{U}_{\text{shared}} \quad (3.6)$$

To address the overall design problem, we define each input signal $u_i(h)$ as the sum of two contributions:

$$u_i(h) = \alpha_i \bar{u}(h) + \delta u_i(h) \quad (3.7)$$

where

- the common input $\bar{u}(h)$ will be computed by a centralized high-level, low-dimensional, and slow-timescale controller designed to fulfill objective (i);
- the terms $\delta u_i(h)$ will be defined by M local low-level, fast controllers to enforce local input constraints and optimize local dynamic performances;

3.2. Statement of the problem and models

- the weights α_i with $\sum_{i=1}^M \alpha_i = 1$ will be chosen off-line to guarantee the feasibility of the problem at both layers and system-wide optimality. Their values are temporarily assumed to be fixed; their choice and possible adaptive tuning, also allowing for plug and play operations, will be discussed in Section 3.6.

The feasibility properties of the two schemes are strictly correlated. In particular, letting $\bar{\mathcal{U}}$ and $\delta\mathcal{U}_i$ be two bounded and convex sets and in view of (3.7), in order to satisfy constraints (3.5), (3.6) we can enforce

$$\bar{u}(h) \in \bar{\mathcal{U}} \quad (3.8a)$$

$$\delta u_i(h) \in \delta\mathcal{U}_i, i = 1, \dots, M \quad (3.8b)$$

and select $\bar{\mathcal{U}}$, $\delta\mathcal{U}_i$, and the parameters α_i such that

$$\delta\mathcal{U}_i \oplus \alpha_i \bar{\mathcal{U}} \subseteq \mathcal{U}_i, \text{ for all } i = 1, \dots, M \quad (3.9a)$$

$$\left(\sum_{i \in \mathcal{S}} \alpha_i \right) \bar{\mathcal{U}} \oplus \left(\bigoplus_{i \in \mathcal{S}} \delta\mathcal{U}_i \right) \subseteq \mathcal{U}_{\text{shared}} \quad (3.9b)$$

3.2.2 System decomposition and low-level models

To develop the models used for control, we rewrite (3.2) as follows

$$y_i(h) = \sum_{j=1}^{T_L} G_j^i u_i(h-j) + \sum_{j=T_L+1}^{+\infty} G_j^i u_i(h-j) \quad (3.10)$$

where the positive integer T_L is in general selected so that $G_{T_L+j}^i \simeq 0, j > 0$. From (3.7) and (3.10) and applying the superposition principle, for each subsystem $i = 1, \dots, M$, we obtain that

$$y_i(h) = \alpha_i \bar{y}_i(h) + \delta y_i(h) \quad (3.11)$$

where

$$\bar{y}_i(h) = \sum_{j=1}^{T_L} G_j^i \bar{u}(h-j) + \sum_{j=T_L+1}^{+\infty} G_j^i \bar{u}(h-j) \quad (3.12)$$

and $\delta y_i(h)$ is the output of the system (3.1) with input $\delta u_i(h)$. The quantity $w_i(h) = \alpha_i \sum_{j=T_L+1}^{+\infty} G_j^i \bar{u}(h-j) + \delta y_i(h)$ can be considered as the output of the following state-space model Σ_i^w , which will be used in the design of the low level controllers

$$\begin{cases} x_i^{(w)}(h+1) &= A_i x_i^{(w)}(h) + A_i^{T_L} B_i \alpha_i \bar{u}(h-T_L) + B_i \delta u_i(h) \\ w_i(h) &= C_i x_i^{(w)}(h) \end{cases} \quad (3.13)$$

Chapter 3. A hierarchical MPC scheme for coordination of independent systems with shared resources and plug-and-play capabilities

In the following we will design a high-level controller that runs at a slower timescale, i.e., that keeps the signal $\bar{u}(h)$ constant for N_L subsequent time steps and equal to $\bar{u}^{[N_L]}(k)$, i.e., $\bar{u}(h) = \bar{u}^{[N_L]}(k)$ for all $h \in \{kN_L, \dots, (k+1)N_L - 1\}$ for all $k \geq 0$. The only requirement is that there exists an integer value T_H such that $T_L = T_H N_L$. We define also, for all $i = 1, \dots, M$, $y_i^{[N_L]}(k) = y_i(kN_L)$. From (3.11) and (3.12) we obtain, for all $k \geq 0$, that

$$y_i^{[N_L]}(k) = \sum_{l=1}^{T_H} \alpha_i G_l^{i,[N_L]} \bar{u}^{[N_L]}(k-l) + w_i(kN_L) \quad (3.14)$$

where $G_l^{i,[N_L]} = \sum_{j=(l-1)N_L+1}^{lN_L} G_j^i$. By inspecting equation (3.14) it becomes clear that the evolution of the variable (3.14) can be described by a pure FIR (finite impulse response) system provided that, for all $k \geq 0$, it is possible to set

$$w_i(kN_L) = 0 \quad (3.15)$$

The low-level controllers will be committed, for all $i = 1, \dots, M$, to guarantee (3.15).

3.2.3 High-level collective model

In order to derive the model used for the design of the controller at the high level, define $y^{[N_L]}(k) = y(kN_L)$. In view of (3.3) and (3.14), and under (3.15) we can write

$$y^{[N_L]}(k) = \sum_{l=1}^{T_H} G_l^{[N_L]} \bar{u}^{[N_L]}(k-l) \quad (3.16)$$

where $G_l^{[N_L]} = \sum_{i=1}^M \alpha_i G_l^{i,[N_L]}$. A state space realization of the model (3.16) can be obtained letting $\bar{x}_u(k) = (\bar{u}^{[N_L]}(k-1), \dots, \bar{u}^{[N_L]}(k-T_H))$, and writing (3.16) as

$$\begin{cases} \bar{x}_u(k+1) &= \bar{A}_u \bar{x}_u(k) + \bar{B}_u \bar{u}^{[N_L]}(k) \\ y^{[N_L]}(k) &= \bar{C}_u \bar{x}_u(k) \end{cases} \quad (3.17)$$

where

$$\bar{A}_u = \begin{bmatrix} 0 & \dots & 0 & 0 \\ I_m & \dots & 0 & 0 \\ \vdots & \ddots & \vdots & \vdots \\ 0 & \dots & I_m & 0 \end{bmatrix}, \bar{B}_u = \begin{bmatrix} I_m \\ 0 \\ \vdots \\ 0 \end{bmatrix}$$

and $\bar{C}_u = [G_1^{[N_L]}, \dots, G_{T_H}^{[N_L]}]$.

Model (3.17) can be transformed into the corresponding *velocity form*,

3.3. The high level regulator

commonly employed for guaranteeing offset free control performances, see for example [19]. To this aim define $\Delta\bar{x}_u(k) = \bar{x}_u(k) - \bar{x}_u(k-1)$ and $\Delta\bar{u}^{[N_L]}(k) = \bar{u}^{[N_L]}(k) - \bar{u}^{[N_L]}(k-1)$. Following the procedure sketched in [19], define $\bar{x}(k) = (y^{[N_L]}(k), \Delta\bar{x}_u(k))$, then the corresponding velocity form is

$$\begin{cases} \bar{x}(k+1) &= \bar{A}\bar{x}(k) + \bar{B}\Delta\bar{u}^{[N_L]}(k) \\ y^{[N_L]}(k) &= \bar{C}\bar{x}(k) \end{cases} \quad (3.18)$$

where

$$\bar{A} = \begin{bmatrix} I_p & \bar{C}_u\bar{A}_u \\ 0 & \bar{A}_u \end{bmatrix}, \bar{B} = \begin{bmatrix} \bar{C}_u\bar{B}_u \\ \bar{B}_u \end{bmatrix} \quad (3.19)$$

and $\bar{C} = [I_p \quad 0 \quad \dots \quad 0]$.

Remark 3.1. *The velocity form (3.18) has a twofold advantage with respect to the original one (3.17). First, it guarantees the presence of an integral action in the final control law to be determined by the high-level controller. Second, it includes in the control law an output feedback term which would not be obtained by using in the synthesis phase the original truncated impulse response model.*

The following assumption is required on system (3.18).

Assumption 3.2. *Model (3.18) is reachable.*

The following result provides a sufficient and necessary condition for Assumption 3.2 to hold.

Proposition 3.1.

Model (3.18) is reachable if and only if $\det(\sum_{i=1}^{T_H} G_i^{[N_L]}) \neq 0$.

3.3 The high level regulator

In this section we define the design algorithm for the high level MPC controller.

3.3.1 Constraints in velocity form

To enforce constraints on absolute input and state variables (e.g., $\bar{u}^{[N_L]}(k)$) through suitable constraints on the inputs and states of the velocity form (3.18), we resort to [19], where it is shown that

$$\bar{u}^{[N_L]}(k-1) = C^*\bar{x}(k) \quad (3.20)$$

Chapter 3. A hierarchical MPC scheme for coordination of independent systems with shared resources and plug-and-play capabilities

where

$$C^* = [0 \quad , \quad I_m] \begin{bmatrix} \bar{C}_u \bar{A}_u & \bar{C}_u \bar{B}_u \\ \bar{A}_u - I_m T_H & \bar{B}_u \end{bmatrix}^{-1}$$

In view of (3.20) and (3.18), (3.4) and (3.8a) are satisfied provided that

$$\begin{bmatrix} \bar{C} \\ C^* \end{bmatrix} \bar{x}(k) = \begin{bmatrix} y^{[N_L]}(k) \\ \bar{u}^{[N_L]}(k-1) \end{bmatrix} \in \mathcal{Y}_u \quad (3.21)$$

where $\mathcal{Y}_u = \mathcal{Y} \times \bar{\mathcal{U}}$.

3.3.2 The auxiliary control law and the maximal output admissible set

As usual in MPC, the definition of an auxiliary control law and a terminal set may be required to guarantee stabilizing properties, therefore the design of these elements is now performed. Preliminarily, recall that y_{ref} is the reference which should be ideally tracked by the collective output, and note that it could not be reached within the considered prediction horizon due to the presence of the input constraints. For this reason, define by r a feasible output reference, which must be computed by the control algorithm to be as near as possible to y_{ref} . Then, the auxiliary control law for system (3.18) reads

$$\Delta \bar{u}^{[N_L]}(k) = K^{aux}(\bar{x}(k) - \bar{x}_{ref}) \quad (3.22)$$

where $\bar{x}_{ref} = E_1 r$, $E_1 = [I_p \quad , \quad 0 \quad , \quad \dots \quad , \quad 0]^T$ and K^{aux} is defined in such a way that $F^{aux} = \bar{A} + \bar{B}K^{aux}$ is Schur stable. A possible choice of K^{aux} is given in the following proposition.

Proposition 3.2.

If $\det(G_1^{[N_L]}) \neq 0$ and

$$\left\| \left[G_2^{[N_L]}(G_1^{[N_L]})^{-1} \quad , \quad \dots \quad , \quad G_{T_H}^{[N_L]}(G_1^{[N_L]})^{-1} \right] \right\|_\infty < 1 \quad (3.23)$$

then, setting $K^{aux} = \left[-(1-\varepsilon)(G_1^{[N_L]})^{-1} \quad , \quad 0 \quad , \quad \dots \quad , \quad 0 \right]$, where $\varepsilon \in [0, 1)$, matrix $F^{aux} = \bar{A} + \bar{B}K^{aux}$ is Schur stable. \square

Letting $r(k+1) = r(k) = r$, we can write

$$\begin{bmatrix} \bar{x}(k+1) \\ r(k+1) \end{bmatrix} = \mathcal{F} \begin{bmatrix} \bar{x}(k) \\ r(k) \end{bmatrix} \quad (3.24)$$

3.3. The high level regulator

where

$$\mathcal{F} = \begin{bmatrix} F^{\text{aux}} & -\bar{B}K^{\text{aux}}E_1 \\ 0 & I_p \end{bmatrix}$$

Recall also that

$$\begin{bmatrix} y^{[N_L]}(k) \\ \bar{u}^{[N_L]}(k-1) \end{bmatrix} = C_{yu} \begin{bmatrix} \bar{x}(k) \\ r(k) \end{bmatrix} \quad (3.25)$$

where

$$C_{yu} = \begin{bmatrix} \bar{C} & 0 \\ C^* & 0 \end{bmatrix}$$

Consider the following assumption.

Assumption 3.3.

- (1) The pair (\mathcal{F}, C_{yu}) is observable.
- (2) \mathcal{Y}_u is a closed polytope.

Under Assumption 3.3 and according to [65] we can compute, in a finite number of steps, an invariant polytopic ε -inner approximation of the maximal output admissible set for the pair (3.24), (3.25), i.e., $\mathbb{O}_\varepsilon := \{(\bar{x}, r) : C_{yu}\mathcal{F}^k(\bar{x}, r) \in \mathcal{Y}_u \text{ for all } k \geq 0 \text{ and } \lim_{k \rightarrow +\infty} C_{yu}\mathcal{F}^k(\bar{x}, r) \in \mathcal{Y}_u(\varepsilon)\}$, where $\mathcal{Y}_u(\varepsilon)$ is a closed and compact set satisfying $\mathcal{Y}_u(\varepsilon) \oplus \mathcal{B}_\varepsilon(0) \subseteq \mathcal{Y}_u$.

3.3.3 The high layer MPC problem

In view of the previous considerations, the problem to be solved at a generic time instant t is

$$\min_{r(t), \Delta\bar{u}^{[N_L]}(t:t+N_H-1)} J_{HL} \quad (3.26a)$$

where

$$J_{HL} = \sum_{k=t}^{t+N_H-1} \left\{ \|\bar{x}(k) - E_1 r(t)\|_Q^2 + \|\Delta\bar{u}(k)^{[N_L]}\|_R^2 \right\} + \|\bar{x}(t+N_H) - E_1 r(t)\|_P^2 + \gamma \|r(t) - y_{\text{ref}}\|^2 \quad (3.26b)$$

subject to the dynamical system (3.18), constraints (3.21) for all $k = t, \dots, t + N_H - 1$, and to the terminal constraint

$$(\bar{x}(t+N_H), r(t)) \in \mathbb{O}_\varepsilon \quad (3.26c)$$

Chapter 3. A hierarchical MPC scheme for coordination of independent systems with shared resources and plug-and-play capabilities

The symmetric and positive definite weighting matrices Q and R are arbitrary tuning knobs. The matrix P must be chosen as the solution to the Lyapunov equation

$$(F^{\text{aux}})^T P F^{\text{aux}} - P = -(Q + (K^{\text{aux}})^T R K^{\text{aux}}) \quad (3.26d)$$

From [19], the parameter γ must be chosen so as to meet the inequality $\gamma I \succ P_{yy}$, where P_{yy} is a block of matrix P , decomposable as follows

$$P = \begin{bmatrix} P_{yy} & P_{y\Delta\bar{x}_u} \\ P_{y\Delta\bar{x}_u}^T & P_{\Delta\bar{x}_u\Delta\bar{x}_u} \end{bmatrix}$$

The stated MPC problem is easily solvable, in view of its QP structure; however, when the weights α_i vary during the system operation (e.g., in a plug and play scenario, see Section 3.6.2) it is impractical to compute the set \mathbb{O}_ε online, especially in case of high-dimensional systems. A possible way to circumvent this issue is to resort the simplified problem presented in the following.

3.3.4 The high layer MPC problem with zero-terminal constraint

The idea proposed in this section consists of replacing (3.26c) with a zero-terminal constraint, that does not require the definition of the terminal set, of the auxiliary control law, and of the terminal weight. Note that the latter are derived, in a non-trivial way, from the parameters α_i . This solution corresponds to set

$$\begin{aligned} \bar{x}(t + N_H) &= E_1 r(t) \\ \begin{bmatrix} \bar{C} \\ C^* \end{bmatrix} \bar{x}(t + N_H) &\in \mathcal{Y}_u(\varepsilon) \end{aligned} \quad (3.27)$$

Also note that, choosing $Q = \text{diag}(Q_y, R, \dots, R)$, we obtain that $\|\bar{x}(k) - E_1 r(t)\|_Q^2 = \|y^{[M_L]}(k) - r(t)\|_{Q_y}^2 + \sum_{s=k-T_H}^{k-1} \|\Delta\bar{u}^{[M_L]}(s)\|_R^2$, so that

$$\begin{aligned} J_{\text{HL}} &= \sum_{k=t}^{t+N_H-1} \left\{ \|y^{[M_L]}(k) - r(t)\|_{Q_y}^2 + \sum_{s=k-T_H}^k \|\Delta\bar{u}^{[M_L]}(s)\|_R^2 \right\} \\ &\quad + \gamma \|r(t) - y_{\text{ref}}\|^2 \end{aligned}$$

3.4. The low level regulators

Since, at time t , the values of $\Delta\bar{u}^{[N_L]}(k)$ for $k \leq t$ are not optimization variables, minimizing J_{HL} actually corresponds to optimizing

$$\begin{aligned} \tilde{J}_{\text{HL}} = & \sum_{k=0}^{N_H-1} \{ \|y^{[N_L]}(t+k) - r(t)\|_{Q_y}^2 \\ & + (\min(N_H - k, T_H)) \| \Delta\bar{u}^{[N_L]}(t+k) \|_R^2 \} + \gamma \|r(t) - y_{\text{ref}}\|^2 \end{aligned} \quad (3.28)$$

Under the simplifications above, the overall optimization problem is

$$\min_{r(t), \Delta\bar{u}^{[N_L]}(t:t+N_H-1)} \tilde{J}_{\text{HL}} \quad (3.29a)$$

subject to the dynamical system (3.16). The constraints are

$$\bar{u}^{[N_L]}(k) \in \bar{\mathcal{U}} \quad (3.29b)$$

$$y^{[N_L]}(k) \in \mathcal{Y} \quad (3.29c)$$

for all $k = t, \dots, t + N_H - 1$, while the terminal constraint (3.27) can be rephrased as follows.

$$\begin{aligned} \bar{u}^{[N_L]}(k) = & \left(\sum_{l=1}^{T_H} G_l^{[N_L]} \right)^{-1} r(t), \\ & \text{for } k = t + N_H - T_H, \dots, t + N_H - 1 \end{aligned} \quad (3.29d)$$

$$y^{[N_L]}(t + N_H) = r(t) \quad (3.29e)$$

$$\begin{bmatrix} I_p \\ \left(\sum_{l=1}^{T_H} G_l^{[N_L]} \right)^{-1} \end{bmatrix} r(t) \in \mathcal{Y}_u(\varepsilon) \quad (3.29f)$$

For well-posedness, it is assumed that $N_H \geq T_H$.

3.4 The low level regulators

The role of the low-level regulators is twofold. Firstly, they are needed to remove the mismatch of the high-level simplified system from its model (3.16) by enforcing (3.15). Secondly, they optimize the performances of the subsystems in transient conditions. Recall that $w_i(h)$ is driven by the dynamical system (3.13). At low level we adopt a shrinking horizon approach and, for each $i = 1, \dots, M$, at time $h \in \{kN_L, (k+1)N_L - 1\}$ we solve

$$\min_{\vec{\delta}u_i(h:(k+1)N_L-1)} J_{\text{LL}}^i \quad (3.30a)$$

Chapter 3. A hierarchical MPC scheme for coordination of independent systems with shared resources and plug-and-play capabilities

where

$$J_{LL}^i = \sum_{s=h}^{(k+1)N_L-1} \left\{ \|w_i(s)\|_{Q_i}^2 + \|\delta u_i(s) + \alpha_i g_i^{[T_L]} \bar{u}^{[N_L]}(k - T_H)\|_{R_i}^2 \right\} \quad (3.30b)$$

subject to the constraints

$$\delta u_i(s) \in \delta \mathcal{U}_i, \quad s = h, \dots, (k+1)N_L - 1 \quad (3.30c)$$

$$w_i((k+1)N_L) = 0 \quad (3.30d)$$

$$x_i^{(w)}((k+1)N_L) \in \mathbb{X}_i^F \quad (3.30e)$$

We have denoted

$$g_i^{[T_L]} = (C_i(I_{n_i} - A_i)^{-1}B_i)^{-1} C_i(I_{n_i} - A_i)^{-1}A_i^{T_L}B_i$$

defined in such a way that if, in steady state, $\delta u_i(h) + \alpha_i g_i^{[T_L]} \bar{u}^{[N_L]}(k - T_H) = 0$, then $w_i(h) = 0$. Note that $g_i^{[T_L]}$ is well defined in view of Assumption 3.1.(3).

The set \mathbb{X}_i^F is a suitable terminal set for $x_i^{(w)}$ that guarantees the feasibility of the low-level problem at the subsequent long sampling time, i.e., for the problem at $h = (k+1)N_L$. Its definition is deferred to Section 3.5.

Note also that, since $w_i(h) = y_i(h) - \alpha_i \sum_{j=1}^{T_L} G_j^i \bar{u}(h-j)$ is given, in view of Assumption 3.1.(4), the estimate of $x_i^{(w)}(h)$ is known at all sampling times.

Remark 3.2. *To account for possible uncertainties, both at low and high layers, a bounded disturbance term can also be considered and the corresponding tube-based robust algorithm can be used, without significant technical issues. Possible uncertainties are intentionally neglected in this chapter to keep the notation and the treatment as simple as possible.*

3.5 Design issues and main results

In this section we discuss the main conditions required to make the two layers consistent and we derive the main feasibility and convergence results of the proposed design method.

Up to this point, the values of the parameters $\alpha_i \geq 0, i = 1, \dots, M$, have been assumed to be fixed. However, in the final part of the paper they will be considered as additional tuning knobs to be possibly retuned on-line and/or to be modified to allow for plug and play operations. For this reason, the

3.5. Design issues and main results

conditions discussed in the following will be formulated to be consistent with all the values the α_i can take. To this end, define $\bar{\alpha}_i$, $i = 1, \dots, M$ as upper bounds to α_i , i.e.

$$\bar{\alpha}_i \geq \alpha_i \quad (3.31a)$$

that must be compatible with the fact that

$$\sum_{i=1}^M \alpha_i = 1 \quad (3.31b)$$

More specifically, we require that

$$\bar{\alpha}_i \geq 0 \quad , \quad \sum_{i=1}^M \bar{\alpha}_i \geq 1 \quad (3.32a)$$

In view of these definitions, the constraints that $\bar{\mathcal{U}}$, $\delta\mathcal{U}_i$, $\bar{\alpha}_i$, \mathbb{X}_i^F , $i = 1, \dots, M$ must fulfill are here listed

- I) Conditions (3.9a), (3.9b) must be verified for all admissible values of α_i , i.e., it must hold that

$$\delta\mathcal{U}_i \oplus \bar{\alpha}_i \bar{\mathcal{U}} \subseteq \mathcal{U}_i \quad (3.32b)$$

$$\left(\sum_{i \in \mathcal{S}} \bar{\alpha}_i \right) \bar{\mathcal{U}} \oplus \left(\bigoplus_{i \in \mathcal{S}} \delta\mathcal{U}_i \right) \subseteq \mathcal{U}_{\text{shared}} \quad (3.32c)$$

- II) The set \mathbb{X}_i^F in (3.30e) must be positively invariant with respect to $A_i^{N_L}$, i.e., it must guarantee that there exists a scalar $\lambda_i \in [0, 1)$ such that

$$A_i^{N_L} \mathbb{X}_i^F \subseteq \lambda_i \mathbb{X}_i^F \quad (3.32d)$$

This is always possible in view of Assumption 3.1.(1).

- III) To make the low-level regulators' optimization problems well posed (i.e., in order to make (3.15) possible and recursively feasible), the set of output conditions that can be reached in N_L steps by using $\delta u_i(h)$ in system (3.13) must be able to compensate for the effect of the input \bar{u} and of possible non-null initial conditions of $x_i^{(w)}$. This can be represented in set-theoretical way as follows

$$\begin{bmatrix} C_i \\ I_{n_i} \end{bmatrix} (\lambda_i \mathbb{X}_i^F \oplus \bar{\alpha}_i \bar{R}_i \bar{\mathcal{U}}) \subseteq \begin{bmatrix} 0 \\ I_{n_i} \end{bmatrix} \mathbb{X}_i^F \oplus \begin{bmatrix} C_i \\ I_{n_i} \end{bmatrix} (-\delta R_i \delta \mathcal{U}_i^{N_L}) \quad (3.32e)$$

Chapter 3. A hierarchical MPC scheme for coordination of independent systems with shared resources and plug-and-play capabilities

where

$$\bar{R}_i = A_i^{T_{L-1}} \sum_{j=0}^{N_L-1} A_i^j B_i, \quad \delta R_i = [A_i^{N_L-1} B_i, \dots, B_i]$$

and C_i^\perp is any matrix whose rows are perpendicular to the rows of C_i and complete the \mathbb{R}^n basis.

IV) Finally, to make such compensation possible also in steady state conditions for all admissible values of α_i ,

$$-\bar{\alpha}_i g_i^{[T_L]} \bar{\mathcal{U}} \subseteq \delta \mathcal{U}_i \quad (3.32f)$$

The following main result can now be stated (the proof is in the Appendix at the end of this chapter).

Theorem 3.1. *Under Assumptions 3.1 and 3.2, if the feasibility of the high-layer problem (3.26) and of the low-layer ones (3.30), for all $i = 1, \dots, M$, is verified at time $t = 0$, then feasibility is guaranteed:*

- for (3.26) at all time instants $h = kN_L, k \geq 0$;
- for (3.30), for all $i = 1, \dots, M$, at all time instants $h, h \geq 0$.

Also, (3.5), (3.6) hold for all $h \geq 0$ and (3.4) holds for all $h = kN_L$, where $k \geq 0$. Finally, as $h \rightarrow \infty, y(h) \rightarrow y_{\text{feas.ref}}$, where

$$y_{\text{feas.ref}} = \underset{E_1 y \in \mathcal{B}_u(\varepsilon)}{\operatorname{argmin}} \begin{bmatrix} \bar{C} \\ C^* \end{bmatrix} \|y - y_{\text{ref}}\|^2 \quad (3.33)$$

3.6 Static and dynamic optimization of the weights α_i and plug and play operations

In the control law (3.7), the term $\bar{u}(t)$ may be regarded as the total input request to the set of subsystems, and the parameters α_i represent the share of input assigned to each subsystem Σ_i . Their values can be chosen according to global optimality criteria by solving a static higher layer optimizer a priori, periodically, or based on an event-driven rationale. The optimization problem proposed here has the role of minimising the control signals, in order to minimize the overall cost for controlling the plant, but other alternative cost functions can be proposed and used.

3.6. Static and dynamic optimization of the weights α_i and plug and play operations

In steady-state, from (3.16), the input \bar{u} must take the value \bar{u}^{ss} such that

$$\left(\sum_{i=1}^M \alpha_i \sum_{l=1}^{T_H} G_l^{i,[N_L]} \right) \bar{u}^{ss} = y_{\text{ref}} \quad (3.34)$$

Note that the matrix $\sum_{i=1}^M \alpha_i \sum_{l=1}^{T_H} G_l^{i,[N_L]}$ has full rank in view of Assumption 3.2 and Proposition 3.1. Also, to make $w_i = 0$, from (3.13), $\delta u_i = -\alpha_i g_i^{[T_L]} \bar{u}^{ss}$, Therefore, in steady state, the input u_i must take the value

$$u_i^{ss} = \alpha_i (I_m - g_i^{[T_L]}) \bar{u}^{ss} \quad (3.35)$$

The proposed minimization problem reads

$$\min_{\bar{u}^{ss}, \{u_i^{ss}, \alpha_i\}_{i=1, \dots, M}} \sum_{i=1}^M q_i^\alpha \|u_i^{ss}\|^2 \quad (3.36)$$

subject to (3.32a), (3.31), and where q_i^α is a suitable cost associated to the use of subsystem Σ_i . Note that the resulting optimization problem is a quadratic one with bilinear constraints.

3.6.1 Time varying weights

We consider now the case where the weights α_i change during the system operation, and how this impacts on the control scheme at both dynamic control layers. This will pave the way for the application in plug and play scenarios in the subsequent Section 3.6.2. At this point, we will only make the assumption that the weight optimization problem (3.36) is run during the system operation, and that the changes are applied at the beginning of long sampling times $h = kN_L$ (resulting constant for the low-layer problems). In general, we denote by $\alpha_i(k)$ the values taken by α_i at time $h = kN_L$, for all $i = 1, \dots, M$.

3.6.1.1 High level control during weight changes

At time $h = kN_L$, the model (3.16) must be rewritten as

$$y^{[N_L]}(k) = \sum_{l=1}^{T_H} G_{l,k}^{[N_L]} \bar{u}^{[N_L]}(k-l) \quad (3.37)$$

where $G_{l,k}^{[N_L]} = \sum_{i=1}^M \alpha_i(k-l) G_l^{i,[N_L]}$. A variation of the weights α_i , $i = 1, \dots, M$ during the system operation may compromise the feasibility properties of the high layer control scheme. For this reason a three-step procedure is proposed.

Chapter 3. A hierarchical MPC scheme for coordination of independent systems with shared resources and plug-and-play capabilities

1. Based on periodic or event-based call, a weight change is proposed by the optimizer running (3.36). The candidate new weights, denoted α_i^* , $i = 1, \dots, M$, are transmitted at time \bar{t} to the high-level dynamic controller, but are not directly applied.
2. The feasibility of the optimization problem (3.29) is checked at a time instant $t = \bar{t}$ where the output variable is computed based on (3.37), with $\alpha_i(k) = \alpha_i^-$ for all $k < t$, where α_i^- is the value taken by the weight before the variation request, while $\alpha_i(k) = \alpha_i^*$ for all $k \geq t$. If the feasibility of the problem is verified, then we can set $\alpha_i(t) = \alpha_i^*$ for all $i = 1, \dots, M$, for all $t \geq \bar{t}$. Otherwise go to step 3.
3. Solve, at any time instant $t \geq \bar{t}$

$$\min_{\substack{\vec{u} \\ r(t), \Delta \vec{u}^{[N_L]}(t:t+N_H-1), \alpha_1(t), \dots, \alpha_M(t)}} \tilde{J}_{\text{HL}} + \gamma_\alpha \sum_{i=1}^M \|\alpha_i(t) - \alpha_i^*\|^2 \quad (3.38)$$

subject to the dynamical system (3.37), where it is assumed that $\alpha_i(k) = \alpha_i(t)$ is kept constant for all $k \geq t$. The constraints are (3.29b)-(3.29f), where the term $G_l^{[N_L]}$ is replaced by $G_{l,k}^{[N_L]}$, and (3.32a), (3.31).

Note that the feasibility of the problem (3.38) is guaranteed by the fact that one can always keep $\alpha_i(t)$ constant at the last feasible value.

3.6.1.2 Low level control during weight changes

The low-level optimization problem (3.30) is less critical than the high-level one. Indeed, as already remarked, it is assumed that weight α_i remains constant over the long sampling time, i.e., during the low-level shrinking-horizon optimization problem for all $h \in [kN_L, \dots, (k+1)N_L - 1]$. Therefore, the results obtained on recursive feasibility still hold thanks to the terminal constraint (3.30e) and to the definition of \mathbb{X}_i^F , which is given for all admissible values of $\alpha_i \leq \bar{\alpha}_i$.

3.6.2 Plug and play operations

The scenario in which one or more subsystems join or leave the network may be naturally included in the framework in which the weights α_i are time varying. We can distinguish two main cases, the plug-in and the unplug cases.

3.6. Static and dynamic optimization of the weights α_i and plug and play operations

3.6.2.1 Plug-in requests

Assume that, at time instants $t \leq \bar{t}$, the system is controlled using the scheme proposed in this paper and is composed of M subsystems. At time \bar{t} a plug-in request is received, i.e., we want to include subsystem $M + 1$ in the network. Note that the case in which Σ_{M+1} is not plugged-in is equivalent to the case in which Σ_{M+1} is plugged-in, but with weight $\alpha_{M+1} = 0$. Thanks to this simple remark, we can define a plug-in procedure, consisting of the following steps.

1. Structural plug-in design: define a triple $(\bar{\alpha}_{M+1}, \delta \mathcal{U}_{M+1}, \mathbb{X}_{M+1}^F)$ satisfying the conditions (3.32).
2. Feasibility plug-in test: set $\alpha_{M+1} = 0$ and check the feasibility of the low-level problem (3.30).

If these steps have been successfully carried out, then the subsystem Σ_{M+1} is formally plugged in. At this point, we may run the procedure sketched in Section 3.6.1 to properly take advantage of the newly-plugged device.

3.6.2.2 Unplug requests

Assume that, at time instants $t \leq \bar{t}$, the system is controlled using the scheme proposed in this paper and is composed of M subsystems. At time \bar{t} , an unplug request is received, i.e., we want to exclude subsystem M from the network. Note that the case in which Σ_M gets unplugged can be achieved by setting $\alpha_M = 0$. In view of this, the unplug operation consists of the following steps.

1. Structural unplug condition: check the feasibility of the optimization problem (3.36) with the further constraint $\alpha_M = 0$.
2. Run the procedure sketched in Section 3.6.1 to adapt the system to the new configuration. Note that, if we resort to the step 3 outlined in Section 3.6.1, the solution $\alpha_i(t) = \alpha_i^*$ is achieved in steady state (i.e., after a large number of steps) and only if y_{ref} is an admissible steady state. To overcome these problems, we suggest to repeat step 2 periodically. If this does not work, it is possible to fix $r(t)$ to its last feasible value and disregard it as optimization variable, and check if, in this way, $\alpha_i(t) = \alpha_i^*$ is achieved at least asymptotically.

If the steps above are successfully carried out, then we can remove the subsystem Σ_M from the overall plant. Otherwise, the system cannot support an unplug event and the request is denied.

Chapter 3. A hierarchical MPC scheme for coordination of independent systems with shared resources and plug-and-play capabilities

3.7 Simulation example

The hierarchical control algorithm described in the previous sections has been used for coordination of a number of synchronous machines.

3.7.1 Description of the models

Consider six diesel generators connected to a network with terminal voltage 240 V and frequency 60 Hz, that must track a total electrical power ($y_{\text{ref}} = 98.32$ kW). The values of their rated powers are $\{16.1, 25.0, 26.5, 30.7, 40.8, 47.6\}$ kW, respectively. The linear continuous models of the generators are obtained from [192], and are of orders, $n_1 = n_6 = 9$, $n_2 = n_3 = 8$, $n_4 = 4$, $n_5 = 5$. The input u_i and output y_i , for all $i = 1, \dots, 6$, are the fuel flow rate and the produced power, respectively, with $m = 1$ and $p = 1$. The six generators' linear continuous-time models have been sampled with $\Delta t = 1s$ to obtain their discrete-time counterpart of the fast time scale. Then, these discrete-time subsystems have been used as the models in (3.1) for the implementation of the hierarchical control structure. The control variables, as well as the controlled variables, are limited by $0 \leq (u_1, \dots, u_6) \leq (0.89, 1.39, 1.48, 1.71, 2.27, 2.64)$ g/s and $0 \leq (y_1, \dots, y_6) \leq (16.1, 25.0, 26.5, 30.7, 40.8, 47.6)$ kW. The considered constraint on input sharing is $0 \leq \sum_{i=3}^5 u_i \leq 4.4$.

3.7.2 Design of the sets

- We first set $T_L = 60$, $T_H = 6$, and $N_L = 10$.
- The parameters $\bar{\alpha}_i$ and the sets $\bar{\mathcal{U}}, \delta\mathcal{U}_i, i = 1, \dots, 6$, have been selected as $(\bar{\alpha}_1, \dots, \bar{\alpha}_6) = (0.1634, 0.1919, 0.2537, 0.2699, 0.3122, 0.4065)$, $\bar{\mathcal{U}} = [1.2, 4.02]$, and $\delta\mathcal{U}_1 = [-0.20, 0.23]$, $\delta\mathcal{U}_2 = [-0.23, 0.62]$, $\delta\mathcal{U}_3 = [-0.30, 0.30]$, $\delta\mathcal{U}_4 = [-0.33, 0.38]$, $\delta\mathcal{U}_5 = [-0.37, 0.36]$, $\delta\mathcal{U}_6 = [-0.49, 1.07]$ so that (3.32b) and (3.32c) are verified.
- The sets $\mathbb{X}_i^F, i = 1, \dots, 6$, have been chosen as $\mathbb{X}_i^F = \{x_i^{(w)} \mid (x_i^{(w)} - \alpha_i g_i^x \bar{u}_{\text{feas.ref}})^T P_i (x_i^{(w)} - \alpha_i g_i^x \bar{u}_{\text{feas.ref}}) \leq \mu_i\}$ where $\bar{u}_{\text{feas.ref}} = (\sum_{l=1}^{T_H} G_l^{[N_L]})^{-1} y_{\text{feas.ref}}$, P_i has been taken as the solution to the Riccati equation related to the infinite horizon control problem with $Q_{x,i} = I_{n_i}$, $R_i = 0.1I_m$, while μ_i here has been set to 0.1. Condition (3.32d) has been checked by verifying the feasibility of the following optimization problem for $i =$

3.7. Simulation example

$1, \dots, 6$:

$$\begin{aligned} & \min \quad \lambda_i \\ & \text{subject to} \quad (A_i^{N_L})^T P_i A_i^{N_L} - \lambda_i^2 P_i < 0 \\ & \quad \quad \quad \lambda_i \in [0, 1) \end{aligned} \quad (3.39)$$

- Condition (3.32e) has been checked for $i = 1, \dots, 6$, by verifying

$$\bar{\alpha}_i \bar{R}_i \bar{\mathcal{U}}_i \subseteq -\delta R_i \delta \mathcal{U}_i^{N_L}$$

and

$$C_i \lambda_i \mathbb{X}_i^F \subseteq \bar{\mathbb{X}}_i$$

where $\bar{\mathbb{X}}_i$ is the maximum volume ellipsoid in $C_i(-\delta R_i \delta \mathcal{U}_i^{N_L}) \ominus C_i \bar{\alpha}_i \bar{R}_i \bar{\mathcal{U}}_i$ and can be computed according to the algorithm described in Section 8.4.2 in [23].

Table 3.1: On-line computation time comparison

Approach		Optimization activated at	Average computation time (s)	
Proposed one	HL regulator	$h = kN_L$	0.360	
	LL regulator	1	each fast time instant h	0.278
		2	each fast time instant h	0.163
		3	each fast time instant h	0.278
		4	each fast time instant h	0.276
		5	each fast time instant h	0.276
Centralized MPC		each fast time instant h	1.756	

3.7.3 Simulation results without plug-and-play operations

The hierarchical control structure has been applied to the system with only five generators, i.e., $M = 5$, assuming that the sixth generator is disconnected from the network. The optimization problem (3.36) has been solved with $(q_1^\alpha, \dots, q_5^\alpha) = (0.779, 0.812, 0.823, 0.830, 0.837)$. The values of the parameters \bar{u}^{ss} , u_i^{ss} and α_i , $i = 1, \dots, 5$, are: $\bar{u}^{ss} = 6.28$, $(u_1^{ss}, \dots, u_5^{ss}) = (0.89, 1.20, 1.19, 1.16, 1.12)$, $(\alpha_1, \dots, \alpha_5) = (0.1496, 0.2107, 0.2191, 0.2028, 0.2178)$. The high layer MPC has been designed with prediction horizon $N_H = 10$, penalties $Q_y = I_p$ and $R_H = 0.1I_m$, while the control gain K^{aux} has been selected according to Proposition 3.2 and the matrix P has been computed as the solution to the Lyapunov equation (3.26d) with Q_y and R_H . The parameter γ has been chosen as $\gamma = 10P_{yy} = 24.99$. The low layer shrinking horizon optimization algorithms have been solved with state and input penalties $Q_i = 10I_p$, $R_i = 0.1I_m$, $i = 1, \dots, 5$. It is worth mentioning that a penalty on the deviation of the input has also been added, having

Chapter 3. A hierarchical MPC scheme for coordination of independent systems with shared resources and plug-and-play capabilities

weight $R_{\Delta,i} = I_m$, during the transient phase to enforce smooth dynamic behavior and must be removed once the regulator is close to its steady state. For comparison, a centralized state-feedback MPC has been designed at any fast time h with cost function $J_c = \sum_{k=h}^{h+N-1} \|\sum_{i=1}^5 C_i x_i(k) - y_{\text{ref}}\|_{Q_c}^2 + \sum_{i=1}^5 q_i^\alpha \|u_i(k)\|^2$ where the penalty $Q_c = 500$ and prediction horizon $N = N_H \cdot N_L = 100$. The terminal set has been chosen as $\mathcal{X}_F = \{x | \sum_{i=1}^5 C_i x_i(t+N) = y_{\text{ref}}\}$. All the simulation tests have been implemented with the MATLAB Yalmip and MPT toolbox, see [108] and [79], in a PC with Intel Core i5-4200U 2.30 GHz and with Windows 10 operating system. The Matlab QUADPROG solver has been used for the implementation of the centralized MPC and the proposed optimization algorithms. The detailed on-line computational time required by each controller is reported in Table 3.1, showing the computational advantages of the proposed hierarchical scheme.

The evolution of the control and output variables of the controlled subsystems are reported in Figures 3.1 and 3.2 which show that, after an initial transient, the inputs and outputs return to their nominal values, and both the separation of total electrical power and the control performance in terms of the proposed two-layer approach are close to those of centralized MPC.

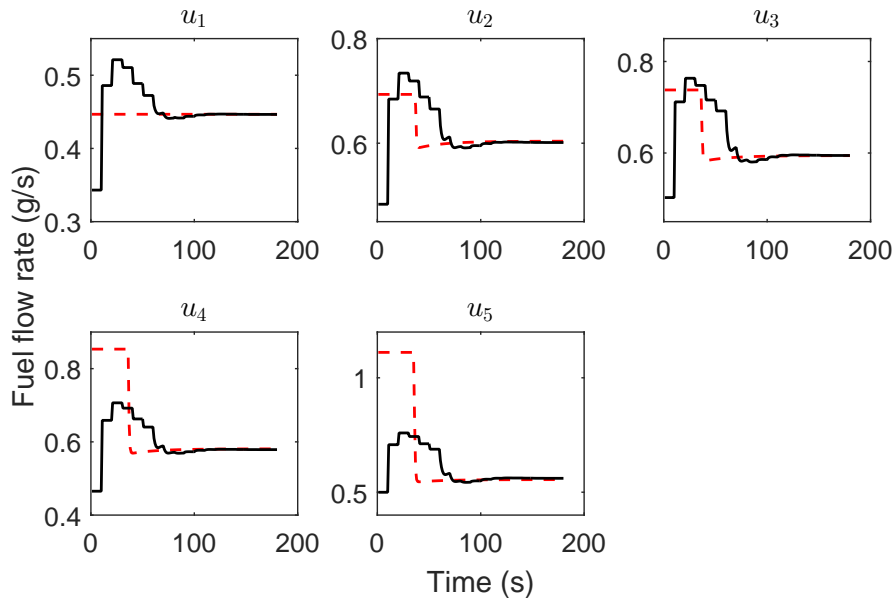


Figure 3.1: Control variables of the controlled generators: overall control actions computed with the two-layer scheme (black solid lines) and control variables computed with the centralized scheme (red dashed lines).

3.8. Conclusions

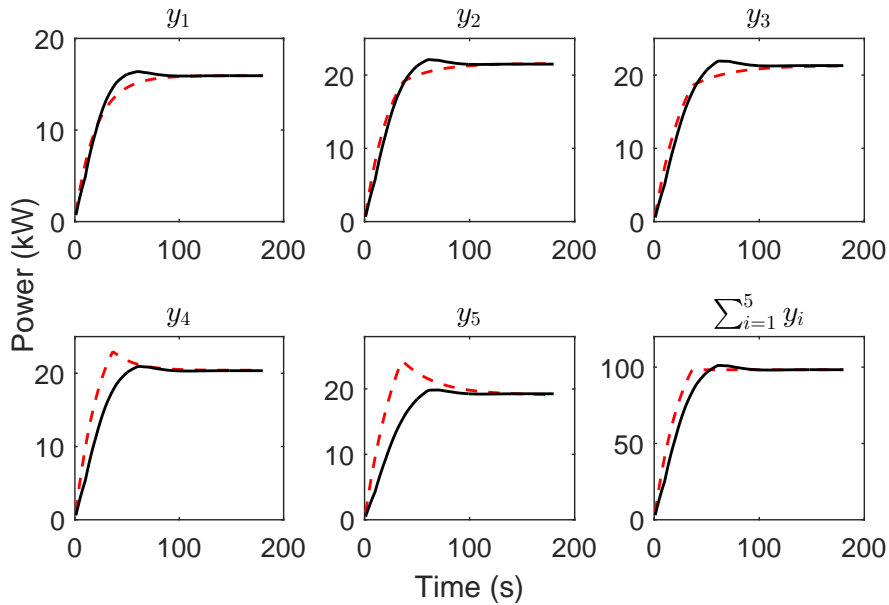


Figure 3.2: Outputs of the controlled generators: outputs obtained with the two-layer scheme (black solid lines) and outputs obtained with the centralized scheme (red dashed lines).

3.7.4 Simulation results with plug-and-play operations

The two-layer control structure has also been applied with plug-and-play operations. Starting from the simulation conditions of scenario 1, at time $t = 180$ s, the 6th generator has been added to the network; then, at time $t = 360$ s, the third generator has been disconnected by setting $\alpha_3 = 0$. The evolution of the output and control variables of the controlled system are reported in Figures 3.3 and 3.4. These figures show that, after an initial transient due to the plug-in procedure, inputs and outputs return to their current nominal values until the next plug-out operation occurs, when the two-layer control system properly reacts to bring the controlled variables to their new reference values.

3.8 Conclusions

In this chapter, a hierarchical control scheme has been proposed for the coordination of independent systems. Among its main characteristics we recall the possibility to consider shared input constraints as well as joint output constraints and the simplicity of the procedure required to obtain the

Chapter 3. A hierarchical MPC scheme for coordination of independent systems with shared resources and plug-and-play capabilities

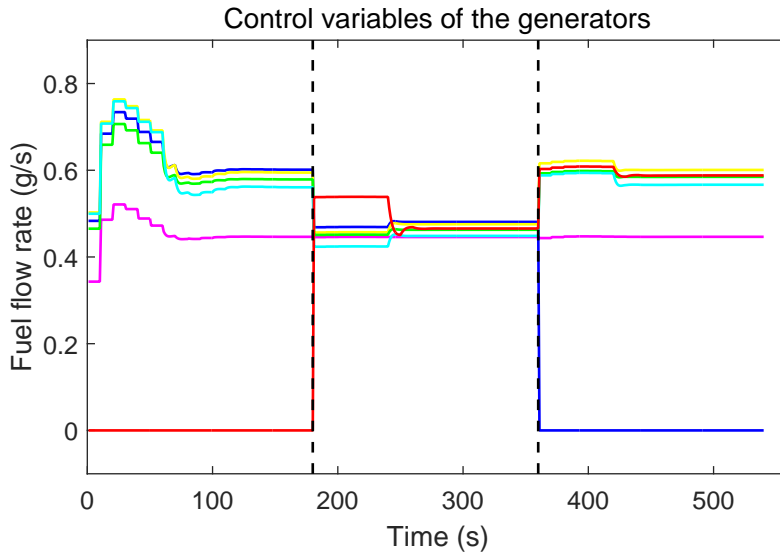


Figure 3.3: Control variables of the controlled generators: overall control actions (u_1, \dots, u_6), (magenta, blue, yellow, green, cyan, and red solid lines). Vertical dashed lines indicate the plug-in/unplug instants.

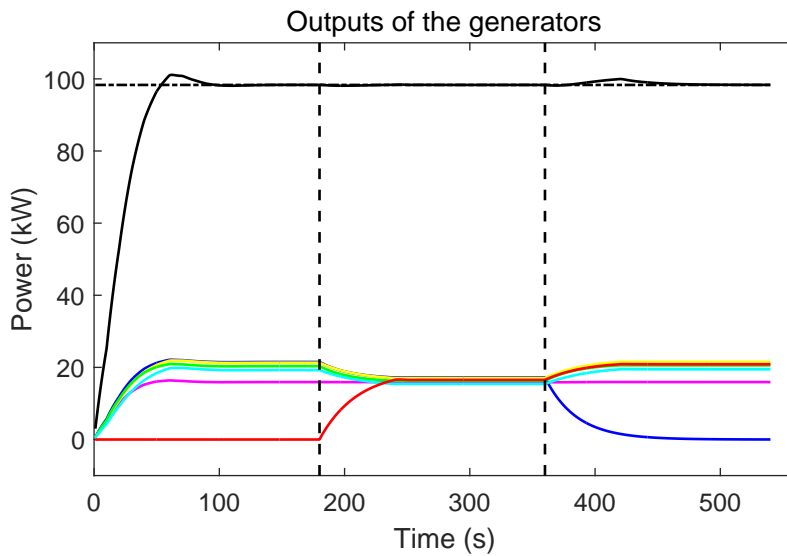


Figure 3.4: Outputs of the controlled generators: outputs ($y_1, \dots, y_6, \sum_{i=1}^6 y_i$), (magenta, blue, yellow, green, cyan, red, and black solid lines) and reference power (black dash-dotted line). Vertical dashed lines indicate the plug-in/unplug instants.

3.9. Appendix

simplified model at the high layer of the hierarchical structure. In addition, the algorithm allows to consider long term objectives at the high layer, for instance based on economic criteria, and short term goals at the low layer, typically fast compensation of disturbances and model mismatch. Finally, a procedure is suggested to determine the optimal usage of the subsystems and to include the possibility to consider plug and play operations, so as to provide flexibility and practical fault tolerance to the scheme. The recursive feasibility and convergence properties of the closed-loop system have been established and a simulation example has been reported to illustrate the algorithm’s behavior.

3.9 Appendix

3.9.1 Proof of Proposition 3.1

According to the PBH test, the pair (\bar{A}, \bar{B}) is reachable if and only if, for all $\lambda \in \mathbb{C}$,

$$\text{rank} \left(\begin{bmatrix} \lambda I_{m \cdot (T_H+1)} - \bar{A} & \bar{B} \end{bmatrix} \right) = m \cdot (T_H + 1)$$

i.e., if and only if

$$\begin{bmatrix} (\lambda I_{m \cdot (T_H+1)} - \bar{A})^T \\ \bar{B}^T \end{bmatrix} v = 0 \quad (3.40)$$

implies that $v = 0$. We take $v = (v_1, \dots, v_{T_H+1})$ where $v_l \in \mathbb{R}^m$ for all $l = 1, \dots, T_H$. Equation (3.40) can be rewritten as

$$\begin{cases} (\lambda - 1)v_1 & = 0 \\ \lambda v_2 - (G_2^{[N_L]})^T v_1 - v_3 & = 0 \\ \vdots & \\ \lambda v_{T_H-1} - (G_{T_H-1}^{[N_L]})^T v_1 - v_{T_H} & = 0 \\ \lambda v_{T_H} - (G_{T_H}^{[N_L]})^T v_1 - v_{T_H+1} & = 0 \\ \lambda v_{T_H+1} & = 0 \\ (G_1^{[N_L]})^T v_1 + v_2 & = 0 \end{cases}$$

It is easy to see that, if $\lambda \neq 1$, the only solution to this homogeneous system is $v_l = 0$ for all $l = 1, \dots, T_H + 1$. If $\lambda = 1$, we obtain $v_{T_H+1} = 0$ and, for all $i = 2, \dots, T_H$, $v_i = \left(\sum_{l=i}^{T_H} (G_l^{[N_L]})^T \right) v_1$ and, from the last equation

Chapter 3. A hierarchical MPC scheme for coordination of independent systems with shared resources and plug-and-play capabilities

$(\sum_{l=1}^{T_H} (G_i^{[N_L]})^T) v_1 = 0$. The latter implies that $v_1 = 0$ is the only admissible solution if and only if $\det(\sum_{l=1}^{T_H} (G_i^{[N_L]})^T) \neq 0$. \square

3.9.2 Proof of Proposition 3.2

Setting $K^{\text{aux}} = \begin{bmatrix} -(1-\varepsilon)(G_1^{[N_L]})^{-1} & 0 & \dots & 0 \end{bmatrix}$, we obtain that

$$F^{\text{aux}} = \begin{bmatrix} \varepsilon I_p & G_2^{[N_L]} & \dots & G_{T_H-1}^{[N_L]} & G_{T_H}^{[N_L]} & 0 \\ -(G_1^{[N_L]})^{-1}(1-\varepsilon) & 0 & \dots & 0 & 0 & 0 \\ 0 & I_m & \dots & 0 & 0 & 0 \\ \vdots & \vdots & \ddots & \vdots & \vdots & \vdots \\ 0 & 0 & \dots & I_m & 0 & 0 \\ 0 & 0 & \dots & 0 & I_m & 0 \end{bmatrix}$$

The eigenvalues of F^{aux} are the solutions to the characteristic equation $I_p z^{T_H+1} - \varepsilon I_m z^{T_H} + (1-\varepsilon)G_2^{[N_L]}(G_1^{[N_L]})^{-1}z^{T_H-2} + \dots + (1-\varepsilon)G_{T_H}^{[N_L]}(G_1^{[N_L]})^{-1}z = 0$. In view of [131], F^{aux} is Schur stable if

$$\left\| \begin{bmatrix} \varepsilon I_p & (1-\varepsilon)G_2^{[N_L]}(G_1^{[N_L]})^{-1} & \dots & (1-\varepsilon)G_{T_H}^{[N_L]}(G_1^{[N_L]})^{-1} \end{bmatrix} \right\|_{\infty} < 1$$

i.e., if

$$(1-\varepsilon) \left\| \begin{bmatrix} G_2^{[N_L]}(G_1^{[N_L]})^{-1} & \dots & G_{T_H}^{[N_L]}(G_1^{[N_L]})^{-1} \end{bmatrix} \right\|_{\infty} < 1 - \varepsilon$$

\square

3.9.3 Proof of Theorem 3.1

Recursive feasibility of the low-level problem (3.30)

Assume that the problem is feasible for subsystem Σ_i at time $h \in \{kN_L, \dots, (k+1)N_L - 1\}$, i.e., an optimal sequence $\delta u_i(h|h), \dots, \delta u_i((k+1)N_L - 1|h)$ is available, allowing to satisfy the constraints (3.30d), (3.30e) in face of input $\bar{u}(s - T_L) = \bar{u}^{[N_L]}(k - T_H)$, constant for all $s = kN_L, \dots, (k+1)N_L - 1$. At time h the input value $\delta u_i(h|h)$ is applied, and the remaining sequence $\delta u_i(h+1|h), \dots, \delta u_i((k+1)N_L - 1|h)$ is feasible at time h , since the problem is a shrinking-horizon one.

Note that, at time $h = (k+1)N_L$ (i.e., at the beginning of the subsequent

3.9. Appendix

high-level sampling time), the state $x_i^{(w)}((k+1)N_L)$ enjoys (3.30e). To guarantee recursive feasibility, for any input $\bar{u}^{[N_L]}(h - T_H) = \bar{u}^{[N_L]}(k+1 - T_H)$ (constant for all $h = (k+1)N_L, \dots, (k+2)N_L - 1$) there must exist an input sequence $\delta \vec{u}_i(k+1) = \delta u_i((k+1)N_L), \dots, \delta u_i((k+2)N_L - 1)$ such that $w_i((k+2)N_L) = 0$ and $x_i^{(w)}((k+2)N_L) \in \mathbb{X}_i^F$. So, we require the existence of $\delta \vec{u}_i(k+1)$ such that, at the same time

$$\begin{aligned} C_i(A_i^{N_L}x_i^{(w)}((k+1)N_L) + \alpha_i\bar{R}_i\bar{u}^{[N_L]}(k+1) + \delta R_i\delta \vec{u}_i(k+1)) &= 0 \\ A_i^{N_L}x_i^{(w)}((k+1)N_L) + \alpha_i\bar{R}_i\bar{u}^{[N_L]}(k+1) + \delta R_i\delta \vec{u}_i(k+1) &\in \mathbb{X}_i^F \end{aligned}$$

Note that, if $x_i^{(w)}((k+1)N_L) \in \mathbb{X}_i^F$, in view of (3.32d), then $A_i^{N_L}x_i^{(w)}((k+1)N_L) \in \lambda_i\mathbb{X}_i^F$. Thanks to (3.32e), there exists a sequence $\delta \vec{u}_i(k+1) \in \delta \mathcal{U}_i^{N_L}$ such that both (3.30d) and (3.30e) can be verified for all inputs $\bar{u}^{[N_L]}(k+1) \in \bar{\mathcal{U}}$. \square

Recursive feasibility and convergence of the high-level problem (3.26)

Thanks to the recursive feasibility properties of the low-level problems (3.30), it is possible to guarantee that $w_i(kN_L) = 0$ for all $i = 1, \dots, M$ and for all $k \geq 0$, in view of the feasibility of the problems (3.30) at time $h = 0$. In view of this, it is possible to describe the evolution of variable $y^{[N_L]}(k)$ using the dynamical model (3.18). This allows to apply Theorem 1 in [19]. In particular, it is proved that the high-level problem (3.26) enjoys recursive feasibility properties and that $y^{[N_L]}(k) \rightarrow y_{\text{feas.ref}}$ and $\bar{u}^{[N_L]}(k) \rightarrow \bar{u}_{\text{feas.ref}}$, as $k \rightarrow +\infty$.

Since constraint (3.21) is respected at all $k \geq 0$, then $y^{[N_L]}(k) = y(kN_L) \in \mathcal{Y}$ and $\bar{u}^{[N_L]}(k) \in \bar{\mathcal{U}}$ for all $k \geq 0$. Furthermore, since constraint (3.30c) is verified at low level then, from (3.9a), (3.9b), and (3.31), for all $i = 1, \dots, M$ and for all $h \geq 0$, $u_i(h) = \alpha_i\bar{u}^{[N_L]}(\lfloor h/N_L \rfloor) + \delta u_i(h) \in \mathcal{U}_i$ and $\sum_{i \in \mathcal{S}} u_i(h) = \sum_{i \in \mathcal{S}} \alpha_i\bar{u}^{[N_L]}(\lfloor h/N_L \rfloor) + \sum_{i \in \mathcal{S}} \delta u_i(h) \in \mathcal{U}_{\text{shared}}$, as required for satisfying (3.5) and (3.6), respectively, for all $h \geq 0$. \square

Convergence of the low-level problem (3.30)

The evolution of variable $x_i^{(w)}(h)$ on a N_L -steps sampling time is

$$\begin{aligned} x_i^{(w)}((k+1)N_L) &= A_i^{N_L}x_i^{(w)}(kN_L) + \delta R_i\delta \vec{u}_i(k) + \alpha_i\bar{R}_i\bar{u}^{[N_L]}(k - T_H) \\ w_i(kN_L) &= C_ix_i^{(w)}(kN_L) \end{aligned} \tag{3.41}$$

Chapter 3. A hierarchical MPC scheme for coordination of independent systems with shared resources and plug-and-play capabilities

Now, define $\varepsilon_i^x(k) = x_i^{(w)}(kN_L) - \alpha_i g_i^x \bar{u}^{[N_L]}(k - T_H)$, where $g_i^x = (I - A_i)^{-1} (A_i^{T_L} B_i - B_i g_i^{[T_L]})$. Also, define $\varepsilon_i^u(k) = \delta \vec{u}_i(k) + \mathbb{1} \otimes (\alpha_i g_i^{[T_L]} \bar{u}^{[N_L]}(k - T_H))$. Under this change of coordinates, we can rewrite (3.41) as

$$\begin{aligned} \varepsilon_i^x(k+1) &= A_i^{N_L} \varepsilon_i^x(k) + \delta R_i \varepsilon_i^u(k) + v_i(k) \\ \bar{w}_i(k) &= w_i(kN_L) = C_i \varepsilon_i^x(k) \end{aligned} \quad (3.42)$$

where $v_i(k) = \alpha_i g_i^x (\bar{u}^{[N_L]}(k - T_H) - \bar{u}^{[N_L]}(k + 1 - T_H))$ can be accounted for as a (vanishing) disturbance. In view of constraint (3.30d), $\bar{w}_i(k) = 0$ for all $k \geq 0$. We can write $\bar{w}_i(k) = w_i^{FREE}(k) + w_i^{FORCED}(k) = 0$, where $w_i^{FREE}(k)$ and $w_i^{FORCED}(k)$ are the free and forced, respectively, motions of variable $\bar{w}_i(k)$. Therefore $w_i^{FORCED}(k) = -w_i^{FREE}(k) = -C_i A_i^{k(N_L)} \varepsilon_i^x(0) \rightarrow 0$ as $k \rightarrow +\infty$ in view of Assumption 3.1. Similarly to Proposition 2.3, if $C_i(zI_{n_i} - A_i^{N_L})^{-1}$ has no zeros on the unitary circle, then

$$\lim_{k \rightarrow +\infty} (\delta R_i \varepsilon_i^u(k) + v_i(k)) = 0$$

Consequently, $\lim_{k \rightarrow +\infty} \varepsilon_i^x(k) = 0$ (i.e., $\lim_{k \rightarrow +\infty} x_i^{(w)}(kN_L) = \alpha_i g_i^x \bar{u}_{\text{feas.ref}}$) follows from the asymptotic stability of (3.42) and from the fact that $\lim_{k \rightarrow +\infty} \bar{u}^{[N_L]}(k) = \bar{u}_{\text{feas.ref}}$. This also implies that $\lim_{h \rightarrow +\infty} \delta u_i(h) + \alpha_i g_i^{[T_L]} \bar{u}_{\text{feas.ref}} = 0$, in view of the fact that, when $x_i^{(w)}(kN_L) = \alpha_i g_i^x \bar{u}_{\text{feas.ref}}$, in stationary conditions $\delta u_i(h) = -\alpha_i g_i^{[T_L]} \bar{u}_{\text{feas.ref}}$ minimizes the cost function (3.30b). This, in turns, implies that $\lim_{h \rightarrow +\infty} w_i(h) = 0$ and that $\lim_{h \rightarrow +\infty} y(h) = \bar{y}_{\text{feas.ref}}$. \square

CHAPTER 4

Hierarchical multi-rate MPC scheme for interconnected systems

4.1 Introduction and main idea

Physical and cyber-physical systems are becoming more and more complex, large-scale, and heterogeneous due to the growing opportunities provided by information technology in terms of computing power, transmission of information, and networking capabilities. As described in Chapter 1, a classic approach in terms of the management and control of these systems consists of resorting to decentralized or distributed MPC, in which distributed MPC algorithms can be cooperative, characterized by an intensive transmission load due to the multiple exchange of information among the regulators within one sampling period, or non-cooperative, characterized conservativeness to compensate for the effects of neglected dynamics. With the aim of reducing the above limitations of distributed MPC algorithms, in this chapter, we extend the hierarchical control structure described in Chapter 2 to large-scale interconnected systems. The control scheme is shown in Figure 4.1. The system under control Σ is assumed to be composed by M interconnected subsystems $\Sigma_1, \dots, \Sigma_M$. A reduced order

Chapter 4. Hierarchical multi-rate MPC scheme for interconnected systems

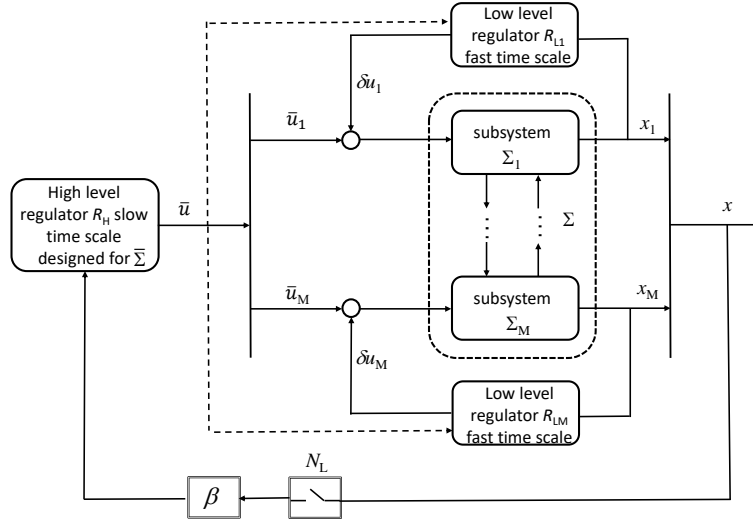


Figure 4.1: Overall control scheme.

model $\bar{\Sigma}$ is first computed and a centralized MPC regulator R_H working at a slow rate is designed to consider the long-term behavior of the system and to compute the control variables \bar{u}_i , $i = 1, \dots, M$. Then, faster local regulators R_{Li} , $i = 1, \dots, M$, are designed for each subsystem Σ_i to compute the control contributions δu_i compensating for the inaccuracies of the high layer design due to the mismatch between Σ and $\bar{\Sigma}$. Notably, the local regulators can be designed and implemented at different rates to cope with subsystems operating at different time scales, as it often happens in many important industrial fields, see the centralized multirate MPC methods reported in [11, 18, 28, 29, 97, 101, 160], or the multirate implementations described in [76, 156, 195].

Compared with Chapter 2, the control structure is similar while the framework is different. For instance, in Chapter 2 only independent systems Σ_i with joint output constraints were considered, no multirate implementations were allowed, and the problem was to coordinate the Σ_i 's to guarantee an overall output request, so that different technical tools, with respect to the ones here considered, had to be adopted at the two layers of the control structure.

The chapter is organized as follows. Section 4.2 introduces the models considered at the two layers. Section 4.3 describes the MPC algorithms adopted at the two layers, while Section 4.4 presents the main feasibility and convergence results as well as a summary of the main implementation aspects. Section 4.5 describes the simulation examples, while in Section

4.2. Models for the two-layer control scheme

4.6 some conclusions are drawn. The proofs of the main results are reported in an Appendix.

4.2 Models for the two-layer control scheme

In this section we present the model of the overall system and the simplified one used for high-level control.

4.2.1 Large-scale system model

In line with [110], we assume that the overall system Σ is composed by M discrete-time, linear, interacting subsystems described by

$$\Sigma_i : \begin{cases} x_i(h+1) &= A_L^{ii}x_i(h) + B_L^{ii}u_i(h) + E_L^i s_i(h) \\ y_i(h) &= C_L^{ii}x_i(h) \\ z_i(h) &= C_L^{zi}x_i(h), \end{cases} \quad (4.1)$$

$i = 1, 2, \dots, M$, where $x_i \in \mathbb{R}^{n_i}$, $u_i \in \mathbb{R}^{m_i}$, and $y_i \in \mathbb{R}^{p_i}$ are the state, input, and output vectors, while h is the discrete-time index in the basic time scale according to which the models are defined and the low level regulators will be designed. The interconnections among the subsystems Σ_i are represented by the coupling input and output vectors $s_i \in \mathbb{R}^{p_{si}}$ and $z_i \in \mathbb{R}^{p_{zi}}$, respectively, where

$$s_i(h) = \sum_{j=1}^M L_{ij}z_j(h) \quad (4.2)$$

with $L_{ii} = 0$, $i = 1, \dots, M$.

From (4.1) and (4.2), the overall dynamical model Σ is

$$\Sigma : \begin{cases} x(h+1) &= A_L x(h) + B_L u(h) \\ y(h) &= C_L x(h) \end{cases} \quad (4.3)$$

where $x = (x_1, \dots, x_M) \in \mathbb{R}^n$, $n = \sum_{i=1}^M n_i$, $u = (u_1, \dots, u_M) \in \mathbb{R}^m$, $m = \sum_{i=1}^M m_i$, and $y = (y_1, \dots, y_M) \in \mathbb{R}^p$, $p = \sum_{i=1}^M p_i$. The diagonal blocks of A_L are state transition matrices A_L^{ii} , whereas the coupling terms among the Σ_i 's correspond to the non-diagonal blocks of A_L , i.e., $A_L^{ij} = E_L^i L_{ij} C_L^{zj}$, with $j \neq i$. The collective input and output matrices are $B_L = \text{diag}(B_L^{11}, \dots, B_L^{MM})$ and $C_L = \text{diag}(C_L^{11}, \dots, C_L^{MM})$, respectively.

Concerning systems (4.1) and (4.3), the following standing assumption is introduced:

Chapter 4. Hierarchical multi-rate MPC scheme for interconnected systems

Assumption 4.1.

(1) The state x_i is measurable, for each $i = 1, \dots, M$;

(2) A_L is Schur stable;

(3) $m = p$ and the system matrix $S_\Sigma = \begin{bmatrix} I_n - A_L & -B_L \\ C_L & 0 \end{bmatrix}$ has full rank $n + m$;

(4) B_L and C_L are full-rank matrices;

(5) the pair (A_L^{ii}, B_L^{ii}) is reachable, for each $i = 1, \dots, M$. \square

4.2.2 Reduced order models

For each subsystem Σ_i , $i = 1, \dots, M$, we define a reduced order model $\bar{\Sigma}_i$, $i = 1, \dots, M$, with state $\bar{x}_i \in \mathbb{R}^{\bar{n}_i}$, $\bar{n}_i \leq n_i$, and input $\bar{u}_i \in \mathbb{R}^{m_i}$. In a collective form, these systems $\bar{\Sigma}_i$ define the overall reduced order model

$$\bar{\Sigma}: \begin{cases} \bar{x}(h+1) &= A_H \bar{x}(h) + B_H \bar{u}(h) \\ \bar{y}(h) &= C_H \bar{x}(h) \end{cases} \quad (4.4)$$

where $\bar{x} = (\bar{x}_1, \dots, \bar{x}_M) \in \mathbb{R}^{\bar{n}}$, $\bar{n} = \sum_{i=1}^M \bar{n}_i$, $\bar{u} = (\bar{u}_1, \dots, \bar{u}_M) \in \mathbb{R}^m$, and $\bar{y} \in \mathbb{R}^p$. The reduced order models $\bar{\Sigma}_i$ can be defined according to different criteria. First, it is necessary that the stability properties of system Σ are inherited by $\bar{\Sigma}$. Moreover, we assume that for each subsystem $i = 1, \dots, M$ there exists a state projection $\beta_i: \mathbb{R}^{n_i} \rightarrow \mathbb{R}^{\bar{n}_i}$, $i = 1, \dots, M$, that allows to establish a connection between the states $x_i(h)$ of the original models and the states of the reduced models $\bar{x}_i(h)$. Collectively, we define $\beta = \text{diag}(\beta_1, \dots, \beta_M)$. In principle, the ideal case would be to verify that, if $\bar{u}(h) = u(h)$, then $\bar{x}(h) = \beta x(h)$ and $\bar{y}(h) = y(h)$ for all $h \geq 0$ for suitable initial conditions. However, due to model reduction approximations, this ideal assumption must be relaxed; instead, we just ask that $\bar{x} = \beta x$ and that $\bar{y} = y$ in steady-state conditions. We also require that, while matrix B_H can be full, the output matrix C_H preserves the block-diagonal form of C_L , i.e., that $C_H = \text{diag}(C_H^{11}, \dots, C_H^{MM})$, where $C_H^{ii} \in \mathbb{R}^{p_i \times \bar{n}_i}$ for all $i = 1, \dots, M$.

Overall, we require the following standing assumption to be satisfied to guarantee the compatibility of the models used at the two layers.

Assumption 4.2.

(1) A_H is Schur stable;

(2) β_i is full rank and is such that $C_H^{ii} \beta_i = C_L^{ii}$, for each $i = 1, \dots, M$;

4.3. Design of the hierarchical control structure

(3) letting $\hat{G}_L(z) = \beta(zI_n - A_L)^{-1}B_L$ and $G_H(z) = (zI_{\bar{n}} - A_H)^{-1}B_H$, it holds that $G_H(1)$ is full rank and $\hat{G}_L(1) = G_H(1)$. \square

An algorithm to compute the projections β_i and the matrices of $\bar{\Sigma}$ is discussed in Appendix 4.7.1, along the lines of Chapter 1.

4.3 Design of the hierarchical control structure

In this section the regulators at the two layers of the hierarchical control structure are designed for the solution to a tracking control problem, i.e., to drive the output $y(h)$ of the system Σ to the reference value y_s , while respecting suitable input constraints.

Thanks to Assumption 4.1.(3), it is possible to compute the reference pair (x_s, u_s) corresponding to y_s , i.e., such that $x_s = A_L x_s + B_L u_s$ and $C_L x_s = y_s$. Correspondingly, we define $\bar{u}_s = u_s$ as the steady-state input reference for the reduced-order system $\bar{\Sigma}$, and the corresponding reference steady-state value as $\bar{x}_s = G_H(1)\bar{u}_s = \beta x_s$ by Assumption 4.2.(3).

At the same time, we aim to enforce input constraints of type $u_i(h) \in \bar{u}_{s,i} \oplus \mathcal{U}_{s,i}$ for all $i = 1, \dots, M$, where $\bar{u}_{s,i}$ is the i -th vector component of \bar{u}_s and $\mathcal{U}_{s,i}$, $i = 1, \dots, M$, are closed and convex sets containing the origin in their interiors. Note that, if the reference $\bar{u}_{s,i}$ changes, also the set $\mathcal{U}_{s,i}$ may vary to enforce absolute input limitations or saturations. At a collective level, the required constraints are $u(h) \in \bar{u}_s \oplus \mathcal{U}_s$, where $\mathcal{U}_s = \prod_{i=1}^M \mathcal{U}_{s,i}$ is a closed and convex set containing the origin in its interior.

4.3.1 Design of the high level regulator

The high level regulator, designed to work at a low frequency, is based on the reduced order model (4.4) sampled with period N_L under the assumption that, $\forall k \in \mathbb{N}$, the \bar{u}_i 's are held constant over the interval $h \in [kN_L, (k+1)N_L - 1]$. Therefore, the sampling time of the high-level model is N_L times larger than the basic sampling time, used in the model (4.1). Denoting by $\bar{u}_i^{[N_L]}(k)$ the constant values of \bar{u}_i in the long sampling period k and by $\bar{u}^{[N_L]}(k)$ the overall input vector, the reduced order model in the slow timescale is

$$\bar{\Sigma}^{[N_L]} : \bar{x}^{[N_L]}(k+1) = A_H^{N_L} \bar{x}^{[N_L]}(k) + B_H^{[N_L]} \bar{u}^{[N_L]}(k) \quad (4.5)$$

where $B_H^{[N_L]} = \sum_{j=0}^{N_L-1} A_H^j B_H$. To enforce the input constraints specified above, we will require that $\bar{u}^{[N_L]}(k) \in \bar{u}_s \oplus \bar{\mathcal{U}}_s$, where $\bar{\mathcal{U}}_s = \prod_{i=1}^M \bar{\mathcal{U}}_{s,i}$, $\bar{\mathcal{U}}_{s,i} \subset \mathcal{U}_{s,i}$ for each $i = 1, \dots, M$, and where the properties of sets $\bar{\mathcal{U}}_{s,i}$ are specified later in Section 4.4.

Chapter 4. Hierarchical multi-rate MPC scheme for interconnected systems

In order to feedback a value of $\bar{x}^{[N_L]}$ related to the real state x of the system, the projected value $\beta_i x_i(kN_L)$ is used, so that the reset

$$\bar{x}_i^{[N_L]}(k) = \beta_i x_i(kN_L) \quad (4.6)$$

must be applied for all $i = 1, \dots, M$. In collective form (4.6) becomes

$$\bar{x}^{[N_L]}(k) = \beta x(kN_L) \quad (4.7)$$

The reset (4.6) at time k may force $\bar{x}^{[N_L]}(k+1)$ to assume a value different from the one computed based on the dynamics (4.5) and the applied input $\bar{u}^{[N_L]}(k)$. This discrepancy, due to the model reduction error and to the actions of the low level controllers, is accounted for by including in (4.5) an additive disturbance $\bar{w}(k)$, i.e.,

$$\bar{\Sigma}_w^{[N_L]} : \bar{x}^{[N_L]}(k+1) = A_H^{N_L} \bar{x}^{[N_L]}(k) + B_H^{[N_L]} \bar{u}^{[N_L]}(k) + \bar{w}(k) \quad (4.8)$$

The size of $\bar{w}(k)$ depends on the action of the low level regulators and its presence requires to resort to a robust MPC method, which is here designed assuming that $\bar{w}(k) \in \mathcal{W}$, where \mathcal{W} is a compact set containing the origin. The characteristics of \mathcal{W} will be defined in the following once the low level regulators have been specified (see Section 4.4).

The robust MPC algorithm is based on the scheme proposed in [121]. To this end, we first need to define the “unperturbed” prediction model

$$\bar{\Sigma}_w^{[N_L],o} : \bar{x}^{[N_L],o}(k+1) = A_H^{N_L} \bar{x}^{[N_L],o}(k) + B_H^{[N_L]} \bar{u}^{[N_L],o}(k) \quad (4.9)$$

and the control gain matrix \bar{K}_H such that, at the same time

- $F_H = A_H^{N_L} + B_H^{[N_L]} \bar{K}_H$ is Schur stable.
- $F_L^{[N_L]} = A_L^{N_L} + B_L^{[N_L]} \bar{K}_H \beta$ is Schur stable, where $B_L^{[N_L]} = \sum_{j=0}^{N_L-1} A_L^j B_L$.

We define $\bar{e}(k) = \bar{x}^{[N_L]}(k) - \bar{x}^{[N_L],o}(k)$ and we let \mathcal{Z} be a robust positively invariant (RPI) set - minimal, if possible - for the autonomous but perturbed system

$$\bar{\Sigma}_w^{[N_L],e} : \bar{e}(k+1) = F_H \bar{e}(k) + \bar{w}(k) \quad (4.10)$$

The prediction horizon for the high-level MPC consists of N_H slow time steps. Accordingly, at each slow time-step t the following optimization

4.3. Design of the hierarchical control structure

problem is solved:

$$\begin{aligned}
 & \min_{\overrightarrow{\bar{x}^{[N_L],o}(t)}, \overrightarrow{\bar{u}^{[N_L],o}(t:t+N_H-1)}} J_H(\bar{x}^{[N_L],o}(t), \overrightarrow{\bar{u}^{[N_L],o}(t:t+N_H-1)}) \\
 & \text{subject to:} \\
 & \bullet \text{ the unperturbed model dynamics (4.9)} \\
 & \bullet \text{ the initial constraint } \beta x(tN_L) - \bar{x}^{[N_L],o}(t) \in \mathcal{Z} \\
 & \bullet \text{ the terminal constraint } \bar{x}^{[N_L],o}(t+N_H) \in \bar{x}_S \oplus \bar{\mathcal{X}}_F \\
 & \bullet \bar{u}^{[N_L],o}(k) \in \bar{u}_S \oplus \bar{\mathcal{U}}_S \ominus \bar{K}_H \mathcal{Z}, k = t, \dots, t+N_H-1,
 \end{aligned} \tag{4.11}$$

where the input constrained set has been properly tightened in accordance with the used tube-based control approach, and where

$$\begin{aligned}
 J_H &= \sum_{k=t}^{t+N_H-1} \|\bar{x}^{[N_L],o}(k) - \bar{x}_S\|_{Q_H}^2 + \|\bar{u}^{[N_L],o}(k) - \bar{u}_S\|_{R_H}^2 \\
 &+ \|\bar{x}^{[N_L],o}(t+N_H) - \bar{x}_S\|_{P_H}^2
 \end{aligned} \tag{4.12}$$

The set $\bar{\mathcal{X}}_F$ is a positively invariant terminal set for the unperturbed system (4.9) controlled with the stabilizing control law $\bar{u}^{[N_L],o}(k) = \bar{K}_H \bar{x}^{[N_L],o}(k)$, satisfying $\bar{K}_H \bar{\mathcal{X}}_F \subseteq \bar{\mathcal{U}}_S \ominus \bar{K}_H \mathcal{Z}$. In view of this, $\bar{x}_S \oplus \bar{\mathcal{X}}_F$ results positively-invariant for (4.9) controlled with the stabilizing auxiliary control law $\bar{u}^{[N_L],o}(k) = \bar{u}_S + \bar{K}_H(\bar{x}^{[N_L],o}(k) - \bar{x}_S)$.

The positive definite and symmetric weighting matrices Q_H , R_H are free design parameters, while P_H is computed as the solution to the Lyapunov equation

$$F_H^T P_H F_H - P_H = -(Q_H + \bar{K}_H^T R_H \bar{K}_H) \tag{4.13}$$

Letting $\bar{x}^{[N_L],o}(t|t), \overrightarrow{\bar{u}^{[N_L],o}(t:t+N_H-1|t)}$ be the solution to the optimization problem (4.11), the control action, applied to system $\bar{\Sigma}_w^{[N_L]}$ at time t , is

$$\bar{u}^{[N_L]}(t) = \bar{u}^{[N_L],o}(t|t) + \bar{K}_H(\beta x(tN_L) - \bar{x}^{[N_L],o}(t|t)) \tag{4.14}$$

4.3.2 Design of the low level regulators

Recall that (see again Figure 4.1) the overall control action to be applied to the real system Σ has components generated by both the high-level and the low-level controllers, i.e.,

$$u_i(h) = \bar{u}_i^{[N_L]}(\lfloor h/N_L \rfloor) + \delta u_i(h) \tag{4.15}$$

The low level regulators are in charge of computing the local control corrections $\delta u_i \in \mathcal{U}_{S,i} \ominus \bar{\mathcal{U}}_{S,i}$ with the specific goal of compensating for the

Chapter 4. Hierarchical multi-rate MPC scheme for interconnected systems

effect of the model inaccuracies at the high level expressed by the term $\bar{w}(k)$ in (4.8). To this end, first define the auxiliary system $\hat{\Sigma}_i$: for $h = kN_L, \dots, (k+1)N_L - 1$

$$\hat{\Sigma}_i : \begin{cases} \hat{x}_i(h+1) &= A_L^{ii} \hat{x}_i(h) + B_L^{ii} \bar{u}_i^{[N_L]}(\lfloor h/N_L \rfloor) + E_L^i \hat{s}_i(h) \\ \hat{s}_i(h) &= \sum_{j=1}^M L_{ij} \hat{z}_j(h) \\ \hat{z}_i(h) &= C_L^{zi} \hat{x}_i(h) \\ \hat{x}_i(kN_L) &= x_i(kN_L) \end{cases} \quad (4.16)$$

and note that $\hat{\Sigma}_i$ can be simulated in a centralized way in the time interval $[kN_L, (k+1)N_L)$ once the high level controller has computed $\bar{u}_i^{[N_L]}(k)$ at the beginning of the time interval.

Also denote by $\Delta\Sigma_i$ the model given by the difference between systems (4.1) and (4.16), with (4.2) and (4.15).

$$\Delta\Sigma_i : \begin{cases} \delta x_i(h+1) &= A_L^{ii} \delta x_i(h) + B_L^{ii} \delta u_i(h) + E_L^i \delta s_i(h) \\ \delta s_i(h) &= \sum_{j=1}^M L_{ij} \delta z_j(h) \\ \delta z_i(h) &= C_L^{zi} \delta x_i(h) \\ \delta x_i(kN_L) &= 0 \end{cases} \quad (4.17)$$

where $\delta x_i(h) = x_i(h) - \hat{x}_i(h)$, $\delta z_i(h) = z_i(h) - \hat{z}_i(h)$ and $\delta s_i(h) = s_i(h) - \hat{s}_i(h)$.

The difference state δx_i is available at each time instant h since x_i is measurable and \hat{x}_i can be computed with (4.16) from the available value $\bar{u}_i^{[N_L]}(\lfloor h/N_L \rfloor)$. However, the difference dynamical system $\Delta\Sigma_i$ is not yet useful for decentralized prediction since it depends upon the interconnection variables $\delta s_i(h)$ that, in turn, depend upon the variables $\delta x_j(h)$, $j \neq i$, not known in advance in the future prediction horizon. For this reason, we define a decentralized (approximated) dynamical system $\Delta\hat{\Sigma}_i$ with input $\delta\hat{u}_i(h)$ and discarding all coupling inputs, i.e.,

$$\Delta\hat{\Sigma}_i : \begin{cases} \delta\hat{x}_i(h+1) &= A_L^{ii} \delta\hat{x}_i(h) + B_L^{ii} \delta\hat{u}_i(h) \\ \delta\hat{x}_i(kN_L) &= 0 \end{cases} \quad (4.18)$$

The decentralized dynamical system $\Delta\hat{\Sigma}_i$ is suitable for prediction, since it does not depend on quantities related to other subsystems. However, the dynamics of the subsystems can be very different from each other and re-sampling can be advisable for the design of the low level regulators. To this end, for any subsystem Σ_i , define a new sampling period $\zeta_i \in \mathcal{N}_+$ such that $N_L/\zeta_i = N_i \in \mathcal{N}_+$ and a corresponding time index l_i . For clarity, the

4.3. Design of the hierarchical control structure

relations among the time scales with indices h , l_i , and k are shown in Figure 4.2 in a specific case.

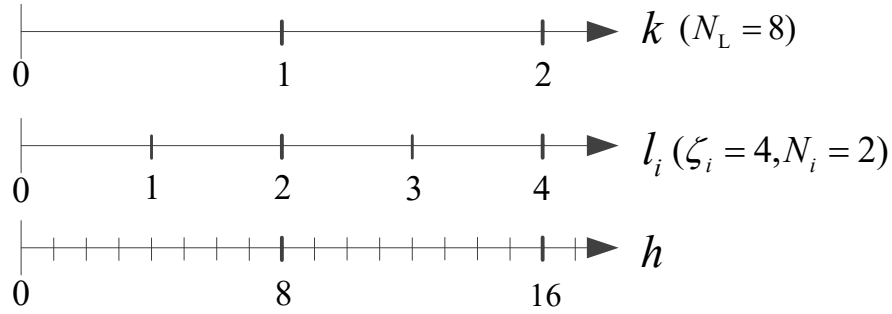


Figure 4.2: Adopted time scales: k (high layer design), $l_i = kN_i$ (low layer design of the i -th local regulator), $h = \zeta_i l_i = k\zeta_i N_i = kN_L$ (basic time scale).

In the time scale of l_i , define the dynamical system $\Delta\hat{\Sigma}_i^{[\zeta_i]}$ as

$$\Delta\hat{\Sigma}_i^{[\zeta_i]} : \begin{cases} \delta\hat{x}_i^{[\zeta_i]}(l_i + 1) = (A_L^{ii})^{\zeta_i} \delta\hat{x}_i^{[\zeta_i]}(l_i) + B_L^{ii[\zeta_i]} \delta\hat{u}_i^{[\zeta_i]}(l_i) \\ \delta\hat{x}_i^{[\zeta_i]}(kN_i) = \delta\hat{x}_i(kN_L) = 0 \end{cases} \quad (4.19)$$

where $B_L^{ii[\zeta_i]} = \sum_{j=0}^{\zeta_i-1} (A_L^{ii})^j B_L^{ii}$. In the short time scale, with time index h , the input $\delta\hat{u}_i(h) = \delta\hat{u}_i^{[\zeta_i]}(\lfloor h/\zeta_i \rfloor)$ is piecewise constant for $h \in [l_i\zeta_i, (l_i + 1)\zeta_i - 1]$. Its value will be computed as the result of a suitable optimization problem formulated for system (4.19).

Given $\delta\hat{u}_i(h)$, the evolution of $\delta\hat{x}_i(h)$ can be computed thanks to the dynamical model (4.18), however $\delta\hat{x}_i(h)$ is in general different from $\delta x_i(h)$ due to the neglected interconnections in systems (4.18) and (4.19). For this reason, and for all $i = 1, \dots, M$, the input $\delta u_i(h)$ to the real model (4.17) is computed based on $\delta\hat{u}_i(h)$, $\delta x_i(h)$, and $\delta\hat{x}_i(h)$ using a standard state-feedback policy, i.e.,

$$\delta u_i(h) = \delta\hat{u}_i(h) + K_i(\delta x_i(h) - \delta\hat{x}_i(h)) \quad (4.20)$$

where K_i is designed in such a way that the matrix $F_L = A_L + B_L K$ is Schur stable, being $K = \text{diag}(K_1, \dots, K_M)$.

Assume now to be at time $h = kN_L$ and to have run the high level controller, so that both $\bar{u}_i^{[N_L]}(k)$ and the predicted value $\bar{x}^{[N_L]}(k+1|k) = A_H^{N_L} \bar{x}^{[N_L]}(k) + B_H^{[N_L]} \bar{u}^{[N_L]}(k)$ are available. Therefore, in order to remove the effect of the

Chapter 4. Hierarchical multi-rate MPC scheme for interconnected systems

mismatch at the high level represented by $\bar{w}(k)$ in (4.8), the low level controller working in the interval $h \in [kN_L, (k+1)N_L - 1]$ should, if possible, aim to fulfill

$$\beta_i x_i((k+1)N_L) = \bar{x}_i^{[N_L]}(k+1|k)$$

or equivalently,

$$\beta_i \delta x_i((k+1)N_L) = \bar{x}_i^{[N_L]}(k+1|k) - \beta_i \hat{x}_i((k+1)N_L) \quad (4.21)$$

Since the model used for low-level control design is the decentralized one (i.e., (4.18)), the constraint (4.21) can only be formulated in an approximated way with reference to the state $\delta \hat{x}_i$ of system (4.18). In turn, if the resampling is used with $\zeta_i \neq 1$, the constraint on $\delta \hat{x}_i$ must be reformulated in terms of the state $\delta \hat{x}_i^{[\zeta_i]}$ of system (4.19), so that

$$\begin{aligned} \beta_i \delta \hat{x}_i^{[\zeta_i]}((k+1)N_i) &= \beta_i \delta \hat{x}_i((k+1)N_L) = \\ &= \bar{x}_i^{[N_L]}(k+1|k) - \beta_i \hat{x}_i((k+1)N_L) \end{aligned} \quad (4.22)$$

Note that the fulfillment of (4.22) does not imply that (4.21) is satisfied due to the neglected interconnections in (4.18) and (4.19) which make the term $\bar{w}(k)$ in (4.5) not identically equal to zero, although it contributes to its reduction.

All these considerations lead to the formulation of the following low-level MPC designs. The low level control action is computed, at time instant $h = kN_L$, based on the solution to the following optimization problem:

$$\begin{aligned} \min_{\overrightarrow{\delta \hat{u}_i^{[\zeta_i]}(kN_i:(k+1)N_i-1)}} J_L \left(\overrightarrow{\delta \hat{u}_i^{[\zeta_i]}(kN_i:(k+1)N_i-1)} \right) \\ \text{subject to:} \end{aligned} \quad (4.23)$$

- the dynamics (4.19)
- the terminal constraint (4.22)
- $\delta \hat{u}_i^{[\zeta_i]}(kN_i + l_i) \in \Delta \hat{\mathcal{U}}_i, l_i = 0, \dots, N_i - 1,$

where J_L is a positive definite function with arguments $\delta \hat{x}_i^{[\zeta_i]}(kN_i + l_i), \delta \hat{u}_i^{[\zeta_i]}(kN_i + l_i), l_i = 0, \dots, N_i - 1$, e.g.,

$$J_L = \sum_{l_i=0}^{N_i-1} \|\delta \hat{x}_i^{[\zeta_i]}(kN_i + l_i)\|_{Q_i}^2 + \|\delta \hat{u}_i^{[\zeta_i]}(kN_i + l_i)\|_{R_i}^2 \quad (4.24)$$

and where a discussion on how to select the set $\Delta \hat{\mathcal{U}}_i$ is deferred to Appendix 4.7.2.

4.4. Properties and algorithm implementation

Finally, for $j = 0, \dots, N_L - 1$, the control component at each (fast) time instant $\delta u_i(kN_L + j)$ is given by

$$\begin{aligned} \delta u_i(kN_L + j) &= \delta \hat{u}_i(kN_L + j|kN_L) \\ &+ K_i(\delta x_i(kN_L + j) - \delta \hat{x}_i(kN_L + j|kN_L)) \end{aligned} \quad (4.25)$$

where

$$\delta \hat{u}_i(kN_L + j|kN_L) = \delta \hat{u}_i^{[\zeta_i]}(kN_i + \lfloor j/\zeta_i \rfloor |kN_L) \quad (4.26)$$

A further clarification is finally due. At the low level, the controller is designed mostly to compensate for the effects of model inaccuracies during each long sampling time (i.e., that of the high-level controller). Therefore, the prediction horizon at low level coincides with one large sampling time of the slow high-level controller, i.e., corresponding to N_L fast sampling times. Due to resampling, the optimization problem computed at the beginning of each slow sampling time, i.e., at time $h = kN_L$, has a prediction horizon of N_i steps of length ζ_i , where indeed $N_i \zeta_i = N_L$. As a result of this optimization problem, the input sequence $\delta \hat{u}_i^{[\zeta_i]}(kN_i|kN_L), \dots, \delta \hat{u}_i^{[\zeta_i]}((k+1)N_i - 1|kN_L)$ is obtained, and at each fast sampling time $kN_L + j$, $j = 0, \dots, N_L - 1$, the real (low-level) input contribution (4.25) is used in (4.15). Note that, in this way, $\delta u_i(h)$ varies at each sampling time. In summary, the on-line implementation procedure of the hierarchical control scheme here proposed is depicted in Algorithm 4.1.

4.4 Properties and algorithm implementation

The main assumptions, the recursive feasibility and convergence properties of the optimization problems stated at the high and low levels are established in this section.

4.4.1 Main assumptions and remarks

Define

$$\kappa(N_L) = \|\mathcal{B}(N_L)\| \quad (4.27)$$

where

$$\mathcal{B}(N_L) = \sum_{j=1}^{N_L} A_H^{N_L-j} B_H - \beta \sum_{j=1}^{N_L} A_L^{N_L-j} B_L$$

Also, let $I_{si} = [0_{\bar{n}_i \times \bar{n}_1} \ \dots \ I_{\bar{n}_i} \ \dots \ 0_{\bar{n}_i \times \bar{n}_M}]$, $\mathcal{A}(N_L) = A_H^{N_L} \beta - \beta A_L^{N_L} \in \mathbb{R}^{\bar{n} \times \bar{n}}$, $\mathcal{B}(N_L) = [B_L \ A_L B_L \ \dots \ (A_L)^{N_L-1} B_L]$, ρ_u be such that $\mathcal{U}_s \subseteq \mathcal{B}_{\rho_u}(0)$. We now introduce the following assumption.

Chapter 4. Hierarchical multi-rate MPC scheme for interconnected systems

Algorithm 4.1 On-line implementation

initialization

while for any integer $k \geq 0$ **do**

(1) set $\bar{x}^{[N_L]}(k) = \beta x(kN_L)$, $\hat{x}(kN_L) = x(kN_L)$, $\delta\hat{x}(kN_L) = 0$ and $\delta x(kN_L) = 0$

(2) compute the high-level control action $\bar{u}^{[N_L],o}(k|k)$ by solving the optimization problem (4.11) with cost (4.12), and obtain $\bar{u}^{[N_L]}(k)$ by (4.14)

(3) update $\bar{x}^{[N_L]}(k+1|k)$ and $\bar{x}^{[N_L],o}(k+1|k)$

(4) for any system $\hat{\Sigma}_i$, generate $\hat{x}_i(h)$ of system (4.16) in an open-loop fashion for N_L fast time steps with high-level control action $\bar{u}^{[N_L]}(\lfloor h/N_L \rfloor)$, for all $h \in [kN_L, kN_L + N_L)$

(5) for any $i = 1, \dots, M$, compute terminal constraint (4.22) for the i -th low-level regulator

(6) for any $i = 1, \dots, M$, compute the sequence $\overrightarrow{\delta\hat{u}_i^{[\zeta_i]}}(kN_i : (k+1)N_i - 1 | kN_L)$ by solving the finite-horizon optimization problem (4.23) with (4.24)

(7) for any system $\Delta\hat{\Sigma}_i$, generate $\delta\hat{u}_i(h)$ in (4.26) with $\delta\hat{u}_i^{[\zeta_i]}(\lfloor h/\zeta_i \rfloor | kN_L)$ and compute $\delta\hat{x}_i(h)$ in (4.18) with $\delta\hat{u}_i(h)$ and for all $h \in [kN_L, kN_L + N_L)$

for $h \leftarrow kN_L$ **to** $kN_L + N_L - 1$ **do**

(f1) for any $i = 1, \dots, M$, compute $\delta u_i(h)$ with (4.25) and compute $u_i(h) = \bar{u}_i^{[N_L]}(\lfloor h/N_L \rfloor) + \delta u_i(h)$

(f2) update $\delta x(h+1)$ and $x(h+1)$

end

(8) $k \leftarrow k+1$

end

Assumption 4.3.

(1) $\|A_L^{N_L}\| < 1$;

(2) letting $\mathcal{R}_i(N_i) = \begin{bmatrix} B_L^{ii[\zeta_i]} & (A_L^{ii})\zeta_i B_L^{ii[\zeta_i]} & \dots & (A_L^{ii})\zeta_i(N_i-1) B_L^{ii[\zeta_i]} \end{bmatrix}$ for each $i = 1, \dots, M$, be the reachability matrix in N_i steps associated to the pair $((A_L^{ii})\zeta_i, B_L^{ii[\zeta_i]})$, matrix

$$\mathcal{H}_i(N_i) = \beta_i \mathcal{R}_i(N_i) \in \mathbb{R}^{\bar{n}_i \times N_i m_i}$$

is full-rank with minimum singular value $\underline{\sigma}_{\mathcal{H}_i(N_i)} > 0$;

(3) letting $\rho_{\bar{u}}$ and $\rho_{\delta\hat{u}_i}$ be such that $\bar{\mathcal{U}} \subseteq \mathcal{B}_{\rho_{\bar{u}}}(0)$ and $\Delta\hat{\mathcal{U}}_i \supseteq \mathcal{B}_{\rho_{\delta\hat{u}_i}}(0)$, respectively, for any $i = 1, \dots, M$ it holds that

$$\rho_{\delta\hat{u}_i} > \frac{\kappa(N_L)\rho_{\bar{u}}}{\sqrt{N_i}\underline{\sigma}_{\mathcal{H}_i(N_i)}} \quad (4.28)$$

(4) for each $i = 1, \dots, M$

$$\chi_i(kN_L) = \frac{\sqrt{N_L}\rho_u \|\mathcal{R}(N_L)\| \|\mathcal{A}(N_L)\|}{(1 - \|A_L^{N_L}\|)(\sqrt{N_i}\underline{\sigma}_{\mathcal{H}_i(N_i)}\rho_{\delta\hat{u}_i} - \kappa(N_L)\rho_{\bar{u}})} \leq 1 \quad (4.29)$$

4.4. Properties and algorithm implementation

(5) Define $\Delta\bar{\mathcal{U}}_i = \Delta\mathcal{U}_i(N_L - 1)$, and $\Delta\mathcal{U}_i(j) = \Delta\hat{\mathcal{U}}_i \oplus \mathcal{B}_{\rho_{\Delta u_i}(j)}(0)$ where $\rho_{\Delta u_i}(j) = \sum_{r=2}^j \|K_i I_{s_i} F_L^{j-r} (A_L - A_L^D)\| \rho_{\delta \hat{x}}(r-1)$ for all $j = 2, \dots, N_L$, $\rho_{\Delta u_i}(j) = 0$ for $j = 0, 1$, and where $A_L^D = \text{diag}(A_L^{11}, \dots, A_L^{MM})$ and $\rho_{\delta \hat{x}}(j) = \sqrt{\sum_{i=1}^M \rho_{\delta \hat{x}_i}^2(j)}$,

$$\rho_{\delta \hat{x}_i}(j) = \rho_{\delta \hat{u}_i} \sum_{r=1}^j \|(A_L^{ii})^{j-r} B_L^{ii}\| \quad (4.30)$$

We require that

$$\bar{\mathcal{U}}_s \oplus \left(\prod_{i=1}^M \Delta\bar{\mathcal{U}}_i \right) \subseteq \mathcal{U}_s \quad (4.31)$$

□

Assumption 4.3 may be viewed, at a first glance, as a list of purely abstract and technical requirements. However, on the one hand, it represents relevant inherent properties of the system under control and, on the other hand, it implicitly includes important design principles, that will be shortly discussed next.

First, note that Assumption 4.3.(1) can always be verified in the light of the Assumption 4.1.(2) on stability of the transition matrix A_L , and establishes a lower bound for the parameter N_L . On the other hand, in view of Assumption 4.2.(2), β_i are full rank and the full rank of matrix $\mathcal{R}_i(N_i)$ is guaranteed by the reachability of the local submodels used at low level control guaranteed by Assumption 4.1.(5): therefore Assumption 4.3.(2) is fulfilled by taking N_i (and so N_L) sufficiently large.

Secondly, Assumptions 4.3.(3)-4.3.(5) provide a tradeoff for the selection of parameters $\rho_{\delta \hat{u}_i}$, $i = 1, \dots, M$ and $\rho_{\bar{u}}$. In fact

- on the one hand, as required by Assumption 4.3.(5), and more specifically by equation (4.31), the input $u(h)$ must be shared between the low-level controllers (with local inputs δu_i , whose maximal amplitude is related to $\rho_{\delta \hat{u}_i}$) and centralized high-level controller (with input \bar{u} , whose maximal amplitude is related to $\rho_{\bar{u}}$);

- on the other hand, the amplitude of δu_i must be sufficiently large to compensate for the model inaccuracies, as expressed by Assumptions 4.3.(3), 4.3.(4), and more specifically by equations (4.28) and (4.29).

Importantly, note that the constraints (4.28) and (4.29) depend upon quantities that are all functions of the number of steps N_L , as clarified in the following.

- In view of Assumptions 4.1.(2), 4.2.(1,3), $\kappa(N_L) = \|\sum_{j=0}^{N_L-1} A_H^j B_H - G_H(1) -$

Chapter 4. Hierarchical multi-rate MPC scheme for interconnected systems

$(\beta \sum_{j=0}^{N_L-1} A_L^j B_L - \hat{G}_L(1))$ and $G_H(1) = \sum_{j=0}^{+\infty} A_H^j B_H$, $\hat{G}_L(1) = \beta \sum_{j=0}^{+\infty} A_L^j B_L$. Therefore $\kappa(N_L) \leq \|\sum_{j=N_L}^{+\infty} A_H^j B_H\| + \|\beta \sum_{j=N_L}^{+\infty} A_L^j B_L\| \leq \|A_H^{N_L}\| \|G_H(1)\| + \|A_L^{N_L}\| \|\beta\| \|G_L(1)\|$, where $G_L(z) = (zI_n - A_L)^{-1} B_L$. Therefore $\kappa(N_L) \rightarrow 0$ exponentially as $N_L \rightarrow +\infty$. This shows that also Assumption 4.3.(3) can be fulfilled by taking N_L sufficiently large.

- Similarly to Proposition 2.2.3, for any $i = 1, \dots, M$ it can be proved that

$$\lim_{N_L \rightarrow +\infty} \|A_L^{N_L}\| = 0, \quad \lim_{N_L \rightarrow +\infty} \chi_i(N_L) = 0 \quad (4.32)$$

This proves that also Assumption 4.3.(4) can be fulfilled - i.e., we can increase the maximum amplitude of \bar{u} as much as possible - by taking a sufficiently large value of parameter N_L . This, as a byproduct, allows to minimize the conservativeness of the overall control scheme, as discussed in the next section.

4.4.2 Main results and conservativeness of the scheme

The size of the uncertainty set \mathcal{W} to be considered in the high level design is given by

$$\mathcal{W} = \mathcal{B}_{\rho_w}(0) \quad (4.33)$$

where $\rho_w = \sum_{j=2}^{N_L} \|\beta F_L^{N_L-j} (A_L - A_L^D)\| \rho_{\delta \hat{x}}(j-1)$.

The main result can now be stated.

Theorem 4.1. *Under Assumption 4.3, if $x(0)$ is such that the problem (4.11) is feasible at $k = 0$ and, for all $i = 1, \dots, M$*

$$\|x(0) - x_s\| \leq \frac{(\sqrt{N_i} \sigma_{\mathcal{H}_i(N_i)} \rho_{\delta \hat{u}_i} - \kappa(N_L) \rho_{\bar{u}})}{\|\mathcal{A}(N_L)\|} := \lambda_i(N_L)$$

then

(i) $\bar{w}(k) \in \mathcal{W}$ and problems (4.11) and (4.23) are feasible for all $k \geq 0$;

(ii) for all $h \geq 0$

$$u(h) \in \bar{u}_s \oplus \mathcal{U}_s \quad (4.34)$$

(iii) the state of the slow time-scale reduced model $\bar{\Sigma}^{[N_L]}$ enjoys robust convergence properties, i.e.,

$$\bar{x}^{[N_L]}(k) \rightarrow \bar{x}_s \oplus \mathcal{Z} \text{ as } k \rightarrow +\infty$$

(iv) the state of the large scale model Σ enjoys robust convergence properties, i.e., for a computable positive constant ρ_x

$$x(kN_L) \rightarrow x_s \oplus \bigoplus_{h=0}^{\infty} (F_L^{[N_L]})^h \mathcal{B}_{\rho_x}(0)$$

4.4. Properties and algorithm implementation

(v) we can define (see (4.67) in Appendix 4.7.3) a function $\sigma(N_L)$ of N_L such that, if

$$\sigma(N_L) < 1 \quad (4.35)$$

then, as $k \rightarrow \infty$, $x(kN_L) \rightarrow x_S$. \square

Theorem 4.1 establishes three important facts. First, it shows that, if the initial state lies in a suitable set (and if Assumption 4.3 holds), the joint feasibility properties of the two control layers can be guaranteed in a recursive fashion. Secondly, it ensures robust convergence of the states of both the reduced-scale and the overall systems to a neighborhood of the corresponding steady-state goals.

Finally, if a suitably-defined function $\sigma(N_L)$ is smaller than one, then convergence of the state to the goal is ensured. The definition of $\sigma(N_L)$ is quite involved and for this reason it is given in Appendix 4.7.3, in particular see equation (4.67). A general remark, however, is due on parameter $\sigma(N_L)$: the more the subsystems are interconnected (in a wide sense, regarding both the existence of dependencies between subsystems and their amplitude), the larger is $\sigma(N_L)$. On the other hand, it is possible to reduce arbitrarily this parameter by increasing the tuning knob N_L . This depends of the fact that, as $N_L \rightarrow +\infty$, both $\|\mathcal{A}(N_L)\| \rightarrow 0$ and $\|\mathcal{B}(N_L)\| \rightarrow 0$.

A further remark is that, similarly to Proposition 2.3, for any $i = 1, \dots, M$ it can be proved that $\lim_{N_L \rightarrow +\infty} \lambda_i(N_L) = +\infty$, allowing to increase at will the feasibility region of the low-level problem.

From the discussion in Section 4.4.1 it has finally become clear that, by tuning the value of the low-level prediction horizon N_L , one can reduce at will the values of $\rho_{\delta u_i}$, related to the maximum required amplitude of inputs δu_i . This, from (4.30) and (4.33), allows to reduce arbitrarily the high-level disturbance set \mathcal{W} . This, in turn, allows to reduce at will the corresponding RPI set \mathcal{L} and to minimize the conservativeness of the present control scheme. We remark that, although a fine tuning of the gain matrices K_i , $i = 1, \dots, M$ and \bar{K}_H can also be beneficial for the reduction of the conservativeness of the scheme, the most relevant tuning knob indeed results parameter N_L , especially since the dependence upon all other design parameters results rather straightforward and simple.

From the discussion above a further consideration is due. Although the case $N_L \rightarrow +\infty$ allows to verify all the requirements, to obtain the best dynamic performances from the application of our control scheme, it would be beneficial to set N_L to an “average” value, such that the assumptions are verified, but at the same time that guarantees to control the system in a

Chapter 4. Hierarchical multi-rate MPC scheme for interconnected systems

dynamic fashion also at high level. It is nevertheless important to remark that, when $N_L \rightarrow +\infty$, the scheme can be regarded as a two-layer algorithm that at high level consists of a static optimizer based on a simplified system model and, at low level, consists of a dynamic, reactive, decentralized, and multi-rate, optimization-based regulator.

4.4.3 Design

The implementation of the multilayer algorithm described in the previous section requires a number of off-line computations here listed for the reader’s convenience.

- design of A_H , B_H , and β_i , $i = 1, \dots, M$, such that Assumption 4.2 is satisfied;
- design of \bar{K}_H such that both $F_H = A_H^{N_L} + B_H^{[N_L]} \bar{K}_H$ and $F_L^{[N_L]} = A_L^{N_L} + B_L^{[N_L]} \bar{K}_H \beta$ are Schur stable;
- design of $K = \text{diag}(K_1, \dots, K_M)$ such that $F_L = A_L + B_L K$ is Schur stable;
- computation of $\rho_{\delta \hat{u}_i}$, $\rho_{\bar{u}_i}$ (see the procedure proposed in Appendix 4.7.2) and of the sets $\mathcal{U}_{s,i}$, $\Delta \hat{\mathcal{U}}_i$;
- computation of \mathcal{W} according to (4.33) and (4.30);
- computation of $\bar{\mathcal{X}}_F$, \mathcal{Z} , see [150], and P_H with (4.13).

4.5 Simulation examples and implementation procedures

In this Section, we present two simulation examples concerning the use of the hierarchical control algorithm described in the previous sections.

4.5.1 Temperature regulation of two apartments

4.5.1.1 Description of the model

Consider the problem of regulating temperatures of the two apartments depicted in Figure 4.3. The first apartment is constituted by rooms A_1 , B_1 , C_1 , D_1 and E_1 , while the second one by A_2 , B_2 , C_2 , D_2 and E_2 . Each apartment is equipped with a radiator supplying heats q_i , $i = 1, 2$. Heat exchange coefficient between neighbouring rooms of different apartment, i.e., E_2 and C_1 , is $k_1^t = 1 \text{ W/m}^2\text{K}$, the one between adjacent rooms inside each apartment

4.5. Simulation examples and implementation procedures

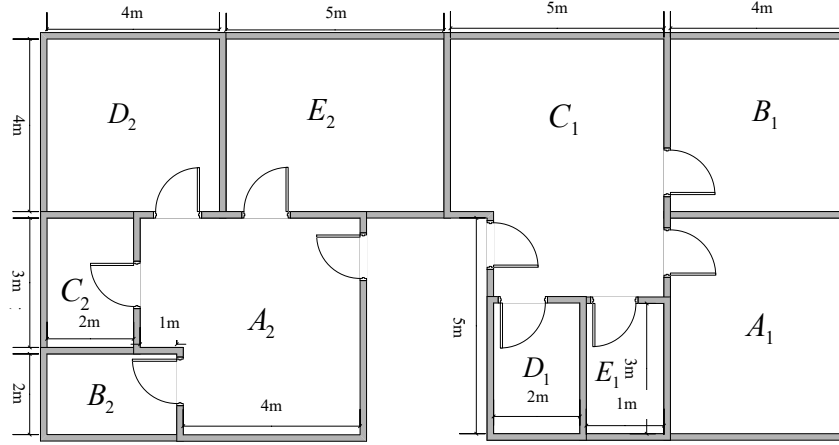


Figure 4.3: Schematic representation of a building with two apartments

is $k_2^t = 2.5 \text{ W/m}^2\text{K}$, and the one between the rooms and the external environment is $k_e^t = 0.5 \text{ W/m}^2\text{K}$. The external temperature is $T_E = 0^\circ\text{C}$ and, for simplicity, we neglect solar radiation. Furthermore, the height of the walls is $H = 4 \text{ m}$. Air density and heat capacity are $\rho = 1.225 \text{ kg/m}^3$ and $c = 1005 \text{ J/kgK}$, respectively. The overall model is made by dynamic energy balance equations of each room. The variables q_1, q_2 are expressed in Watts, while all the temperature variables are expressed in $^\circ\text{C}$. The considered equilibrium point is: $\bar{q} = (\bar{q}_1, \bar{q}_2) = (354.2, 320.8)$, with $\bar{T} = (\bar{T}_{A_1}, \bar{T}_{B_1}, \bar{T}_{C_1}, \bar{T}_{D_1}, \bar{T}_{E_1}, \bar{T}_{A_2}, \bar{T}_{B_2}, \bar{T}_{C_2}, \bar{T}_{D_2}, \bar{T}_{E_2}) = (19.6, 20.3, 20.2, 21.7, 18.2, 17.2, 21.2, 21.7, 19.6, 19.4)$. Let $\delta T_{j_i} = T_{j_i} - \bar{T}_{j_i}$ and $\delta q_i = q_i - \bar{q}_i$, for $j = A, B, C, D$ and $i = 1, 2$. In this way, $x_i = (\delta T_{A_i}, \delta T_{B_i}, \delta T_{C_i}, \delta T_{D_i}, \delta T_{E_i})$ and $u_i = \delta q_i$ are the state and input variables of the i -th subsystem, i.e., $n_i = 5$ and $m_i = 1$, with $i = 1, 2$. The control variables are limited by $-50 \leq u_1, u_2 \leq 50$.

4.5.1.2 Design and implementation procedures

Devising the high-level and low-level models

The two subsystems' continuous-time models have been sampled using the algorithm described in [56] with $\Delta t = 90\text{s}$ to obtain their discrete-time counterpart in the fast time scale. The eigenvalues of the first subsystem are $\{0.73, 0.97, 0.9, 0.85, 0.88\}$, and the eigenvalues of the second one are $\{0.97, 0.76, 0.82, 0.91, 0.87\}$. Then the procedure described in the appendix 4.7.1 has been used to compute the discrete-time reduced order

Chapter 4. Hierarchical multi-rate MPC scheme for interconnected systems

model with $A_H = \text{diag}(0.97, 0.97)$, i.e., $\bar{n} = 2$, as well as the transformation matrices $\beta_1 = [0 \ 0 \ -1 \ 0 \ 0]$ and $\beta_2 = [0 \ 0 \ 0 \ 0 \ -1]$. The plant model at the slow time scale has been constructed with $N_L = 20$. As the dynamics of the two subsystems is close, the resampling procedure is not considered for the two models used at the low level, i.e., $\zeta_1 = \zeta_2 = 1$.

Off-line design of the low-level regulators

- At the low level, the finite-horizon optimization algorithms described in (4.23) have been implemented with state and input penalties $Q_1 = \beta_1^T \beta_1$, $Q_2 = \beta_2^T \beta_2$, $R_1 = R_2 = 10$.
- The decentralized feedback gains K_1 and K_2 guaranteeing that F_L is Schur stable can in principle be computed according to the algorithm described in [20] and based on the solution of LMI problems. However, in our case, we simply solved two independent LQ problems and we checked that the resulting F_L is Schur stable.
- The parameters $\rho_{\delta\hat{u}_1}$, $\rho_{\delta\hat{u}_2}$, $\rho_{\bar{u}_1}$ and $\rho_{\bar{u}_2}$ have been computed according to (4.41) in Appendix 4.7.2. Specifically we used the cost function $J_\rho = \gamma_1 \mathbb{1}_{1 \times M} \vec{\rho}_{\delta\hat{u}} - (\vec{\rho}_{\bar{u}} - \gamma_2 \vec{\rho}_u)' (\vec{\rho}_{\bar{u}} - \gamma_2 \vec{\rho}_u)$, where γ_1, γ_2 are positive constants selected as $\gamma_1 = 1$ and $\gamma_2 = 0.3$. Note that the choice of γ_1, γ_2 allows one to modify the feasibility region of the high level optimization problem (4.11) with cost (4.12); typically setting $\gamma_1 = 1$, the feasibility properties of (4.11) grow with γ_2 . The computed values are $\rho_{\delta\hat{u}_1} = 35.3$, $\rho_{\delta\hat{u}_2} = 35.3$, $\rho_{\bar{u}_1} = 14.5$, $\rho_{\bar{u}_2} = 14.5$. In view of this, the conservativeness of the algorithm related to the computation of the input constraint sets described in Appendix 4.7.2 is small for both subsystems.

Off-line design of the high-level regulator

- Tube-based robust MPC has been designed at the high level according to the algorithm described in [121] with prediction horizon, $N_H = 5$, state and input penalties, $Q_H = I_{\bar{n}}$ and $R_H = 0.1I_{\bar{m}}$.
- The gain matrix \bar{K}_H guaranteeing that both F_H and $F_L^{[N_L]}$ are Schur stable, can be computed according to the algorithm described in [20] and based on the solution of LMI problems. However, in our case, we simply solved a LQ problem and we checked that the resulting F_H and $F_L^{[N_L]}$ were Schur stable.

4.5. Simulation examples and implementation procedures

- The disturbance set has been obtained according to (4.33) and (4.30) with $\rho_w = 0.04$, and the RPI set has been computed with the algorithms described at pp. 231-233 of [150], i.e., $\mathcal{Z} = \{z \mid -(0.067, 0.067) \leq z \leq (0.067, 0.067)\}$ and $\bar{K}_H \mathcal{Z} = \{\bar{K}_H z \mid -(0.022, 0.021) \leq \bar{K}_H z \leq (0.022, 0.021)\}$. The terminal penalty P_H has been computed with (4.13), that is

$$P_H = \begin{bmatrix} 1.49 & -0.02 \\ -0.02 & 1.50 \end{bmatrix}$$

and the terminal set has been calculated under nominal input constraints in (4.11), i.e., $\tilde{\mathcal{X}}_F = \{\bar{x}^{[N_L],o} \mid (\bar{x}^{[N_L],o} - \bar{x}_s)^T P_H (\bar{x}^{[N_L],o} - \bar{x}_s) \leq 0.996\}$, see [80].

The values taken by ρ_w , \mathcal{Z} and $\bar{K}_H \mathcal{Z}$ reveal that the reduction of the feasibility region of the high-level regulator caused by the use of tightened input constraint set is negligible.

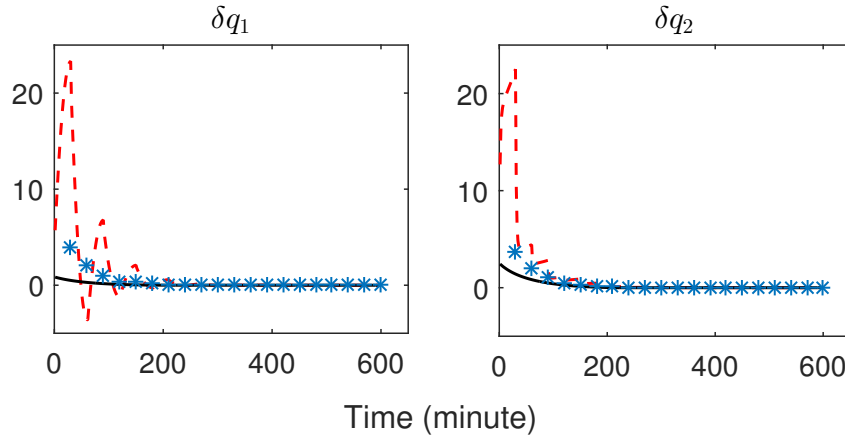


Figure 4.4: Inputs of the controlled two apartments: blue * markers are the values of the inputs computed at the high level with the two-layer scheme, red dashed lines are the values of the overall control actions computed with the two-layer scheme, while black continuous lines are the values of the control variables computed with the centralized scheme.

4.5.1.3 Simulation results

The overall control actions computed by the high and low level controllers have been applied to the two apartments at each fast sampling time with initial condition $x(0) = (x_1(0), x_2(0)) = (-2, \dots, -2)$ and $\bar{x}(0) = \beta x(0)$.

Chapter 4. Hierarchical multi-rate MPC scheme for interconnected systems

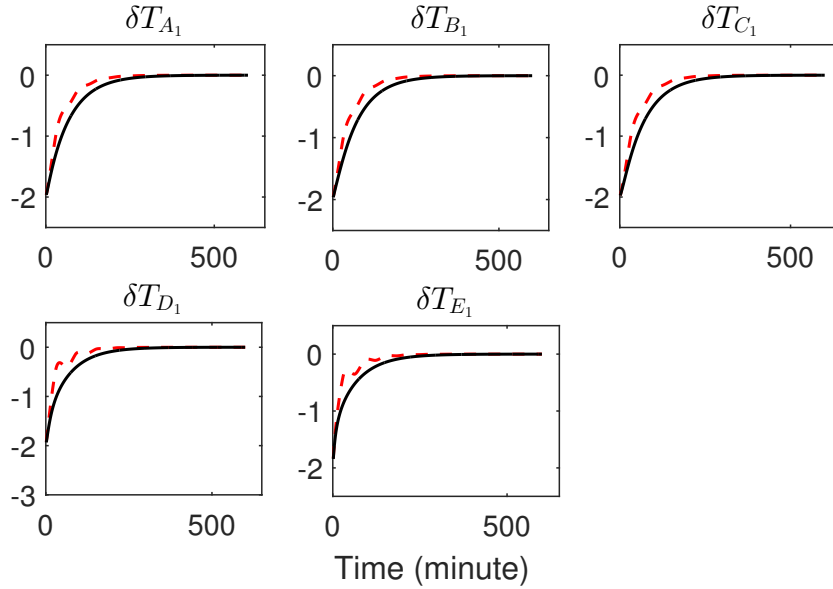


Figure 4.5: States of the first apartment: red dashed lines are the values of the states with the two-layer scheme, while black continuous lines are the ones with the centralized scheme.

For comparison, a centralized state-feedback stabilizing MPC has been designed with an auxiliary state-feedback control law computed with LQ control, state penalty matrix $Q = \text{diag}(Q_1, Q_2)$, input penalty $R = \text{diag}(R_1, R_2)$ and prediction horizon $N = N_H \cdot N_L = 100$. The terminal set has been chosen as $\mathcal{X}_F = \{x | (x - x_s)^T P (x - x_s) \leq 1\}$ where the terminal penalty P has been taken as the steady state solution of the Riccati equation according to the infinite horizon control problem with Q, R . All the simulation tests have been implemented within MATLAB Yalmip and MPT toolbox, see [108] and [79], in a PC with Intel Core i5-4200U 2.30 GHz and with Windows 10 operating system. The SDPT3 solver has been used for the implementation of the centralized MPC and of the high-level regulator of the proposed approach, while the Matlab QUADPROG solver has been used for the low-level optimization problems. The detailed on-line computational time required by each controller is reported in Table 4.1. This table shows that the on-line computational time of the proposed hierarchical approach for each interval $[kN_L, kN_L + N_L)$, i.e., 1.31 s, is reduced dramatically compared to that of the centralized MPC, i.e., $1.48 \cdot N_L$ s.

The transients of the state and control variables of the controlled linear

4.5. Simulation examples and implementation procedures

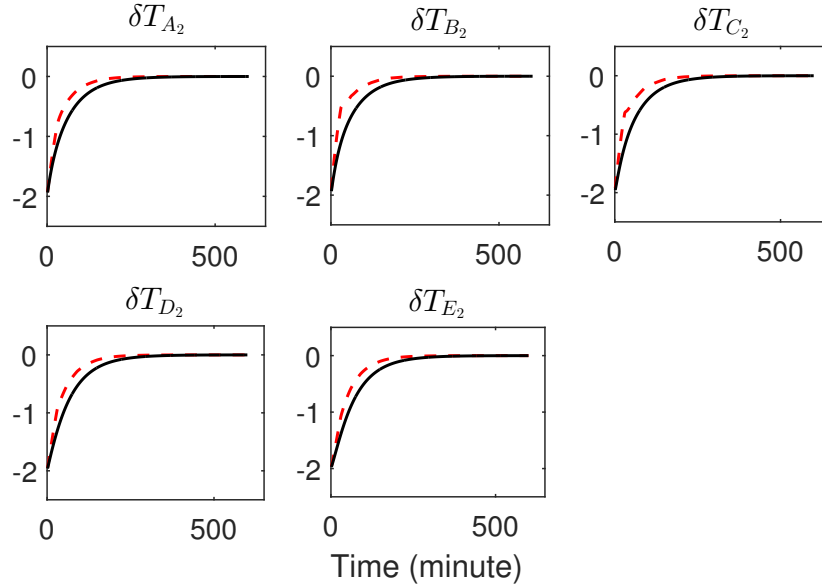


Figure 4.6: States of the second apartment: red dashed lines are the values of the states with the two-layer scheme, while black continuous lines are the ones with the centralized scheme.

Table 4.1: On-line computation time comparison: two apartments

Approach		Optimization activated at	Computation time (s)	
Proposed one	HL regulator	$h = kN_L$	0.38	
	LL regulator	1 st one	$h = kN_L$	0.90
		2 nd one	$h = kN_L$	0.93
Centralized stabilizing MPC		each fast time instant h	1.48	

system are reported in Figures 4.4-4.6 which show that, after an initial transient, the inputs and states return to their nominal values, and the performance of the proposed two-layer approach is close to that of centralized stabilizing MPC.

4.5.2 Multi-rate control of a chemical plant

4.5.2.1 Description of the plant and linearized model

Consider the large-scale chemical plant described in [111], [164]. The system is composed of three reactors R_1, R_2, R_3 , three distillation columns C_1, C_2, C_3 , two recycle streams and six chemical components: A, B, C, D, E, F . The flow diagram of the system is reported in Figure 4.7, where D_1, D_2, D_3 are the top products of the columns, while B_1, B_2, B_3 are their bottom prod-

Chapter 4. Hierarchical multi-rate MPC scheme for interconnected systems

ucts. The following reactions occur inside the reactors $R_1 : A + B \rightarrow C + D$, $R_2 : D + E \rightarrow F + B$, and $R_3 : D + E \rightarrow F + B$. The system has six control variables, namely the refluxes (v_1, v_3, v_5) and the vapour (v_2, v_4, v_6) flow rates in the columns C_1, C_2, C_3 , respectively, and six outputs: the liquid molar fraction (r_1) of component A at the top product of C_1 , the liquid molar fraction (r_2) of component D at the bottom product of C_1 , the liquid molar fraction (r_3) of component C at the top product of C_2 , the liquid molar fraction (r_4) of component D at the bottom product of C_2 , the liquid molar fraction (r_5) of component B at the top product of C_3 , and the liquid molar fraction (r_6) of component F at the bottom product of C_3 . A detailed description of the model equations and of the model parameters is reported in [164]. The considered nominal operating point is characterized by the vector of inputs $v_{nominal} = [330 \ 410 \ 283 \ 385 \ 141 \ 282]^T$ lb mol/h, to which it corresponds the vector of outputs $r_{nominal} = [0.942 \ 0.552 \ 0.827 \ 0.941 \ 0.705 \ 0.991]^T$. The linearized model at this operating condition is of order $n = 192$, and shows strong interactions among the control and controlled variables, see again [164].

In order to apply the hierarchical control structure described in this chapter, the system and the corresponding linearized model have been partitioned into two subsystems (i.e. $M = 2$). The first one includes reactors R_1, R_2 and columns C_1, C_2 , while the second one is made by R_3 and C_3 . The continuous-time linearized models of the two subsystems have been

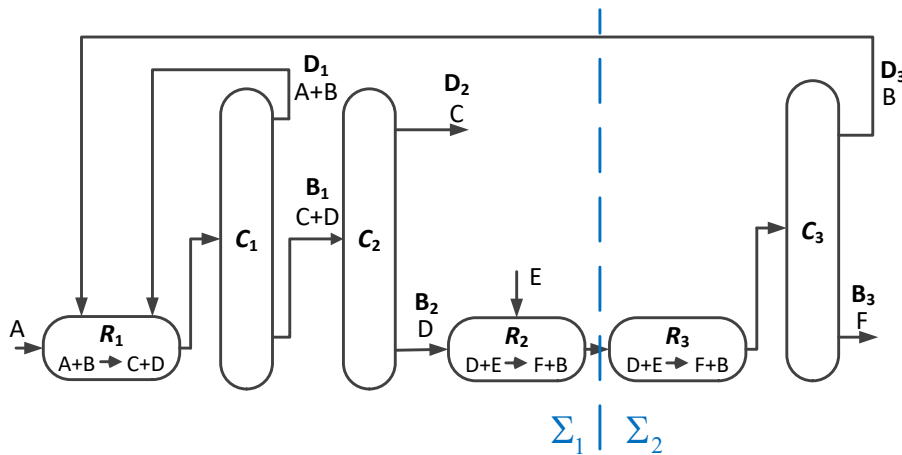


Figure 4.7: Flow diagram of the chemical plant: for $i = 1, 2, 3$, R_i and C_i are the reactors and distillation columns, while D_i and B_i are the top and bottom products.

discretized with the algorithm described in [56] and basic sampling time $T = 0.05$ h and a standard model order reduction procedure has been used

4.5. Simulation examples and implementation procedures

to remove the unreachable states of the two linear subsystems. Denoting by δv_i and δr_i the deviations of the inputs v_i and the outputs r_i , respectively, with respect to their nominal values, the first resulting linear reduced order model is of order $n_1 = 25$, with $m_1 = 4$ inputs, i.e., $u_1 = (\delta v_1, \dots, \delta v_4)$, $p_1 = 4$ outputs, i.e., $y_1 = (\delta r_1, \dots, \delta r_4)$, and $p_{z1} = 3$ coupling outputs, while the second one has $n_2 = 16$ states, $m_2 = 2$ inputs, i.e., $u_2 = (\delta v_5, \delta v_6)$, $p_2 = 2$ outputs, i.e., $y_2 = (\delta r_5, \delta r_6)$, and $p_{z2} = 2$ coupling outputs. These two linear subsystems have been used as the linear models described in (4.1) for the implementation of the hierarchical control structure. The control variables are limited by

$$\|u_i - u_{s,i}\|_\infty \leq 100, \quad (4.36)$$

for $i = 1, 2$, where $u_{s,i}$ is the steady state value corresponding to the output set-point values given by $y_s = 10^{-3} \cdot (9.4, 5.5, 8.3, 9.4, 7.0, 9.9)$.

4.5.2.2 Design and implementation procedures

Along the same lines of Section 4.5.1.2, the procedures used to implement the hierarchical control structure and the computational details regarding the chemical plant are now listed.

Tuning the hierarchical control scheme with $N_L = 28$, $N_H = 3$

(1) *Devising the high-level simplified model and the low-level submodels*

- The procedure described in Appendix 4.7.1 has been used to compute the matrices β_1 and β_2 , and the reduced order model (4.4) with order $\bar{n} = 6$. The dynamic matrix $A_H = \text{diag}(0.972, 0.984, 0.969, 0.969, 0.874, 0.869)$ has been computed; its parameters have been selected as the maximum singular values of the reachability matrix of each subsystem previously discretized. The matrix B_H has been computed as described in Appendix 4.7.1. The resulting model has been resampled with $N_L = 28$ to obtain the model (4.5) to be used at the high level in the slow time scale.
- The models (4.18) have been re-sampled with $\zeta_1 = 4$ and $\zeta_2 = 1$ to obtain the models (4.19) to be used at the low level in the fast time scale.

(2) *Off-line design of the low-level regulators*

Chapter 4. Hierarchical multi-rate MPC scheme for interconnected systems

- The low level finite-horizon optimization algorithms described in (4.23) and (4.24) have been implemented with state and input penalties $Q_1 = 10^3 \cdot \beta_1^T \beta_1$, $Q_2 = 10^4 \cdot \beta_2^T \beta_2$, $R_1 = I_{m_1}$ and $R_2 = I_{m_2}$.
- The decentralized feedback gains K_1 and K_2 have been computed by solving two independent LQ problems and then we have checked that the resulting F_L is Schur stable.
- The parameters $\rho_{\delta \hat{u}_1}$, $\rho_{\delta \hat{u}_2}$, $\rho_{\bar{u}_1}$ and $\rho_{\bar{u}_2}$ have been computed according to (4.41) in Appendix 4.7.2 with cost function $J_\rho = \gamma_1 \mathbb{1}_{1 \times M} \vec{\rho} \delta \hat{u} - (\vec{\rho}_{\bar{u}} - \gamma_2 \vec{\rho}_u)' (\vec{\rho}_{\bar{u}} - \gamma_2 \vec{\rho}_u)$, where γ_1 , γ_2 have been selected as $\gamma_1 = 1$ and $\gamma_2 = 0.3$. The computed values are $\rho_{\delta \hat{u}_1} = 145.2$, $\rho_{\delta \hat{u}_2} = 115.7$, $\rho_{\bar{u}_1} = 49.3$, $\rho_{\bar{u}_2} = 25.2$. The input vectors of each subsystem, namely \bar{u}_i , $\delta \hat{u}_i$, $i = 1, 2$, have been limited as follows: $-\rho_{\bar{u}_i} / \sqrt{m_i} \mathbb{1}_{m_i \times 1} \leq \bar{u}_i - \bar{u}_{s,i} \leq \rho_{\bar{u}_i} / \sqrt{m_i} \mathbb{1}_{m_i \times 1}$, $-\rho_{\delta \hat{u}_i} / \sqrt{m_i} \mathbb{1}_{m_i \times 1} \leq \delta \hat{u}_i \leq \rho_{\delta \hat{u}_i} / \sqrt{m_i} \mathbb{1}_{m_i \times 1}$; and the corresponding sets $\bar{\mathcal{U}}_{s,i}$, $\Delta \hat{\mathcal{U}}_{s,i}$, $i = 1, 2$ have been obtained.

Note that $\rho_{\bar{u}_1} / \sqrt{m_1} + \rho_{\delta \hat{u}_1} / \sqrt{m_1} = 97.3$ and $\rho_{\bar{u}_2} / \sqrt{m_2} + \rho_{\delta \hat{u}_2} / \sqrt{m_2} = 99.6$ and we can write $\bar{\mathcal{U}}_{s,1} \oplus \Delta \hat{\mathcal{U}}_{s,1} = \{\bar{u}_1 + \delta \hat{u}_1 | -97.3 \cdot \mathbb{1}_{m_1 \times 1} \leq \bar{u}_1 + \delta \hat{u}_1 - \bar{u}_{s,1} \leq 97.3 \cdot \mathbb{1}_{m_1 \times 1}\}$ and $\bar{\mathcal{U}}_{s,2} \oplus \Delta \hat{\mathcal{U}}_{s,2} = \{\bar{u}_2 + \delta \hat{u}_2 | -99.6 \cdot \mathbb{1}_{m_2 \times 1} \leq \bar{u}_2 + \delta \hat{u}_2 - \bar{u}_{s,2} \leq 99.6 \cdot \mathbb{1}_{m_2 \times 1}\}$. These results show that the size of both the sets $\bar{\mathcal{U}}_{s,1} \oplus \Delta \hat{\mathcal{U}}_{s,1}$ and $\bar{\mathcal{U}}_{s,2} \oplus \Delta \hat{\mathcal{U}}_{s,2}$ is close to that of the real input constraint in (4.36). In addition, the radius of the sets $\mathcal{B}_{\rho_{\Delta u_i(N_L-1)}}(0)$, $i = 1, 2$, resulting from the feedback policy in (4.20) for compensating the couplings terms between subsystems have been computed according to Assumption 4.3.(5) with $\rho_{\Delta u_1(N_L-1)} = 4.0$ and $\rho_{\Delta u_2(N_L-1)} = 0.37$. Therefore, we can also write $\bar{\mathcal{U}}_{s,1} \oplus \Delta \hat{\mathcal{U}}_{s,1} = \{\bar{u}_1 + \delta u_1 | -99.3 \cdot \mathbb{1}_{m_1 \times 1} \leq \bar{u}_1 + \delta u_1 - \bar{u}_{s,1} \leq 99.3 \cdot \mathbb{1}_{m_1 \times 1}\}$ and $\bar{\mathcal{U}}_{s,2} \oplus \Delta \hat{\mathcal{U}}_{s,2} = \{\bar{u}_2 + \delta u_2 | -99.9 \cdot \mathbb{1}_{m_2 \times 1} \leq \bar{u}_2 + \delta u_2 - \bar{u}_{s,2} \leq 99.9 \cdot \mathbb{1}_{m_2 \times 1}\}$. In view of this, the conservativeness of the algorithm related to the computation of the input constraint sets described in Appendix 4.7.2 is small, especially for the second subsystem.

(3) Off-line design of the high-level regulator

- The high-level tube-based robust MPC has been designed with state and input penalties $Q_H = I_{\bar{n}}$ and $R_H = 0.1I_m$.
- The gain matrix \bar{K}_H has been computed by solving a LQ problem and we have checked that the resulting F_H and $F_L^{[M_L]}$ are Schur stable.
- The disturbance set has been obtained according to (4.33) and (4.30) with $\rho_w = 1.25$, and the RPI set has been computed, i.e., $\mathcal{Z} = \{z | -$

4.5. Simulation examples and implementation procedures

$(2.66, 3.61, 1.93, 2.64, 1.30, 1.30) \leq z \leq (2.66, 3.61, 1.93, 2.64, 1.30, 1.30)$ and $\bar{K}_H \mathcal{Z} = \{\bar{K}_H z | -(1.64, 1.63, 1.02, 1.02, 0.10, 0.10) \leq \bar{K}_H z \leq (1.64, 1.63, 1.02, 1.02, 0.10, 0.10)\}$. The terminal penalty P_H has been computed with (4.13), and the terminal set has been calculated under nominal input constraints in (4.11), i.e., $\bar{\mathcal{Z}}_F = \{\bar{x}^{[N_L],o} | (\bar{x}^{[N_L],o} - \bar{x}_s)^T P_H (\bar{x}^{[N_L],o} - \bar{x}_s) \leq 0.997\}$, see [80].

The values taken by ρ_w , \mathcal{Z} and $\bar{K}_H \mathcal{Z}$ reveal that the feasibility region of high-level regulator might be slightly reduced compared to the one of stabilizing MPC due to the use of tightened input constraint set, i.e., $\bar{u}_s \oplus \bar{\mathcal{U}}_s \ominus \bar{K}_H \mathcal{Z}$ in optimization problem (4.11) and the computation formulas of the disturbance set in (4.33) and (4.30), but can be enlarged by increasing the tuning knobs $\rho_{\bar{u}_1}$ and $\rho_{\bar{u}_2}$.

Tuning the hierarchical control scheme with $N_L = 84$, $N_H = 1$

Along the same line with the tuning case $N_L = 28$, $N_H = 3$, the computational results corresponding to tuning $N_L = 84$ and $N_H = 1$ are also listed here.

- The following parameters $\rho_{\delta \hat{u}_1}$, $\rho_{\delta \hat{u}_2}$, $\rho_{\bar{u}_1}$ and $\rho_{\bar{u}_2}$ have been computed: $\rho_{\delta \hat{u}_1} = 125.6$, $\rho_{\delta \hat{u}_2} = 98.3$, $\rho_{\bar{u}_1} = 59.5$, $\rho_{\bar{u}_2} = 41.9$. The amplitude of both $\rho_{\delta \hat{u}_1}$ and $\rho_{\delta \hat{u}_2}$ ($\rho_{\bar{u}_1}$ and $\rho_{\bar{u}_2}$) is smaller (larger) than that with the parameters $N_L = 28$, $N_H = 3$.
- The sets $\bar{\mathcal{U}}_{s,1} \oplus \Delta \hat{\mathcal{U}}_{s,1} = \{\bar{u}_1 + \delta \hat{u}_1 | -92.6 \cdot \mathbb{1}_{m_1 \times 1} \leq \bar{u}_1 + \delta \hat{u}_1 - \bar{u}_{s,1} \leq 92.6 \cdot \mathbb{1}_{m_1 \times 1}\}$ and $\bar{\mathcal{U}}_{s,2} \oplus \Delta \hat{\mathcal{U}}_{s,2} = \{\bar{u}_2 + \delta \hat{u}_2 | -99.1 \cdot \mathbb{1}_{m_2 \times 1} \leq \bar{u}_2 + \delta \hat{u}_2 - \bar{u}_{s,2} \leq 99.1 \cdot \mathbb{1}_{m_2 \times 1}\}$. These results show that the size of both the sets $\bar{\mathcal{U}}_{s,1} \oplus \Delta \hat{\mathcal{U}}_{s,1}$ and $\bar{\mathcal{U}}_{s,2} \oplus \Delta \hat{\mathcal{U}}_{s,2}$ has been reduced slightly, compared to that with the parameters $N_L = 28$, $N_H = 3$; however, it is still close to that of the real input constraint in (4.36). In addition, the radius of the sets $\mathcal{B}_{\rho_{\Delta u_i(N_L-1)}}(0)$, $i = 1, 2$, have been computed with $\rho_{\Delta u_1(N_L-1)} = 11.3$ and $\rho_{\Delta u_2(N_L-1)} = 0.91$. Therefore, we can also write $\bar{\mathcal{U}}_{s,1} \oplus \Delta \mathcal{U}_{s,1} = \{\bar{u}_1 + \delta u_1 | -98.2 \cdot \mathbb{1}_{m_1 \times 1} \leq \bar{u}_1 + \delta u_1 - \bar{u}_{s,1} \leq 98.2 \cdot \mathbb{1}_{m_1 \times 1}\}$ and $\bar{\mathcal{U}}_{s,2} \oplus \Delta \mathcal{U}_{s,2} = \{\bar{u}_2 + \delta u_2 | -99.8 \cdot \mathbb{1}_{m_2 \times 1} \leq \bar{u}_2 + \delta u_2 - \bar{u}_{s,2} \leq 99.8 \cdot \mathbb{1}_{m_2 \times 1}\}$. In view of this, the conservativeness of the algorithm related to the computation of the input constraint sets described in Appendix 4.7.2 is still small, especially for the second subsystem.

Chapter 4. Hierarchical multi-rate MPC scheme for interconnected systems

- The disturbance set has been obtained with $\rho_w = 1.56$, and the RPI set has been computed i.e., $\mathcal{Z} = \{z | -(1.83, 2.11, 1.69, 1.82, 1.58, 1.58) \leq z \leq (1.83, 2.11, 1.69, 1.82, 1.58, 1.58)\}$ and $\bar{K}_H \mathcal{Z} = \{\bar{K}_H z | -(0.37, 0.29, 0.17, 0.18, 0.01, 0.01) \leq \bar{K}_H z \leq (0.37, 0.29, 0.17, 0.18, 0.01, 0.01)\}$. The terminal penalty P_H is computed with (4.13), and the terminal set is calculated under nominal input constraints in (4.11), i.e., $\mathcal{X}_F = \{\bar{x}^{[N_L, o]} | (\bar{x}^{[N_L, o]} - \bar{x}_s)^T P_H (\bar{x}^{[N_L, o]} - \bar{x}_s) \leq 0.98\}$.

Note that, the size of both the sets \mathcal{Z} and $\bar{K}_H \mathcal{Z}$ is smaller than that with $N_L = 28$, $N_H = 3$. The amplitude of $\rho_{\bar{u}_1}$ and $\rho_{\bar{u}_2}$ has been enlarged and the feasibility region of the high-level regulator can be increased significantly.

Table 4.2: On-line computation time comparison: chemical plant

Approach		Optimization activated at	Computation time (s)
Proposed one with $N_L = 28$	HL regulator	$h = kN_L$	1.1
	LL regulator	1 st one	$h = kN_L$
		2 nd one	$h = kN_L$
Proposed one with $N_L = 84$	HL regulator	$h = kN_L$	1.07
	LL regulator	1 st one	$h = kN_L$
		2 nd one	$h = kN_L$
Centralized stabilizing MPC		each fast time instant h	21.9

4.5.2.3 Simulation results: application to the linearized model

The overall control actions computed by the high and low level controllers have been applied to the linear system at each fast sampling time. The output reference values for the linear system have been initially maintained at the nominal setpoints $y_s = 10^{-3} \cdot (9.4, 5.5, 8.3, 9.4, 7.0, 9.9)$; then, at time $t = 25.2$ h, they have been set equal to $10^{-2} \cdot (2.43, -1.01, -0.43, 0.15, -0.70, 0.41)$. For comparison, a centralized state-feedback stabilizing MPC has been designed with an auxiliary state-feedback control law computed with LQ control, state penalty matrix $Q = \text{diag}(Q_1, Q_2)$, input penalty $R = I_m$ and prediction horizon $N = N_H \cdot N_L = 84$. The terminal set has been chosen as $\mathcal{X}_F = \{x | (x - x_s)^T P (x - x_s) \leq 1\}$ where the terminal penalty P has been taken as the steady state solution of the Riccati equation with Q, R . All the simulation tests have been implemented with the MATLAB Yalmip and MPT toolbox in a PC with Intel Core i5-4200U 2.30 GHz and with Windows 10 operating system. The SDPT3 solver has been used for the implementation of the centralized MPC and of the high-level regulator of the proposed approach, while the Matlab QUADPROG solver has been used for the low-level optimization problems. The detailed on-line computational time required by each controller is reported in Table 4.2. This table

4.5. Simulation examples and implementation procedures

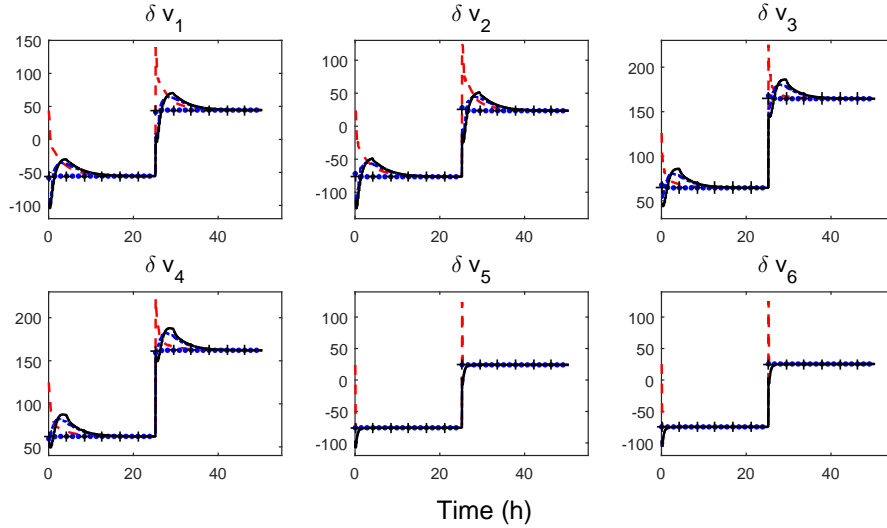


Figure 4.8: Control variables of the controlled linear system: black + markers (blue · markers) are the values of the inputs computed at the high level with the two-layer scheme with $N_L = 84$ and $N_H = 1$ (with $N_L = 28$ and $N_H = 3$), black continuous lines (blue dot-dashed lines) are the values of the overall control actions computed with the two-layer scheme with $N_L = 84$ and $N_H = 1$ (with $N_L = 28$ and $N_H = 3$), while red dashed lines are the values of the control variables computed with the centralized scheme.

shows that the on-line computational time of the proposed hierarchical approach for each interval $[kN_L, kN_L + N_L)$ with $N_L = 28$ and $N_H = 3$ ($N_L = 84$ and $N_H = 1$), i.e., 2.49 s (6.87 s), is reduced dramatically compared to that of the centralized MPC, i.e., $21.9 \cdot N_L$ s.

The evolution of the output and control variables of the controlled linear system is reported in Figures 4.8-4.9 which show that, after an initial transient, inputs and outputs return to their nominal values until the change of the reference occurs, when both the centralized and the two-layer control systems properly react to bring the controlled variables to their reference values, and the performance of the proposed two-layer approach with both tuning cases $N_L = 28$, $N_H = 3$ and $N_L = 84$, $N_H = 1$ is close to that of centralized stabilizing MPC.

4.5.2.4 Simulation results: application to the nonlinear system

The two-layer control structure has also been applied to the nonlinear chemical plant with $N_L = 84$ and $N_H = 1$. Since in a realistic scenario the state is unmeasurable, the distributed Kalman filter described in [55] has been

Chapter 4. Hierarchical multi-rate MPC scheme for interconnected systems

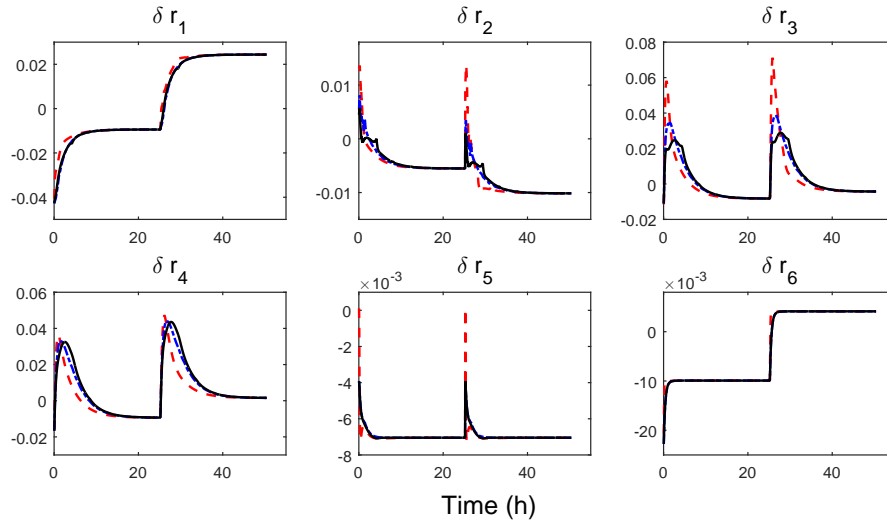


Figure 4.9: Outputs of the controlled linear system: black continuous lines (blue dot-dashed lines) are the values of the outputs computed with the two-layer scheme with $N_L = 84$ and $N_H = 1$ (with $N_L = 28$ and $N_H = 3$), while red dashed lines are the values of the outputs computed with the centralized scheme.

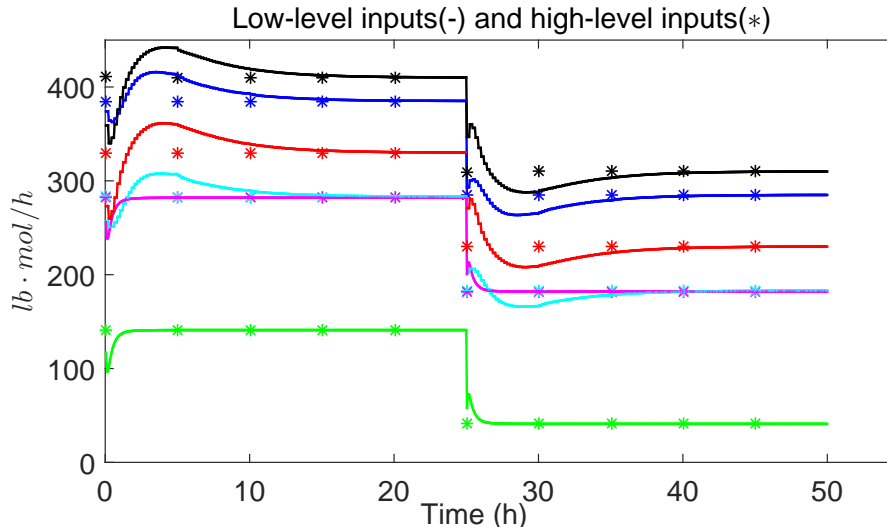


Figure 4.10: Control variables of the controlled nonlinear system: * markers are the values of the control variables computed at the high level in the long sampling time, i.e., (\bar{u}_1, \bar{u}_2) , (red, black, cyan, blue, green and magenta), while continuous lines are the values of the overall control actions in the multi rate, i.e., (u_1, u_2) , (red, black, cyan, blue, green and magenta).

4.6. Extensions and conclusions

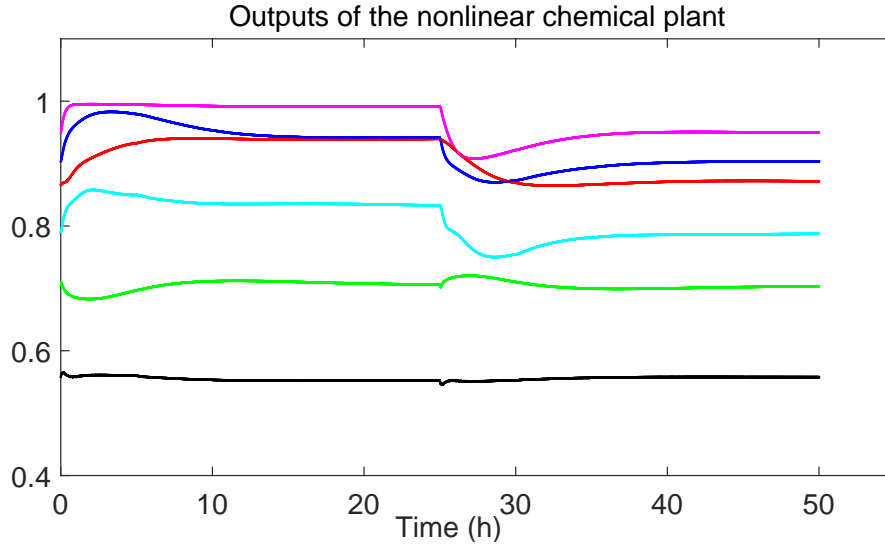


Figure 4.11: Outputs of the controlled nonlinear system, i.e., (r_1, \dots, r_6) , (red, black, cyan, blue, green and magenta).

used. The covariances of the noises acting on the states have been set equal to $\hat{Q}_1 = 0.1I_{n_1}$, $\hat{Q}_2 = 0.1I_{n_2}$, while the covariances of the output noises have been chosen as $\hat{R}_1 = 0.01I_{p_1}$, $\hat{R}_2 = 0.01I_{p_2}$. Finally, the covariances of the initial state estimates have been selected as $P_1(0) = 0.01I_{n_1}$, $P_2(0) = 0.01I_{n_2}$.

Starting from the nominal operating conditions, the overall control actions computed by high and low level controllers have been applied to the original nonlinear system at each fast time instant. The output reference values for the nonlinear system have been initially maintained at the nominal point $r_{nominal}$; then, at time $t = 25.2$ h, they have been set equal to $[0.866, 0.558, 0.791, 0.903, 0.704, 0.948]$. The evolution of the output and control variables of the controlled nonlinear system are reported in Figure 4.10-4.11. These figures show that, after an initial transient due to the state filter, inputs and outputs return to their nominal values until the change of the reference occurs, when the two-layer control system properly reacts to bring the controlled variables to their reference values.

4.6 Extensions and conclusions

In this chapter a two-layer control scheme for systems made by interconnected subsystems has been presented. The algorithm is based on the solution, at the two layers, of MPC problems of reduced size and allows for

Chapter 4. Hierarchical multi-rate MPC scheme for interconnected systems

a multirate implementation, suitable to deal with systems characterized by significantly different dynamics. Its main properties of recursive feasibility and convergence have been established and its performances have been tested in two simulation examples.

The main rationale of the proposed control architecture is grounded on the use, at the high level, of a reduced and slow-timescale model for centralized control. At the low-level, each subsystem is endowed of a local controller and is in charge of both compensating for the model inaccuracies introduced at the high level and dealing with the distributed nature of the system.

At high level, we use a tracking control algorithm based on robust tube-based MPC. This choice, however, is somehow arbitrary, since many alternative (robust) control solutions can be used instead, e.g., the offset-free robust MPC scheme proposed in [19].

The reference signals are here assumed to be previously computed, for instance by an additional Real Time Optimization layer (RTO), e.g., based on the current and predicted external conditions, such as prices of energy or costs of raw materials, see [3, 38, 39, 53, 61, 87, 88, 191]. It is important to remark that RTO-based structures must be properly designed to guarantee the compatibility of the models used at the two layers, see [39, 53, 191]. Also, dynamic RTO structures may be prone to stability issues, as noted in [50].

To overcome problems related to the use of RTO to generate reference signals, a robust economic MPC approach can be used, see [13], for the design of a high level regulator which, at the same time, computes the optimal reference values for the controlled outputs. This, in our opinion, would not entail significant differences in the algorithm implementation and in the theoretical results.

4.7 Appendix

4.7.1 Construction of β_i and of the reduced order model

A constructive procedure for the computation of the matrices β_i , $i = 1, \dots, M$, and the reduced order model satisfying Assumption 4.2 is listed here following the same line as in Chapter 2. Note however that in Chapter 2 the case of dynamically decoupled subsystems was considered, and full system reduction actually could be carried out subsystem-by-subsystem. On the contrary, in this case, system reduction must be performed at a full system level and structural additional constraints must be satisfied, i.e. the block-diagonality of matrix β . In view of the presence of these constraints, the

4.7. Appendix

sufficient and necessary condition given in Proposition 2.2 for guaranteeing the fulfillment of Assumption 4.2 (i.e., that $\bar{n} \geq p + \dim(\text{Im}G_L^x \cap \text{Ker}C_L)$) is, in our case, only necessary.

Here we now describe a (possibly conservative) procedure:

- a** find a subspace $\text{Ker}\beta_i$ of dimension $n_i - \bar{n}_i$ so that $\text{Ker}\beta_i \subseteq \text{Ker}C_L^{ii}$ and $\mathcal{L}_{ii} \cap \text{Ker}\beta_i = \{0\}$, where $\mathcal{L}_{ii} = \text{Im}\tilde{G}_L^{ii}(1) \cap \text{Ker}C_L^{ii}$, and $\tilde{G}_L^{ii}(z) = (zI_{n_i} - A_L^{ii})^{-1} [B_L^{ii} \ E_i]$;
- b** let $\{\kappa_1, \dots, \kappa_{n_i - \bar{n}_i}\}$ be a set of independent vectors in $\mathcal{K}_{\beta_i} = \text{Ker}\beta_i$ and complete this set to a basis $\mathcal{B}_i = \{v_1, \dots, v_{\bar{n}_i}, \kappa_1, \dots, \kappa_{n_i - \bar{n}_i}\}$ of the whole space \mathbb{R}^{n_i} ;
- c** let $\{r_1, \dots, r_{\bar{n}_i}\}$ be a basis of $\mathbb{R}^{\bar{n}_i}$, define

$$\hat{\beta}_i = [r_1 \mid \dots \mid r_{\bar{n}_i} \mid 0 \mid \dots \mid 0]$$

and T_L be the matrix whose columns are the vectors in \mathcal{B}_i , then $\beta_i = \hat{\beta}_i T_L^{-1}$;

- d** define collective matrix $\beta = \text{diag}(\beta_1, \dots, \beta_M)$;
- e** choose matrix A_H being Schur stable, and let

$$B_H = (I_{\bar{n}} - A_H) \hat{G}_L(1)$$

where the suitable choices for A_H are those modeling the dominant dynamics of the low-level collective model.

Steps **a-c** imply that Assumption 2.(2) is fulfilled, while step **e** guarantees that Assumption 2.(1) and 2.3 are satisfied.

Note that a less conservative choice can be taken, i.e., defining, in step **a**, $\tilde{G}_L^{ii}(z) = (zI_{n_i} - A_L^{ii})^{-1} B_L^{ii}$. However this choice does not guarantee a-priori that the property $\mathcal{L} \cap \mathcal{K}_\beta = \{0\}$, where $\mathcal{L} = \text{Im}G_L^x \cap \text{Ker}C_L$, $G_L^x = (I_n - A_L)^{-1} B_L$, and $\mathcal{K}_\beta = \prod_{i=1}^M \mathcal{K}_\beta^i$. This must be verified after the reduction phase has been carried out.

4.7.2 Computation of the input constraint sets

In the scheme proposed in this chapter, the dimensions of the input constraint sets $\mathcal{U}_{s,i}$ and $\Delta\hat{\mathcal{U}}_i$ are key tuning knobs, which must be selected in order to satisfy, at the same time, the inequalities (4.28), for all $i = 1, \dots, M$, and (4.31). To address the design issue, in this appendix we propose a simple and lightweight algorithm based on a linear program. As a simplifying assumption, we set $\Delta\hat{\mathcal{U}}_i = \mathcal{B}_{\rho_{\delta\hat{u}_i}}(0)$ and $\mathcal{U}_{s,i} = \mathcal{B}_{\rho_{\hat{u}_i}}(0)$. Under

Chapter 4. Hierarchical multi-rate MPC scheme for interconnected systems

this assumption, the tuning knobs are the vectors $\vec{\rho}_{\delta\hat{u}} = (\rho_{\delta\hat{u}_1}, \dots, \rho_{\delta\hat{u}_M})$ and $\vec{\rho}_{\bar{u}} = (\rho_{\bar{u}_1}, \dots, \rho_{\bar{u}_M})$. Note that, in case of need, such assumption can be relaxed, at the price of a slightly different definition of the inequalities below.

First consider inequality (4.28), to be verified for all $i = 1, \dots, M$. Here the constant $\rho_{\bar{u}}$ appears, defined in such a way that $\bar{\mathcal{U}}_S = \prod_{i=1}^M \mathcal{B}_{\rho_{\bar{u}_i}}(0) \subseteq \mathcal{B}_{\rho_{\bar{u}}}(0)$. We can define, for example, $\rho_{\bar{u}} = \sqrt{\sum_{i=1}^M \rho_{\bar{u}_i}^2} \leq \sum_{i=1}^M \rho_{\bar{u}_i}$. Therefore, to fulfill (4.28) it is sufficient to verify the following matrix inequality

$$\vec{\rho}_{\delta\hat{u}} > \kappa(N_L) \text{diag}\left(\frac{1}{\sqrt{N_1} \underline{\sigma}_{\mathcal{H}_1(N_1)}}, \dots, \frac{1}{\sqrt{N_M} \underline{\sigma}_{\mathcal{H}_M(N_M)}}\right) \mathbb{1}_{M \times M} \vec{\rho}_{\bar{u}} \quad (4.37)$$

where $\mathbb{1}_{M \times M}$ is the $M \times M$ matrix whose entries are all equal to 1. The second main inclusion to be fulfilled is (4.31), which is verified if, for all $i = 1, \dots, M$,

$$\Delta \bar{\mathcal{U}}_i \oplus \bar{\mathcal{U}}_{S,i} \subseteq \mathcal{U}_{S,i} \quad (4.38)$$

By definition, $\Delta \bar{\mathcal{U}}_i = \Delta \hat{\mathcal{U}}_i \oplus \mathcal{B}_{\rho_{\Delta u_i(N_L-1)}}(0)$, where

$$\begin{aligned} \rho_{\Delta u_i(N_L-1)} &= \\ &= \sum_{r=2}^{N_L-1} \|K_i I_{Si} F_L^{N_L-r-1} (A_L - A_L^D)\| \sqrt{\sum_{j=1}^M \rho_{\delta\hat{x}_j}^2 (r-1)} \\ &\leq \sum_{r=2}^{N_L-1} \|K_i I_{Si} F_L^{N_L-r-1} (A_L - A_L^D)\| \sum_{j=1}^M \rho_{\delta\hat{x}_j} (r-1) \\ &= \sum_{r=2}^{N_L-1} \|K_i I_{Si} F_L^{N_L-r-1} (A_L - A_L^D)\| \sum_{j=1}^M \sum_{k=1}^{r-1} \|(A_L^{jj})^{r-1-k} B_L^{jj}\| \rho_{\delta\hat{u}_j} \\ &= \sum_{j=1}^M \lambda_{ij} \rho_{\delta\hat{u}_j} \end{aligned} \quad (4.39)$$

where $\lambda_{ij} = \sum_{r=2}^{N_L-1} \|K_i I_{Si} F_L^{N_L-r-1} (A_L - A_L^D)\| \sum_{k=1}^{r-1} \|(A_L^{jj})^{r-1-k} B_L^{jj}\|$. This implies that $\Delta \hat{\mathcal{U}}_i \subseteq \mathcal{B}_{\rho_{\delta\hat{u}_i} + \sum_{j=1}^M \lambda_{ij} \rho_{\delta\hat{u}_j}}(0)$. Therefore, to verify (4.38) it is sufficient to enforce the constraint

$$(\Lambda + I_M) \vec{\rho}_{\delta\hat{u}} + \vec{\rho}_{\bar{u}} \leq \vec{\rho}_u \quad (4.40)$$

where Λ is the $M \times M$ matrix whose entries are λ_{ij} , $i, j = 1, \dots, M$, while $\vec{\rho}_u = (\rho_{u_1}, \dots, \rho_{u_M})$, where $\mathcal{B}_{\rho_i}(0) \subseteq \mathcal{U}_{S,i}$ for all $i = 1, \dots, M$. Eventually, a suitable choice of $\vec{\rho}_{\delta\hat{u}}$ and $\vec{\rho}_{\bar{u}}$ is obtained as the solution to the following problem:

$$\begin{aligned} &\max && J_\rho \\ &\vec{\rho}_{\delta\hat{u}}, \vec{\rho}_{\bar{u}} && \\ &\text{subject to} && \text{constraint (4.37) and (4.40)} \end{aligned} \quad (4.41)$$

where J_ρ is a suitable (linear or quadratic, if possible) cost function that allows to maximize the size of the constraint set.

4.7. Appendix

4.7.3 Proof of Theorem 4.1

The proof of Theorem 4.1 lies on the intermediate results stated below.

Proposition 4.1.

A) Under Assumption 4.3 and if $\bar{x}^{[N_L]}(k) = \beta x(kN_L)$, then for any initial condition $\hat{x}(kN_L) = x(kN_L)$ such that, for all $i = 1, \dots, M$

$$\|x(kN_L) - x_s\| \leq \lambda_i(N_L) \quad (4.42)$$

and for any $\bar{u}^{[N_L]} \in \bar{u}_s \oplus \bar{\mathcal{W}}_s$ there exists a feasible sequence $\overrightarrow{\delta \hat{u}_i^{[\zeta_i]}}(kN_i : (k+1)N_i - 1 | kN_L) \in \Delta \hat{\mathcal{W}}_i^{N_i}$ such that the terminal constraint (4.22) is satisfied.

B) if $x(kN_L)$ satisfies condition (4.42), $\|A_L^{N_L}\| < 1$, and, for all $i = 1, \dots, M$, (4.29) is verified, then recursive feasibility of the terminal constraint (4.22) is guaranteed.

Proof of Proposition 4.1

A) Note that, since $\delta \hat{x}_i^{[\zeta_i]}(kN_i) = \delta \hat{x}_i(kN_L) = 0$,

$$\begin{aligned} \beta_i \delta \hat{x}_i((k+1)N_L) &= \beta_i \delta \hat{x}_i^{[\zeta_i]}((k+1)N_i) = \\ &= \mathcal{H}_i(N_i) \overrightarrow{\delta \hat{u}_i^{[\zeta_i]}}(kN_i : (k+1)N_i - 1 | kN_L) \end{aligned} \quad (4.43)$$

Moreover, in view of (4.5)

$$\bar{x}^{[N_L]}(k+1) = A_H^{N_L} \beta x(kN_L) + \sum_{j=1}^{N_L} A_H^{N_L-j} B_H \bar{u}^{[N_L]}(k) \quad (4.44a)$$

$$\bar{x}_s = A_H^{N_L} \beta x_s + \sum_{j=1}^{N_L} A_H^{N_L-j} B_H \bar{u}_s \quad (4.44b)$$

Analogously, from (4.16) written in collective form we have

$$\beta \hat{x}(kN_L + N_L) = \beta A_L^{N_L} x(kN_L) + \beta \sum_{j=1}^{N_L} A_L^{N_L-j} B_L \bar{u}^{[N_L]}(k) \quad (4.45a)$$

$$\beta x_s = \beta A_L^{N_L} x_s + \beta \sum_{j=1}^{N_L} A_L^{N_L-j} B_L \bar{u}_s \quad (4.45b)$$

Therefore, in view of (4.43), (4.44a), (4.45a), and the definition $\mathcal{A}(N_L)$,

Chapter 4. Hierarchical multi-rate MPC scheme for interconnected systems

$\mathcal{B}(N_L)$, I_{si} , the constraint (4.22) can be written as

$$\begin{aligned} \mathcal{H}_i(N_i) \overrightarrow{\delta \hat{u}_i^{[\zeta_i]}}(kN_i : (k+1)N_i - 1 | kN_L) = \\ = I_{si}[\mathcal{A}(N_L)(x(kN_L) - x_s) + \mathcal{B}(N_L)(\bar{u}^{[N_L]}(k) - \bar{u}_s)] \end{aligned} \quad (4.46)$$

From this expression, the definitions of $\underline{\sigma}_{\mathcal{H}_i(N_i)}$, $\rho_{\bar{u}}$, $\rho_{\delta \hat{u}_i}$, and in view of (4.27), it can be concluded that a feasible sequence $\overrightarrow{\delta \hat{u}_i^{[\zeta_i]}}(kN_i : (k+1)N_i - 1 | kN_L)$ can be computed provided that

$$\sqrt{N_i} \underline{\sigma}_{\mathcal{H}_i(N_i)} \rho_{\delta \hat{u}_i} \geq \|\mathcal{A}(N_L)\| \|x(kN_L) - x_s\| + \kappa(N_L) \rho_{\bar{u}} \quad (4.47)$$

from which the result follows.

B) From (4.3) it holds that

$$\begin{aligned} x((k+1)N_L) - x_s = A_L^{N_L} (x(kN_L) - x_s) \\ + \mathcal{R}(N_L) (\overrightarrow{u}(kN_L : kN_L + N_L - 1 | kN_L) - \mathbb{1}_{N_L \times 1} \otimes \bar{u}_s) \end{aligned} \quad (4.48)$$

where \otimes is the Kronecker product. Hence

$$\|x((k+1)N_L) - x_s\| \leq \|A_L^{N_L}\| \|x(kN_L) - x_s\| + \sqrt{N_L} \|\mathcal{R}(N_L)\| \rho_u \quad (4.49)$$

and, in view of (4.42)

$$\begin{aligned} \|x((k+1)N_L) - x_s\| \leq \\ \leq \|A_L^{N_L}\| \frac{(\sqrt{N_i} \underline{\sigma}_{\mathcal{H}_i(N_i)} \rho_{\delta \hat{u}_i} - \kappa(N_L) \rho_{\bar{u}})}{\|\mathcal{A}(N_L)\|} + \sqrt{N_L} \|\mathcal{R}(N_L)\| \rho_u \end{aligned} \quad (4.50)$$

for all $i = 1, \dots, M$. From this expression and Assumption 4.3.(4)

$$\|x((k+1)N_L) - x_s\| \leq \frac{(\sqrt{N_i} \underline{\sigma}_{\mathcal{H}_i(N_i)} \rho_{\delta \hat{u}_i} - \kappa(N_L) \rho_{\bar{u}})}{\|\mathcal{A}(N_L)\|} = \lambda_i(N_L) \quad (4.51)$$

for all $i = 1, 2, \dots, M$ and the result follows. \square

Proposition 4.2. *If Problem (4.23) is feasible at time $h = kN_L$, then*

$$\|\bar{w}(k)\| \leq \rho_w \quad (4.52)$$

$$\delta u_i(kN_L + j) \in \Delta \mathcal{U}_i(j) \quad (4.53)$$

4.7. Appendix

Also it holds that

$$\Delta \bar{\mathcal{U}}_i \supseteq \Delta \mathcal{U}_i(j) \quad (4.54)$$

for all $j = 0, \dots, N_L - 1$. \square

Proof of Proposition 4.2

Defining the collective vectors $\hat{x} = (\hat{x}_1, \dots, \hat{x}_M)$, $\delta x = (\delta x_1, \dots, \delta x_M)$, $\delta \hat{x} = (\delta \hat{x}_1, \dots, \delta \hat{x}_M)$, and $\varepsilon(kN_L + j|kN_L) = \delta x(kN_L + j|kN_L) - \delta \hat{x}(kN_L + j|kN_L)$, we have that $\bar{w}(k) = \beta x(kN_L + N_L) - \bar{x}^{[N_L]}(k+1|k) = \beta \hat{x}(kN_L + N_L) + \beta \delta x(kN_L + N_L) - \bar{x}^{[N_L]}(k+1|k) = (\beta \hat{x}(kN_L + N_L) + \beta \delta \hat{x}(kN_L + N_L) - \bar{x}^{[N_L]}(k+1|k)) + \beta \varepsilon(kN_L + j|kN_L) = \beta \varepsilon(kN_L + j|kN_L)$. The latter equality holds in view of the fact that Problem (4.23) is feasible, and therefore equality (4.22) is verified. From (4.17), (4.18), (4.20), we collectively have that

$$\begin{aligned} \varepsilon(kN_L + j + 1|kN_L) &= F_L \varepsilon(kN_L + j|kN_L) \\ &\quad + (A_L - A_L^D) \delta \hat{x}(kN_L + j|kN_L) \end{aligned} \quad (4.55)$$

In view of the fact that $\varepsilon(kN_L|kN_L) = \delta \hat{x}(kN_L|kN_L) = 0$, then $\bar{w}(k) = \beta \sum_{j=2}^{N_L} F_L^{N_L-j} (A_L - A_L^D) \delta \hat{x}(kN_L + j - 1|kN_L)$. From this it follows that

$$\|\bar{w}(k)\| \leq \sum_{j=2}^{N_L} \|\beta F_L^{N_L-j} (A_L - A_L^D)\| \|\delta \hat{x}(kN_L + j - 1|kN_L)\| \quad (4.56)$$

Since $\delta \hat{u}_i$ are bounded for all $i = 1, \dots, M$, i.e., scalar $\rho_{\delta \hat{u}_i}$ are defined such that $\delta \hat{u}_i \in \mathcal{B}_{\rho_{\delta \hat{u}_i}}(0)$. In view of this, we compute that $\|\delta \hat{x}(kN_L + j|kN_L)\| \leq \rho_{\delta \hat{x}}(j)$, where $\rho_{\delta \hat{x}}(j)$ is defined in (4.30). Therefore, $\delta \hat{x}(kN_L + j|kN_L)$ are bounded, for all $j = 1, \dots, N_L - 1$ and more specifically we get that $\|\delta \hat{x}(kN_L + j|kN_L)\| \leq \sqrt{\sum_{i=1}^M \rho_{\delta \hat{x}_i}^2(j)}$. Therefore one has (4.52) for all $k \geq 0$.

From (4.55) we have that $\varepsilon(kN_L + j|kN_L) = \sum_{r=2}^j F_L^{j-r} (A_L - A_L^D) \delta \hat{x}(kN_L + r - 1|kN_L)$ and therefore $\delta u_i(kN_L + j) - \delta \hat{u}_i(kN_L + j|kN_L) = K_i \varepsilon_i(kN_L + j|kN_L) = K_i I_{si} \sum_{r=2}^j F_L^{j-r} (A_L - A_L^D) \delta \hat{x}(kN_L + r - 1|kN_L)$. From this it follows that $\delta u_i(kN_L + j) \in \delta \hat{u}_i(kN_L + j|kN_L) \oplus \mathcal{B}_{\rho_{\Delta u_i}(j)}(0)$ and therefore $\delta u_i(kN_L + j) \in \Delta \mathcal{U}_i(j)$. In view of the monotonicity property $\rho_{\Delta u_i}(j+1) \geq \rho_{\Delta u_i}(j)$ for all j , it holds that $\mathcal{B}_{\rho_{\Delta u_i}(j+1)}(0) \supseteq \mathcal{B}_{\rho_{\Delta u_i}(j)}(0)$, which implies (4.54). \square

Proof of Theorem 4.1

(i) If $\|x(0) - x_s\| \leq \lambda_i(N_L)$ and recalling that Assumption 4.3 holds, from Proposition 4.1, recursive feasibility of the optimization problems (4.23)

Chapter 4. Hierarchical multi-rate MPC scheme for interconnected systems

is guaranteed, i.e., that there exists, for all $k \geq 0$, a feasible sequence $\overrightarrow{\delta \hat{u}_i^{\zeta_i}}(kN_i : (k+1)N_i - 1 | kN_L) \in \Delta \hat{\mathcal{U}}_i^{N_i}$ such that the terminal constraint (4.22) is satisfied.

Also, from Proposition 4.2, it follows that $\bar{w}(k) \in \mathcal{W}$ for all $k \geq 0$, which allows to apply the recursive feasibility arguments of [121], proving that also (4.11) enjoys recursive feasibility properties.

(ii) It is now possible to conclude that, in view of the feasibility of (4.11), $\bar{u}^{[N_L]}(k) \in \bar{u}_s \oplus \mathcal{U}_s$; also, from Proposition 4.2 it follows that $\delta u_i(kN_L + j) \in \Delta \hat{\mathcal{U}}_i$ for all $k \geq 0$, $j = 0, \dots, N_L - 1$, and $i = 1, \dots, M$. From this, under (4.31), the inclusion (4.34) can also be proved.

(iii) We apply the results in [121], which guarantee robust convergence properties. In other words, it holds that $\bar{x}^{[N_L], o}(k) \rightarrow \bar{x}_s$ as $k \rightarrow +\infty$, and that $\bar{x}^{[N_L]}(k)$ is asymptotically driven to lie in the robust positively invariant set $\bar{x}_s \oplus \mathcal{X}$.

(iv) To show robust convergence of the global system state, from (4.3) we obtain that

$$\begin{aligned} x((k+1)N_L) &= A_L^{N_L} x(kN_L) + B_L^{[N_L]} \bar{u}^{[N_L]}(k) \\ &\quad + \sum_{h=0}^{N_L-1} A_L^h B_L \delta u((k+1)N_L - h - 1) \end{aligned} \quad (4.57)$$

Denoting $\mathcal{B}_{L, N_L}^C = [A_L^{N_L-1} B_L \quad \dots \quad B_L]$, we obtain that

$$\sum_{h=0}^{N_L-1} A_L^h B_L \delta u((k+1)N_L - h - 1) = \mathcal{B}_{L, N_L}^C \overrightarrow{\delta u}(kN_L : kN_L + N_L - 1)$$

Also, recall that $\overrightarrow{\delta u}(kN_L : kN_L + N_L - 1) = \overrightarrow{\delta \hat{u}}(kN_L : kN_L + N_L - 1) + \text{diag}(K, \dots, K) \overrightarrow{\epsilon}(kN_L : kN_L + N_L - 1)$ and that, by defining

$$\mathcal{F}_{N_L} = \begin{bmatrix} 0 & 0 & \dots & 0 & 0 & 0 \\ I_n & 0 & \dots & 0 & 0 & 0 \\ F_L & I_n & \dots & 0 & 0 & 0 \\ \vdots & \vdots & \ddots & \vdots & \vdots & \vdots \\ F_L^{N_L-2} & F_L^{N_L-3} & \dots & I_n & 0 & 0 \end{bmatrix},$$

then

$$\begin{aligned} \overrightarrow{\epsilon}(kN_L : kN_L + N_L - 1) &= \\ &= \mathcal{F}_{N_L} \text{diag}(A_L^C, \dots, A_L^C) \mathcal{B}_L \overrightarrow{\delta \hat{u}}(kN_L : kN_L + N_L - 1) \end{aligned}$$

4.7. Appendix

where $A_L^C = A_L - A_L^D$ and

$$\mathcal{B}_L = \begin{bmatrix} 0 & \cdots & 0 \\ \vdots & \ddots & \vdots \\ (A_L^D)^{N_L-1} B_L & \cdots & B_L \end{bmatrix}$$

Recalling that $\bar{x}^{[N_L]}(k) = \beta x(kN_L)$ and that

$$\bar{u}^{[N_L]}(k) = \bar{u}^{[N_L],o}(k) + \bar{K}_H(\bar{x}^{[N_L]}(k) - \bar{x}^{[N_L],o}(k)) \quad (4.58)$$

we can rewrite (4.57) as

$$\begin{aligned} x((k+1)N_L) &= (A_L^{N_L} + B_L^{[N_L]} \bar{K}_H \beta) x(kN_L) \\ &+ B_L^{[N_L]} (\bar{u}^{[N_L],o}(k) - \bar{K}_H \bar{x}^{[N_L],o}(k)) + \mathcal{B}_{L,N_L}^C \vec{\delta u}(kN_L : kN_L + N_L - 1) \end{aligned} \quad (4.59)$$

Recall that $\bar{x}^{[N_L],o}(k) \rightarrow \bar{x}_s$, $\bar{u}^{[N_L],o}(k) \rightarrow \bar{u}_s$ as $k \rightarrow +\infty$. Also, we compute that

$$\begin{aligned} \vec{\delta u}(kN_L : kN_L + N_L - 1) &= (I_{mN_L} + \text{diag}(K, \dots, K) \mathcal{F}_{N_L} \\ &\cdot \text{diag}(A_L^C, \dots, A_L^C) \mathcal{B}_L) \vec{\delta \hat{u}}(kN_L : kN_L + N_L - 1) \end{aligned} \quad (4.60)$$

Based on this, we define $\kappa_{\delta u} = \|\mathcal{B}_{L,N_L}^C (I_{mN_L} + \text{diag}(K, \dots, K) \mathcal{F}_{N_L} \text{diag}(A_L^C, \dots, A_L^C) \mathcal{B}_L)\|$ and we write (4.59) as

$$\begin{aligned} x((k+1)N_L) &= (A_L^{N_L} + B_L^{[N_L]} \bar{K}_H \beta) x(kN_L) \\ &+ B_L^{[N_L]} (\bar{u}^{[N_L],o}(k) - \bar{K}_H \bar{x}^{[N_L],o}(k)) + w_L(k) \end{aligned} \quad (4.61)$$

where $\|w_L(k)\| \leq \kappa_{\delta u} \sqrt{N_L} \max_{h \in \{kN_L, \dots, (k+1)N_L - 1\}} \|\delta \hat{u}(h)\| \leq \kappa_{\delta u} \sqrt{N_L} \sqrt{\sum_{i=1}^M \rho_{\delta \hat{u}_i}^2}$. Since $x_s = A_L^{N_L} x_s + B_L^{[N_L]} \bar{u}_s$ and $B_L^{[N_L]} \bar{K}_H \bar{x}_s = B_L^{[N_L]} \bar{K}_H \beta x_s$, we can rewrite (4.61) as

$$\begin{aligned} x((k+1)N_L) - x_s &= (A_L^{N_L} + B_L^{[N_L]} \bar{K}_H \beta) (x(kN_L) - x_s) + w_L(k) \\ &+ B_L^{[N_L]} \left((\bar{u}^{[N_L],o}(k) - \bar{u}_s) - \bar{K}_H (\bar{x}^{[N_L],o}(k) - \bar{x}_s) \right) \end{aligned}$$

Eventually, since $F_L^{[N_L]} = A_L^{N_L} + B_L^{[N_L]} \bar{K}_H \beta$ is Schur stable, then the asymptotic result follows, where $\rho_x = \kappa_{\delta u} \sqrt{N_L} \sqrt{\sum_{i=1}^M \rho_{\delta \hat{u}_i}^2}$.

(v) We can reformulate problem (4.23) as

$$\begin{aligned} \min \quad & \|\vec{\delta \hat{u}}(kN_L : kN_L + N_L - 1)\|_2^2 \\ \text{subject to:} \quad & \beta \mathcal{B}^D(N_L) \vec{\delta \hat{u}}(kN_L : kN_L + N_L - 1) = \delta \bar{x}_{end} \\ & A_{in} \vec{\delta \hat{u}}(kN_L : kN_L + N_L - 1) \leq b_{in}, \end{aligned} \quad (4.62)$$

Chapter 4. Hierarchical multi-rate MPC scheme for interconnected systems

where $\mathcal{Q} = \text{diag}(R, \dots, R) + \mathcal{B}_L^T \text{diag}(Q, \dots, Q) \mathcal{B}_L$, $R = \text{diag}(R_1, \dots, R_M)$, $Q = \text{diag}(Q_1, \dots, Q_M)$, $\delta \bar{x}_{end} = \bar{x}^{[N_L]}(k+1|k) - \beta \hat{x}(kN_L + N_L)$ and $\mathcal{R}^D(N_L) = [(A_L^D)^{N_L-1} B_L \ \dots \ B_L]$. Recalling that $b_{in} > 0$ elementwise, in view of continuity arguments, there exists a ball $\mathcal{B}_{\rho_{end}}(0)$ for $\delta \bar{x}_{end}$ such that the solution to problem (4.62) satisfies $A_{in} \overrightarrow{\delta \hat{u}}(kN_L : kN_L + N_L - 1) \leq b_{in}$. If $\delta \bar{x}_{end} \in \mathcal{B}_{\rho_{end}}(0)$, then

$$\overrightarrow{\delta \hat{u}}(kN_L : kN_L + N_L - 1) = [I_{mN_L} \ 0] \begin{bmatrix} 2\mathcal{Q} & (\beta \mathcal{R}^D(N_L))^T \\ \beta \mathcal{R}^D(N_L) & 0 \end{bmatrix}^{-1} \begin{bmatrix} 0 \\ I_{\bar{n}} \end{bmatrix} \delta \bar{x}_{end}$$

Also, it holds that the optimal constrained solution fulfills

$$\|\overrightarrow{\delta \hat{u}}(kN_L : kN_L + N_L - 1)\|_{\mathcal{Q}}^2 \leq \max_{A_{in} \overrightarrow{\delta \hat{u}} \leq b_{in}} \|\overrightarrow{\delta \hat{u}}\|_{\mathcal{Q}}^2 = J_L^{max}$$

and therefore $\|\overrightarrow{\delta \hat{u}}(kN_L : kN_L + N_L - 1)\| \leq \sqrt{\frac{J_L^{max}}{\lambda_{min}(\mathcal{Q})}}$; in view of this, for $\|\delta \bar{x}_{end}\| \notin \mathcal{B}_{\rho_{end}}(0)$, then $\|\overrightarrow{\delta \hat{u}}(kN_L : kN_L + N_L - 1)\| \leq \sqrt{\frac{J_L^{max}}{\lambda_{min}(\mathcal{Q})}} \frac{1}{\rho_{end}} \|\delta \bar{x}_{end}\|$. Defining now

$$\bar{\kappa} = \max \left\{ \left\| [I_{mN_L} \ 0] \begin{bmatrix} 2\mathcal{Q} & (\beta \mathcal{R}^D(N_L))^T \\ \beta \mathcal{R}^D(N_L) & 0 \end{bmatrix}^{-1} \begin{bmatrix} 0 \\ I_{\bar{n}} \end{bmatrix} \right\|, \sqrt{\frac{J_L^{max}}{\lambda_{min}(\mathcal{Q})}} \frac{1}{\rho_{end}} \right\}$$

then we conclude that

$$\|\overrightarrow{\delta \hat{u}}(kN_L : kN_L + N_L - 1)\| \leq \bar{\kappa} \|\delta \bar{x}_{end}\| \quad (4.63)$$

Therefore, from (4.60) and (4.63), we have that

$$\begin{aligned} \|\overrightarrow{\delta u}(kN_L : kN_L + N_L - 1)\| &\leq \kappa_u \|\overrightarrow{\delta \hat{u}}(kN_L : kN_L + N_L - 1)\| \\ &\leq \kappa_u \bar{\kappa} \|\mathcal{A}(N_L)(x(kN_L) - x_s) + \mathcal{B}(N_L)(\bar{u}^{[N_L]}(k) - \bar{u}_s)\| \end{aligned} \quad (4.64)$$

where

$$\kappa_u = \|I_{mN_L} + \text{diag}(K, \dots, K) \mathcal{F}_{N_L} \text{diag}(A_L^C, \dots, A_L^C) \mathcal{B}_L\|$$

In view of this, we can rewrite (4.59) as

$$x((k+1)N_L) - x_s = F_L^{[N_L]}(x(kN_L) - x_s) + w_x(k) + w_o(k) \quad (4.65)$$

where $\|w_x(k)\| \leq \kappa_x(N_L) \|x(kN_L) - x_s\|$, $\kappa_x(N_L) = \kappa_u \bar{\kappa} \|\mathcal{B}_{L, N_L}^C\| \|\mathcal{A}(N_L) + \mathcal{B}(N_L) \bar{K}_H \beta\|$, $\|w_o(k)\| \leq \kappa_u^o \|\bar{u}^{[N_L], o}(k) - \bar{u}_s\| + \kappa_x^o \|\bar{x}^{[N_L], o}(k) - \bar{x}_s\|$, $\kappa_u^o = \|B_L^{[N_L]}\| + \kappa_u \bar{\kappa} \|\mathcal{B}_{L, N_L}^C\| \|\mathcal{B}(N_L)\|$, and

$$\kappa_x^o = \|B_L^{[N_L]} \bar{K}_H\| + \kappa_u \bar{\kappa} \|\mathcal{B}_{L, N_L}^C\| \|\mathcal{B}(N_L) \bar{K}_H\|$$

4.7. Appendix

To derive a stability condition, we recast (4.65) as the following redundant dynamic system

$$\begin{aligned}\delta x_1^+ &= F_L^{[N_L]} \delta x_1 + w_{\delta x_2} + w_o \\ \delta x_2^+ &= F_L^{[N_L]} \delta x_2 + w_{\delta x_1} + w_o\end{aligned}\tag{4.66}$$

where the initial conditions for δx_1 and δx_2 coincide and are equal to $x(0) - x_S$, and where $\|w_{\delta x_i}\| \leq \kappa_x(N_L) \|\delta x_i\|$, $i = 1, 2$. Recall also that, as already discussed, w_o is an asymptotically vanishing input.

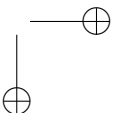
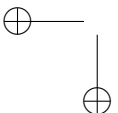
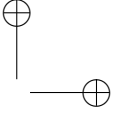
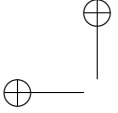
The stability of the system (4.66) can be studied using the (ISS) small gain theorem in [40], according to which the interconnected system above enjoys asymptotic stability properties if the matrix

$$\Gamma = \begin{bmatrix} 0 & \sigma(N_L) \\ \sigma(N_L) & 0 \end{bmatrix}$$

is Schur stable, where

$$\sigma(N_L) = \kappa_x(N_L) \sum_{k=0}^{+\infty} \|(F_L^{[N_L]})^k\|\tag{4.67}$$

Also, Γ is Schur stable if and only if the inequality (4.35) is verified. Then, under the latter condition, $x(kN_L) \rightarrow x_S$ as $k \rightarrow +\infty$. \square



CHAPTER 5

Conclusions

This chapter summarizes the main contributions of the Thesis and proposes some hints for future research on hierarchical control structures based on MPC.

5.1 Conclusions

In this Thesis, novel hierarchical control structures for large-scale systems have been developed.

Specifically, in Chapter 2, a two-layer control scheme for coordination of linear system with input and joint output constraints has been first considered. Its main characteristics are: *(i)* time scale separation is employed at different layers; *(ii)* it requires simplified models to be used at the high layer of the control structure; *(iii)* it allows to consider long-term objectives at the high layer, for instance based on economic criteria or output throughput, and short-term goals at the low layer, typically fast compensation of disturbances and model mismatch. A novel model reduction technique has been proposed to guarantee the consistency between the two layers of the control structure. The overall convergence, recursive feasibility, as well as the fulfillment of the joint constraints, have been obtained under mild

Chapter 5. Conclusions

assumptions.

A fully scalable hierarchical control scheme for coordination of similar independent systems with joint output and input constraints has been discussed in Chapter 3. Compared to the technique developed in Chapter 2, this approach includes a significant improvement for the following reasons: *(i)* the problem at the high level is fully scalable with the number of subsystems, so allowing for plug and play operations, *(ii)* the high-level model is easily determined from the impulse responses of the subsystems and its state is measurable, being composed by past inputs, *(iii)* constraints on the shared resources (inputs) are included, *(iv)* the possibility to perform static high level optimization is explicitly considered to optimize the subsystems’ usage and provide flexibility to the control configuration. The recursive feasibility has been guaranteed also during plug-in and plug-out operations, and overall convergence of the system output to the set-point has been proven.

Then in Chapter 4, the analysis has been extended to interconnected systems. Differently from Chapter 2, the control framework includes a robust centralized MPC algorithm at the high layer, optimizing a long-term performance index with respect to a reduced order model, and a set of lower layer local MPC regulators for the full order models of the subsystems refining the control action computed at the higher layer. Notably, the local regulators can be designed and implemented at different rates to cope with subsystems operating at different time scales. The recursive feasibility and robustness of the two layer algorithms have been guaranteed and the convergence of the state to the steady state has been discussed.

5.2 Hints for future research

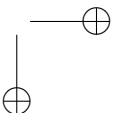
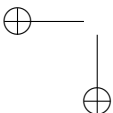
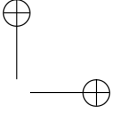
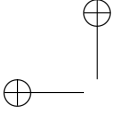
Some possible hints for future research are listed below:

- In Chapter 2 and 3, we propose two hierarchical control solutions for coordination of independent systems, in these schemes the decentralized regulators at the low level are designed to work at a short time scale. Future work will consider the use of multi-rate low-level algorithms to deal with systems with significantly different dynamics and the application of this approach to industrial control problems.
- In Chapter 4, the proposed solutions for interconnected systems consists in considering the couplings between subsystems as disturbances to be rejected. The influence of couplings between subsystems on the global performance is still not clear. In future work we will include

5.2. Hints for future research

dynamic network topology optimization at the high layer by resorting to game-theoretic methods according to a global criterion so as to determine the most appropriate partition for the overall system. Preliminary results can be found in [4, 126, 141].

- In this Thesis, system reconfiguration for coordination of independent systems is considered. However, for the interconnected system, controller reconfiguration is also very useful when a local fault is detected so that local controller redesign is required and plug-and-play operations are advisable. Future work will also exploit the possibility to allow controller reconfiguration in the hierarchical control framework for interconnected systems in order to preserve closed-loop theoretical properties and constraint satisfaction.



Bibliography

- [1] E. Abed. Decomposition and stability for multiparameter singular perturbation problems. *IEEE Transactions on Automatic Control*, 31(10):925–934, 1986.
- [2] E. Abed. Strong D-stability. *Systems & Control Letters*, 7(3):207–212, 1986.
- [3] V. Adetola and M. Guay. Integration of real-time optimization and model predictive control. *Journal of Process Control*, 20(2):125–133, 2010.
- [4] W. Al-Gherwi, H. Budman, and A. Elkamel. Selection of control structure for distributed model predictive control in the presence of model errors. *Journal of Process Control*, 20(3):270–284, 2010.
- [5] A. Alessio and A. Bemporad. Decentralized model predictive control of constrained linear systems. In *2007 European Control Conference*, pages 2813–2818. IEEE, 2007.
- [6] R. Amrit. *Optimizing process economics in model predictive control*. PhD thesis, University of Wisconsin–Madison, 2011.
- [7] R. Amrit, J. B. Rawlings, and D. Angeli. Economic optimization using model predictive control with a terminal cost. *Annual Reviews in Control*, 35(2):178–186, 2011.
- [8] D. Angeli, R. Amrit, and J. B. Rawlings. On average performance and stability of economic model predictive control. *IEEE Transactions on Automatic Control*, 57(7):1615–1626, 2012.
- [9] L. Bakule and J. Lunze. Decentralized design of feedback control for large-scale systems. *Kybernetika*, 24(8):1–3, 1988.
- [10] M. Baldea and P. Daoutidis. Control of integrated process networks—a multi-time scale perspective. *Computers & Chemical Engineering*, 31(5):426–444, 2007.
- [11] M. Baldea and P. Daoutidis. *Dynamics and Nonlinear Control of Integrated Process Systems*. Cambridge University Press, 2012.
- [12] D. Barcelli, A. Bemporad, and G. Ripaccioli. Hierarchical multi-rate control design for constrained linear systems. In *49th IEEE Conference on Decision and Control*, pages 5216–5221. IEEE, 2010.
- [13] F. A. Bayer, M. A. Müller, and F. Allgöwer. Tube-based robust economic model predictive control. *Journal of Process Control*, 24(8):1237–1246, 2014.

Bibliography

- [14] A. Bemporad and D. Barcelli. Decentralized model predictive control. In *Networked Control Systems*, pages 149–178. Springer, 2010.
- [15] A. Bemporad, F. Borrelli, and M. Morari. Robust model predictive control: Piecewise linear explicit solution. In *2001 European Control Conference*, pages 939–944. IEEE, 2001.
- [16] A. Bemporad, F. Borrelli, and M. Morari. Min-max control of constrained uncertain discrete-time linear systems. *IEEE Transactions on Automatic Control*, 48(9):1600–1606, 2003.
- [17] J. Bendtsen, K. Trangbaek, and J. Stoustrup. Hierarchical model predictive control for resource distribution. In *49th IEEE Conference on Decision and Control*, pages 2468–2473. IEEE, 2010.
- [18] B.W. Bequette. Nonlinear predictive control using multi-rate sampling. *The Canadian Journal of Chemical Engineering*, 69(1):136–143, 1991.
- [19] G. Betti, M. Farina, and R. Scattolini. A robust MPC algorithm for offset-free tracking of constant reference signals. *IEEE Transactions on Automatic Control*, 58(9):2394–2400, 2013.
- [20] G. Betti, M. Farina, and R. Scattolini. Distributed MPC: A noncooperative approach based on robustness concepts. In *Distributed Model Predictive Control Made Easy*, pages 421–435. Springer, 2014.
- [21] F. Blanchini. Set invariance in control. *Automatica*, 35(11):1747–1767, 1999.
- [22] F. Blanchini and S. Miani. *Set-theoretic methods in control*. Springer, 2008.
- [23] S. Boyd and L. Vandenberghe. *Convex optimization*. Cambridge university press, 2004.
- [24] M. A. Brdys, M. Grochowski, T. Gminski, K. Konarczak, and M. Drewa. Hierarchical predictive control of integrated wastewater treatment systems. *Control Engineering Practice*, 16(6):751–767, 2008.
- [25] E. F. Camacho and C. Bordons. *Model predictive control in the process industry*. Springer Science & Business Media, 2012.
- [26] E. F. Camacho and C. Bordons. *Model predictive control*. Springer Science & Business Media, 2013.
- [27] E. Camponogara, D. Jia, B. H. Krogh, and S. Talukdar. Distributed model predictive control. *IEEE Control Systems*, 22(1):44–52, 2002.
- [28] X. Chen, M. Heidarinejad, J. Liu, , and P. D. Christofides. Composite fast-slow MPC design for nonlinear singularly perturbed systems. *AIChE Journal*, 58(6):1802–1811, 2012.
- [29] X. Chen, M. Heidarinejad, J. Liu, D. Munoz de la Pena, and P. D. Christofides. Model predictive control of nonlinear singularly perturbed systems: Application to a large-scale process network. *Journal of Process Control*, 21(9):1296–1305, 2011.
- [30] X. Chen, M. Heidarinejad, L. Liu, and P. D. Christofides. Composite fast-slow MPC design for nonlinear singularly perturbed systems: Stability analysis. In *2012 American Control Conference*, pages 4136–4141. IEEE, 2012.
- [31] X. B. Chen and S. S. Stanković. Decomposition and decentralized control of systems with multi-overlapping structure. *Automatica*, 41(10):1765–1772, 2005.
- [32] L. Chisci, J. A. Rossiter, and G. Zappa. Systems with persistent disturbances: Predictive control with restricted constraints. *Automatica*, 37(7):1019–1028, 2001.
- [33] S. Raimondi Cominesi, A. La Bella, M. Farina, and R. Scattolini. A multi-layer control scheme for microgrid energy management. *IFAC-PapersOnLine*, 49(27):256–261, 2016.
- [34] S. Raimondi Cominesi, M. Farina, L. Giulioni, B. Picasso, and R. Scattolini. A two-layer stochastic model predictive control scheme for microgrids. *IEEE Transactions on Control Systems Technology*, PP(99):1–13, 2017.

Bibliography

- [35] C. Conte, M. N. Zeilinger, M. Morari, and C. Jones. Robust distributed model predictive control of linear systems. In *2013 European Control Conference*, pages 2764–2769. IEEE, 2013.
- [36] S. Conti, R. Nicolosi, S. A. Rizzo, and H. H. Zeineldin. Optimal dispatching of distributed generators and storage systems for MV islanded microgrids. *IEEE Trans. on Power Delivery*, 27:1243–1251, 2012.
- [37] B. Coulbeck, M. Brdyś, C. H. Orr, and J. P. Rance. A hierarchical approach to optimized control of water distribution systems: Part I decomposition. *Optimal Control Applications and Methods*, 9(1):51–61, 1988.
- [38] C. R. Cutler and R. T. Perry. Real-time optimization with multivariable control is required to maximize profits. *Computers & Chemical Engineering*, 7(5):663–667, 1983.
- [39] M. L. Darby, M. Nikolaou, J. Jones, and D. Nicholson. RTO: An overview and assessment of current practice. *Journal of Process Control*, 21:874–884, 2011.
- [40] S. Dashkovskiy, B. S. Rüffer, and F. R. Wirth. An ISS small gain theorem for general networks. *Mathematics of Control, Signals, and Systems*, 19(2):93–122, 2007.
- [41] E. J. Davison and T. N. Chang. Decentralized stabilization and pole assignment for general proper systems. *IEEE Transactions on Automatic Control*, 35(6):652–664, 1990.
- [42] M. Diehl, R. Amrit, and J. B. Awlings. A Lyapunov function for economic optimizing model predictive control. *IEEE Transactions on Automatic Control*, 56(3):703–707, 2011.
- [43] B. Ding. Distributed robust MPC for constrained systems with polytopic description. *Asian Journal of Control*, 13(1):198–212, 2011.
- [44] X. Du, Y. Xi, and S. Li. Distributed model predictive control for large-scale systems. In *2001 American Control Conference*, volume 4, pages 3142–3143. IEEE, 2001.
- [45] W. B. Dunbar. Distributed receding horizon control of dynamically coupled nonlinear systems. *IEEE Transactions on Automatic Control*, 52(7):1249–1263, 2007.
- [46] W. B. Dunbar and R. M. Murray. Distributed receding horizon control for multi-vehicle formation stabilization. *Automatica*, 42(4):549–558, 2006.
- [47] D. Elixmann, J. Busch, and W. Marquardt. Integration of model-predictive scheduling, dynamic real-time optimization and output tracking for a wastewater treatment process. *IFAC Proceedings Volumes*, 43(6):90–95, 2010.
- [48] M. Ellis and P. D. Christofides. Optimal time-varying operation of nonlinear process systems with economic model predictive control. *Industrial & Engineering Chemistry Research*, 53(13):4991–5001, 2013.
- [49] M. Ellis and P. D. Christofides. Integrating dynamic economic optimization and model predictive control for optimal operation of nonlinear process systems. *Control Engineering Practice*, 22:242–251, 2014.
- [50] M. Ellis, H. Durand, and P. D. Christofides. A tutorial review of economic model predictive control methods. *Journal of Process Control*, 24(8):1156–1178, 2014.
- [51] M. Ellis, M. Heidarinejad, and P. D. Christofides. Economic model predictive control of nonlinear singularly perturbed systems. *Journal of Process Control*, 23(5):743–754, 2013.
- [52] W. Ellis and P. D. Christofides. Unifying dynamic economic optimization and model predictive control for optimal process operation. In *2013 American Control Conference*, pages 3135–3140. IEEE, 2013.
- [53] S. Engell. Feedback control for optimal process operation. *Journal of Process Control*, 17:203–219, 2007.

Bibliography

- [54] A. Farhadi and A. Khodabandehlou. Distributed model predictive control with hierarchical architecture for communication: Application in automated irrigation channels. *International Journal of Control*, 89(8):1725–1741, 2016.
- [55] M. Farina and R. Carli. Partition-based distributed Kalman filter with plug and play features. *IEEE Transactions on Control of Network Systems*, 2016.
- [56] M. Farina, P. Colaneri, and R. Scattolini. Block-wise discretization accounting for structural constraints. *Automatica*, 49(11):3411–3417, 2013.
- [57] M. Farina, A. Perizzato, and R. Scattolini. Application of distributed predictive control to motion and coordination problems for unicycle autonomous robots. *Robotics and Autonomous Systems*, 72:248–260, 2015.
- [58] M. Farina and R. Scattolini. Distributed non-cooperative MPC with neighbor-to-neighbor communication. *IFAC Proceedings Volumes*, 44(1):404–409, 2011.
- [59] M. Farina and R. Scattolini. Distributed predictive control: a non-cooperative algorithm with neighbor-to-neighbor communication for linear systems. *Automatica*, 48(6):1088–1096, 2012.
- [60] M. Farina and R. Scattolini. Tube-based robust sampled-data MPC for linear continuous-time systems. *Automatica*, 48(7):1473–1476, 2012.
- [61] J. F. Forbes and T. E. Marlin. Design cost: A systematic approach to technology selection for model-based real-time optimization systems. *Computers & Chemical Engineering*, 20(6-7):717–734, 1996.
- [62] M. G. Forbes, R.S. Patwardhan, H. Hamadah, and R.B. Gopaluni. Model predictive control in industry: Challenges and opportunities. *IFAC-PapersOnLine*, 48(8):531–538, 2015.
- [63] E. Franco, L. Magni, T. Parisini, M. M. Polycarpou, and D. M. Raimondo. Cooperative constrained control of distributed agents with nonlinear dynamics and delayed information exchange: A stabilizing receding-horizon approach. *IEEE Transactions on Automatic Control*, 53(1):324–338, 2008.
- [64] C. E. Garcia, D. M. Prett, and M. Morari. Model predictive control: Theory and practice - a survey. *Automatica*, 25(3):335–348, 1989.
- [65] E. G. Gilbert and K. T. Tan. Linear systems with state and control constraints: The theory and application of maximal output admissible sets. *IEEE Transactions on Automatic Control*, 36(9):1008–1020, 1991.
- [66] K. Glover. All optimal hankel-norm approximations of linear multivariable systems and their L-infinity error bounds. *International Journal of Control*, 39(6):1115–1193, 1984.
- [67] G. C. Goodwin, M. E. Salgado, and E. I. Silva. Time-domain performance limitations arising from decentralized architectures and their relationship to the RGA. *International Journal of control*, 78(13):1045–1062, 2005.
- [68] G. Grimm, M. J. Messina, S. E. Tuna, and A. R. Teel. Examples when nonlinear model predictive control is nonrobust. *Automatica*, 40(10):1729–1738, 2004.
- [69] L. Grüne. Economic receding horizon control without terminal constraints. *Automatica*, 49(3):725–734, 2013.
- [70] S. Gugercin. *Projection methods for model reduction of large-scale dynamical systems*. PhD thesis, Rice University, 2003.
- [71] K. E. Häggblom. Partial relative gain: A new tool for control structure selection. In *AICHE Annual Meeting*. Citeseer, 1997.

Bibliography

- [72] R. Halvgaard, N. K. Poulsen, H. Madsen, and J. B. Jørgensen. Thermal storage power balancing with model predictive control. In *2013 European Control Conference*, pages 2567–2572. IEEE, 2013.
- [73] R. Halvgaard, L. Vandenberghe, N. K. Poulsen, H. Madsen, and J. B. Jørgensen. Distributed model predictive control for smart energy systems. *IEEE Transactions on Smart Grid*, 7(3):1675–1682, 2016.
- [74] M. J. He, W. J. Cai, and B. F. Wu. Control structure selection based on relative interaction decomposition. *International Journal of Control*, 79(10):1285–1296, 2006.
- [75] M. Heidarnejad, J. Liu, and P. D. Christofides. Economic model predictive control of nonlinear process systems using Lyapunov techniques. *AIChE Journal*, 58(3):855–870, 2012.
- [76] M. Heidarnejad, J. Liu, D. M. de la Peña, J. F. Davis, and P. D. Christofides. Multirate Lyapunov-based distributed model predictive control of nonlinear uncertain systems. *Journal of Process Control*, 21(9):1231–1242, 2011.
- [77] A. Helbig, O. Abel, and W. Marquardt. Structural concepts for optimization based control of transient processes. In *Nonlinear Model Predictive Control*, pages 295–311. Springer, 2000.
- [78] E. J. Van Henten and J. Bontsema. Time-scale decomposition of an optimal control problem in greenhouse climate management. *Control Engineering Practice*, 17(1):88–96, 2009.
- [79] M. Herceg, M. Kvasnica, C. N. Jones, and M. Morari. Multi-parametric toolbox 3.0. In *Control Conference (ECC), 2013 European*, pages 502–510. IEEE, 2013.
- [80] X. B. Hu and W. H. Chen. Model predictive control: terminal region and terminal weighting matrix. *Proceedings of the Institution of Mechanical Engineers, Part I: Journal of Systems and Control Engineering*, 222(2):69–79, 2008.
- [81] C. Huang, X. Chen, Y. Zhang, S. Qin, Y. Zeng, and X. Li. Hierarchical model predictive control for multi-robot navigation. Available Online at <http://hdl.handle.net/10149/607441>, 2016.
- [82] R. Huang, E. Harinath, and L. T. Biegler. Lyapunov stability of economically oriented NMPC for cyclic processes. *Journal of Process Control*, 21(4):501–509, 2011.
- [83] I. M. Jaimoukha and E. M. Kasenally. Implicitly restarted krylov subspace methods for stable partial realizations. *SIAM Journal on Matrix Analysis and Applications*, 18(3):633–652, 1997.
- [84] D. Jia and B. Krogh. Min-max feedback model predictive control for distributed control with communication. In *Proceedings of the 2002 American Control Conference*, volume 6, pages 4507–4512. IEEE, 2002.
- [85] M. Jilg and O. Stursberg. Hierarchical distributed control for interconnected systems. *IFAC Proceedings Volumes*, 46(13):419–425, 2013.
- [86] S. S. Jogwar, S. Rangarajan, and P. Daoutidis. Multi-time scale dynamics in energy-integrated networks: A graph theoretic analysis. *IFAC Proceedings Volumes*, 44(1):6085–6090, 2011.
- [87] J. V. Kadam and W. Marquardt. Integration of economical optimization and control for intentionally transient process operation. In *Assessment and Future Directions of Nonlinear Model Predictive Control*, pages 419–434. Springer, 2007.
- [88] J. V. Kadam, W. Marquardt, M. Schlegel, T. Backx, O. H. Bosgra, P. J. Brouwer, G. Dunnebler, D. van Hessem, A. Tiagounov, and S. de Wolf. Towards integrated dynamic real-time optimization and control of industrial processes. In *Foundations of Computer-Aided Process Operations*, 2003.
- [89] F. Kennel, D. Görge, and S. Liu. Energy management for smart grids with electric vehicles based on hierarchical MPC. *IEEE Transactions on Industrial Informatics*, 9(3):1528–1537, 2013.

Bibliography

- [90] T. Keviczky, F. Borrelli, and G. J. Balas. Hierarchical design of decentralized receding horizon controllers for decoupled systems. In *43rd IEEE Conference on Decision and Control*, volume 2, pages 1592–1597. IEEE, 2004.
- [91] T. Keviczky, F. Borrelli, and G. J. Balas. Decentralized receding horizon control for large scale dynamically decoupled systems. *Automatica*, 42(12):2105–2115, 2006.
- [92] H. K. Khalil and P. V. Kokotovic. D-stability and multi-parameter singular perturbation. *SIAM Journal on Control and Optimization*, 17(1):56–65, 1979.
- [93] P. V. Kokotovic, R. E. O’malley, and P. Sannuti. Singular perturbations and order reduction in control theory—an overview. *Automatica*, 12(2):123–132, 1976.
- [94] M. V. Kothare, V. Balakrishnan, and M. Morari. Robust constrained model predictive control using linear matrix inequalities. *Automatica*, 32(10):1361–1379, 1996.
- [95] A. Kouvelas, K. Aboudolas, E. B. Kosmatopoulos, and M. Papageorgiou. Adaptive performance optimization for large-scale traffic control systems. *IEEE Transactions on Intelligent Transportation Systems*, 12(4):1434–1445, 2011.
- [96] C. Kuehn. *Multiple time scale dynamics*, volume 191. Springer, 2015.
- [97] A. Kumar and P. Daoutidis. Nonlinear dynamics and control of process systems with recycle. *Journal of Process Control*, 12:475–484, 2002.
- [98] W. Langson, I. Chrysochoos, S.V. Raković, and D. Q. Mayne. Robust model predictive control using tubes. *Automatica*, 40(1):125–133, 2004.
- [99] T. Larsson and S. Skogestad. Plantwide control—a review and a new design procedure. *Modeling, Identification and Control*, 21(4):209, 2000.
- [100] M. Lawryczuk, P. M. Marisa, and P. Tatjewski. Efficient model predictive control integrated with economic optimisation. In *2007 Mediterranean Conference on Control & Automation*, pages 1–6. IEEE, 2007.
- [101] J. H. Lee, M. S. Gelormino, and M. Morari. Model predictive control of multi-rate sampled-data systems: A state-space approach. *International Journal of Control*, 55:153–191, 1992.
- [102] J. H. Lee and Z. Yu. Worst-case formulations of model predictive control for systems with bounded parameters. *Automatica*, 33(5):763–781, 1997.
- [103] S. Leirens, C. Zamora, R. R. Negenborn, and B. D. Schutter. Coordination in urban water supply networks using distributed model predictive control. In *2010 American Control Conference*, pages 3957–3962. IEEE, 2010.
- [104] S. Li, Y. Zhang, and Q. Zhu. Nash-optimization enhanced distributed model predictive control applied to the shell benchmark problem. *Information Sciences*, 170(2):329–349, 2005.
- [105] D. Limon, I. Alvarado, T. Alamo, and E.F. Chamacho. MPC for tracking piecewise constant references for constrained linear systems. *Automatica*, 44(9):2382–2387, 2008.
- [106] J. Liu, D. M. de la Peña, and P. D. Christofides. Distributed model predictive control of nonlinear process systems. *AIChE Journal*, 55(5):1171–1184, 2009.
- [107] J. Liu, D. M. de la Peña, and P. D. Christofides. Distributed model predictive control of nonlinear systems subject to asynchronous and delayed measurements. *Automatica*, 46(1):52–61, 2010.
- [108] J. Lofberg. Yalmip: A toolbox for modeling and optimization in matlab. In *2004 IEEE International Symposium on Computer Aided Control Systems Design*, pages 284–289. IEEE, 2004.
- [109] Y. Long, S. Liu, L. Xie, and K. H. Johansson. A hierarchical distributed MPC for HVAC systems. In *2016 American Control Conference*, pages 2385–2390. IEEE, 2016.

Bibliography

- [110] J. Lunze. *Feedback control of large-scale systems*. Prentice Hall International Series in Systems and Control Engineering, 1992.
- [111] M. L. Luyben and W. L. Luyben. Design and control of a complex process involving two reaction steps, three distillation columns, and two recycle streams. *Industrial & Engineering chemistry research*, 34(11):3885–3898, 1995.
- [112] J. M. Maciejowski. *Predictive control: with constraints*. Prentice Hall, 2001.
- [113] J. M. Maestre and R. R. Negenborn. *Distributed Model Predictive Control Made Easy*, volume 69. Springer Science & Business Media, 2013.
- [114] L. Magni and R. Scattolini. Stabilizing decentralized model predictive control of nonlinear systems. *Automatica*, 42(7):1231–1236, 2006.
- [115] D. L. Marruedo, T. Alamo, and E. F. Camacho. State stable MPC for constrained discrete-time nonlinear systems with bounded additive uncertainties. In *Proceedings of the 41st IEEE Conference on Decision and Control*, volume 4, pages 4619–4624. IEEE, 2002.
- [116] D. L. Marruedo, T. Alamo, D. M. Raimondo, D. M. De La Peña, J. M. Bravo, A. Ferramosca, and E.F. Camacho. Input-to-state stability: A unifying framework for robust model predictive control. In *Nonlinear Model Predictive Control*, pages 1–26. Springer, 2009.
- [117] R. Martí, D. Sarabia, and C. de Prada. Price-driven coordination for distributed NMPC using a feedback control law. In *Distributed Model Predictive Control Made Easy*, pages 73–88. Springer, 2014.
- [118] P. Marusak and P. Tatjewski. Multilayer and integrated structures for predictive control and economic optimisation. *IFAC Proceedings Volumes*, 40(9):198–205, 2007.
- [119] D. Q. Mayne, S. V. Raković, R. Findeisen, and F. Allgöwer. Robust output feedback model predictive control of constrained linear systems. *Automatica*, 42(7):1217–1222, 2006.
- [120] D. Q. Mayne, J. B. Rawlings, C. V. Rao, and P. O. Scokaert. Constrained model predictive control: Stability and optimality. *Automatica*, 36(6):789–814, 2000.
- [121] D. Q. Mayne, M. M. Seron, and S. V. Raković. Robust model predictive control of constrained linear systems with bounded disturbances. *Automatica*, 41(2):219–224, 2005.
- [122] B. Moore. Principal component analysis in linear systems: Controllability, observability, and model reduction. *IEEE Transactions on Automatic Control*, 26(1):17–32, 1981.
- [123] H. Morais, P. Kadar, P. Faria, Z.A. Vale, and H.M. Khodr. Optimal scheduling of a renewable micro-grid in an isolated load area using mixed-integer linear programming. *Renewable Energy*, 35:151–156, 2010.
- [124] M. Morari and J.H. Lee. Model predictive control: Past, present and future. *Computers & Chemical Engineering*, 23(4):667–682, 1999.
- [125] P. D. Morosan, R. Bourdais, D. Dumur, and J. Buisson. A distributed MPC strategy based on Benders’ decomposition applied to multi-source multi-zone temperature regulation. *Journal of Process Control*, 21(5):729–737, 2011.
- [126] F. J. Muros, J. M. Maestre, E. Algaba, T. Alamo, and E. F. Camacho. Networked control design for coalitional schemes using game-theoretic methods. *Automatica*, 78:320–332, 2017.
- [127] R. R. Negenborn. *Multi-agent model predictive control with applications to power networks*. Delft University of Technology, 2007.
- [128] R. R. Negenborn, A. G. Beccuti, T. Demiray, S. Leirens, G Damm, B. D. Schutter, and M. Morari. Supervisory hybrid model predictive control for voltage stability of power networks. In *2007 American Control Conference*, pages 5444–5449. IEEE, 2007.

Bibliography

- [129] R. R. Negenborn, B. D. Schutter, and J. Hellendoorn. Efficient implementation of serial multi-agent model predictive control by parallelization. In *2007 IEEE International Conference on Networking, Sensing and Control*, pages 175–180. IEEE, 2007.
- [130] R. R. Negenborn, B. D. Schutter, and J. Hellendoorn. Multi-agent model predictive control for transportation networks: Serial versus parallel schemes. *Engineering Applications of Artificial Intelligence*, 21(3):353–366, 2008.
- [131] K. T. Ngo and K. T. Erickson. Stability of discrete-time matrix polynomials. *IEEE Transactions on Automatic Control*, 42(4):538–542, 1997.
- [132] J. Niu, J. Zhao, Z. Xu, and J. Qian. A two-time scale decentralized model predictive controller based on input and output model. *Journal of Analytical Methods in Chemistry*, 2009, 2009.
- [133] G.VJ. Pappas, G. Lafferriere, and S. Sastry. Hierarchically consistent control systems. *IEEE Transactions on Automatic Control*, 45(6):1144–1160, 2000.
- [134] A. Parisio, E. Rikos, and L. Glielmo. A model predictive control approach to microgrid operation optimization. *IEEE Transactions on Control Systems Technology*, 22(5):1813–1827, 2014.
- [135] A. Perizzato, M. Farina, and R. Scattolini. Stochastic distributed predictive control of independent systems with coupling constraints. In *2014 IEEE 53rd Annual Conference on Decision and Control (CDC)*, pages 3228–3233. IEEE, 2014.
- [136] B. Picasso, C. Romani, and R. Scattolini. Hierarchical model predictive control of Wiener models. In *Nonlinear Model Predictive Control*, pages 139–152. Springer, 2009.
- [137] B. Picasso, D.D. Vito, R. Scattolini, and P. Colaneri. An MPC approach to the design of two-layer hierarchical control systems. *Automatica*, 46(5):823–831, 2010.
- [138] N. Prljaca and Z. Gajic. General transformation for block diagonalization of multi time-scale singularly perturbed linear systems. In *2007 American Control Conference*, pages 1670–1675. IEEE, 2007.
- [139] V. Puig, C. Ocampo-Martinez, and S. M. De Oca. Hierarchical temporal multi-layer decentralised MPC strategy for drinking water networks: Application to the Barcelona case study. In *20th Mediterranean Conference on Control & Automation*, pages 740–745. IEEE, 2012.
- [140] S. J. Qin and T. A. Badgwell. A survey of industrial model predictive control technology. *Control Engineering Practice*, 11(7):733–764, 2003.
- [141] T. Rahwan, T. Michalak, E. Elkind, P. Faliszewski, and J. Sroka. Constrained coalition formation. In *Proceedings of the Twenty-Fifth AAAI Conference on Artificial Intelligence*, 2011.
- [142] D. M. Raimondo, D. Limon, M. Lazar, L. Magni, and E.F. Camacho. Min-max model predictive control of nonlinear systems: A unifying overview on stability. *European Journal of Control*, 15(1):5–21, 2009.
- [143] D. M. Raimondo, L. Magni, and R. Scattolini. Decentralized MPC of nonlinear systems: An Input-to-State stability approach. *International Journal of Robust and Nonlinear Control*, 17(17):1651–1667, 2007.
- [144] S. V. Rakovic, E. C. Kerrigan, K. I. Kouramas, and D. Q. Mayne. Invariant approximations of the minimal robust positively invariant set. *IEEE Transactions on Automatic Control*, 50(3):406–410, 2005.
- [145] S. V. Raković and D. Q. Mayne. A simple tube controller for efficient robust model predictive control of constrained linear discrete time systems subject to bounded disturbances. *IFAC Proceedings Volumes*, 38(1):241–246, 2005.

Bibliography

- [146] S.V. Rakovic and M. Baric. Parameterized robust control invariant sets for linear systems: Theoretical advances and computational remarks. *IEEE Transactions on Automatic Control*, 55(7):1599–1614, 2010.
- [147] S.V. Raković, B. Kouvaritakis, M. Cannon, and C. Panos. Fully parameterized tube model predictive control. *International Journal of Robust and Nonlinear Control*, 22(12):1330–1361, 2012.
- [148] C. V. Rao, S. J. Wright, and J. B. Rawlings. Application of interior-point methods to model predictive control. *Journal of Optimization Theory and Applications*, 99(3):723–757, 1998.
- [149] J. B. Rawlings and R. Amrit. Optimizing process economic performance using model predictive control. In *Nonlinear Model Predictive Control*, pages 119–138. Springer, 2009.
- [150] J. B. Rawlings and D. Q. Mayne. *Model Predictive Control: Theory and Design*. Nob Hill Publishing, 2009.
- [151] A. Richards and J. P. How. Robust distributed model predictive control. *International Journal of Control*, 80(9):1517–1531, 2007.
- [152] S. Rivero. *Distributed and plug-and-play control for constrained systems*. PhD thesis, University of Pavia, 2014.
- [153] S. Rivero, M. Farina, and G. Ferrari-Trecate. Plug-and-play decentralized model predictive control. In *51st IEEE Conference on Decision and Control*, pages 4193–4198. IEEE, 2012.
- [154] S. Rivero, M. Farina, and G. Ferrari-Trecate. Plug-and-play decentralized model predictive control for linear systems. *IEEE Transactions on Automatic Control*, 58(10):2608–2614, 2013.
- [155] S. Rivero and G. Ferrari-Trecate. Tube-based distributed control of linear constrained systems. *Automatica*, 48(11):2860–2865, 2012.
- [156] S. Roshany-Yamchi, M. Cychowski, R. R. Negenborn, B. De Schutter, K. Delaney, and J. Connell. Kalman filter-based distributed predictive control of large-scale multi-rate systems: Application to power networks. *IEEE Transactions on Control Systems Technology*, 21(1):27–39, 2013.
- [157] W. I. Rowen. Simplified mathematical representations of heavy-duty Gas turbines. *Journal of Engineering for Power*, 105(4):865–869, 1983.
- [158] V. R. Saksena, J. O’reilly, and P. V. Kokotovic. Singular perturbations and time-scale methods in control theory: Survey 1976–1983. *Automatica*, 20(3):273–293, 1984.
- [159] M.E. Salgado and A. Conley. MIMO interaction measure and controller structure selection. *International Journal of Control*, 77(4):367–383, 2004.
- [160] R. Scattolini. Self-tuning control of systems with infrequent and delayed output sampling. *Proc. IEE, Part D*, 135:213–221, 1988.
- [161] R. Scattolini. Architectures for distributed and hierarchical model predictive control—a review. *Journal of Process Control*, 19(5):723–731, 2009.
- [162] R. Scattolini and P. Colaneri. Hierarchical model predictive control. In *46th IEEE Conference on Decision and Control*, pages 4803–4808. IEEE, 2007.
- [163] R. Scattolini, P. Colaneri, and D. D. Vito. A switched MPC approach to hierarchical control. *IFAC Proceedings Volumes*, 41(2):7790–7795, 2008.
- [164] R. Scattolini, D. Doan, T. Keviczky, and B. De Schutter. D2.1: Report on literature survey and preliminary definition of the selected methods for the definition of system decomposition and hierarchical control architectures. In <http://www.ict-hd-mpc.eu/deliverables>, 2009.

Bibliography

- [165] P. O. Scokaert and D. Q. Mayne. Min-max feedback model predictive control for constrained linear systems. *IEEE Transactions on Automatic Control*, 43(8):1136–1142, 1998.
- [166] P. O. Scokaert and J. B. Rawlings. Constrained linear quadratic regulation. *IEEE Transactions on Automatic Control*, 43(8):1163–1169, 1998.
- [167] D. E. Seborg, D. A. Mellichamp, T. F. Edgar, and F. J. Doyle III. *Process dynamics and control*. John Wiley & Sons, 2010.
- [168] G. Seenumani, H. Peng, and J. Sun. A reference governor-based hierarchical control for failure mode power management of hybrid power systems for all-electric ships. *Journal of Power Sources*, 196(3):1599–1607, 2011.
- [169] D. H. Shim, H. J. Kim, and S. Sastry. Decentralized nonlinear model predictive control of multiple flying robots. In *Proceedings of the 42nd IEEE conference on Decision and Control*, volume 4, pages 3621–3626. IEEE, 2003.
- [170] S. Skogestad and I. Postlethwaite. *Multivariable feedback control: Analysis and design*, volume 2. Wiley New York, 2007.
- [171] J. Soustrup. Plug and play control: Control technology towards new challenges. *European Journal of Control*, 15:311–330, 2009.
- [172] B. T. Stewart, J. B. Rawlings, and S. J. Wright. Hierarchical cooperative distributed model predictive control. In *2010 American Control Conference*, pages 3963–3968. IEEE, 2010.
- [173] B. T. Stewart, A. N. Venkat, J. B. Rawlings, S. J. Wright, and G. Pannocchia. Cooperative distributed model predictive control. *Systems & Control Letters*, 59(8):460–469, 2010.
- [174] B. T. Stewart, S. J. Wright, and J. B. Rawlings. Cooperative distributed model predictive control for nonlinear systems. *Journal of Process Control*, 21(5):698–704, 2011.
- [175] D. C. Tarraf and H. H. Asada. Decentralized hierarchical control of multiple time scale systems.
- [176] P. Tatjewski. Advanced control and on-line process optimization in multilayer structures. *Annual Reviews in Control*, 32(1):71–85, 2008.
- [177] P. Tatjewski. Supervisory predictive control and on-line set-point optimization. *International Journal of Applied Mathematics and Computer Science*, 20(3):483–495, 2010.
- [178] P. Tøndel, T. A. Johansen, and A. Bemporad. An algorithm for multi-parametric quadratic programming and explicit MPC solutions. *Automatica*, 39(3):489–497, 2003.
- [179] C. R. Touretzky and M. Baldea. A hierarchical scheduling and control strategy for thermal energy storage systems. *Energy and Buildings*, 110:94–107, 2016.
- [180] J. Tran, K. Ling, and J. M. Maciejowski. Economic model predictive control—a review. In *Proceedings of International Symposium on Automation and Robotics in Construction*, pages 9–11, 2014.
- [181] K. Trangbaek and J. Bendtsen. Exact constraint aggregation with applications to smart grids and resource distribution. In *IEEE 51st Annual Conference on Decision and Control*, pages 4181–4186. IEEE, 2012.
- [182] P. Trodden and A. Richards. Robust distributed model predictive control using tubes. In *2006 American Control Conference*, pages 6–pp. IEEE, 2006.
- [183] T. Tu, M. Ellis, and P. D. Christofides. Model predictive control of a nonlinear large-scale process network used in the production of vinyl acetate. *Industrial & Engineering Chemistry Research*, 52(35):12463–12481, 2013.

Bibliography

- [184] A. N. Venkat, J. B. Rawlings, and S. J. Wright. Stability and optimality of distributed model predictive control. In *Proceedings of the 44th IEEE Conference on Decision and Control*, pages 6680–6685. IEEE, 2005.
- [185] S. H. Wang and E. Davison. On the stabilization of decentralized control systems. *IEEE Transactions on Automatic Control*, 18(5):473–478, 1973.
- [186] X. Wang, M. Chen, C. Lefurgy, and T. W. Keller. SHIP: Scalable hierarchical power control for large-scale data centers. In *18th International Conference on Parallel Architectures and Compilation Techniques*, pages 91–100. IEEE, 2009.
- [187] B. Wittenmark and M.E. Salgado. Hankel-norm based interaction measure for input-output pairing. *IFAC Proceedings Volumes*, 35(1):429–434, 2002.
- [188] M. Wogrin and L. Glielmo. An MPC scheme with guaranteed stability for linear singularly perturbed systems. In *49th IEEE Conference on Decision and Control*, pages 5289–5295. IEEE, 2010.
- [189] I. J. Wolf, D. A. Munoz, and W. Marquardt. Consistent hierarchical economic NMPC for a class of hybrid systems using neighboring-extremal updates. *Journal of Process Control*, 24(2):389–398, 2014.
- [190] K. Worthmann, C. M. Kellett, P. Braun, L. Grüne, and S. R. Weller. Distributed and decentralized control of residential energy systems incorporating battery storage. *IEEE Transactions on Smart Grid*, 6(4):1914–1923, 2015.
- [191] L. Würth, R. Hannemann, and W. Marquardt. A two-layer architecture for economically optimal process control and operation. *Journal of Process Control*, 21(3):311–321, 2011.
- [192] T. Zabaoui, L. A. Dessaint, and P. R. Brunelle. Development of a new library of IEEE excitation systems and its validation with PSS/E. In *2012 IEEE Power and Energy Society General Meeting*, pages 1–8. IEEE, 2012.
- [193] Y. Zhang and S. Li. Networked model predictive control based on neighbourhood optimization for serially connected large-scale processes. *Journal of process control*, 17(1):37–50, 2007.
- [194] Y. Zhang, D. S. Naidu, C. Cai, and Y. Zou. Singular perturbation and time scales in control theories and applications: An overview 2002–2012. *International Journal of Information and Systems Sciences*, 9(1):1–36, 2014.
- [195] Y. Zou, T. Chen, and S. Li. Network-based predictive control of multirate systems. *IET Control Theory & Applications*, 4(7):1145–1156, 2010.